A three-dimensional approach to in vitro culture of immune-related cells

Hartmann, Sofie Bruun

Publication date:
2016

Document Version
Publisher's PDF, also known as Version of record

A three-dimensional approach to *in vitro* culture of immune-related cells

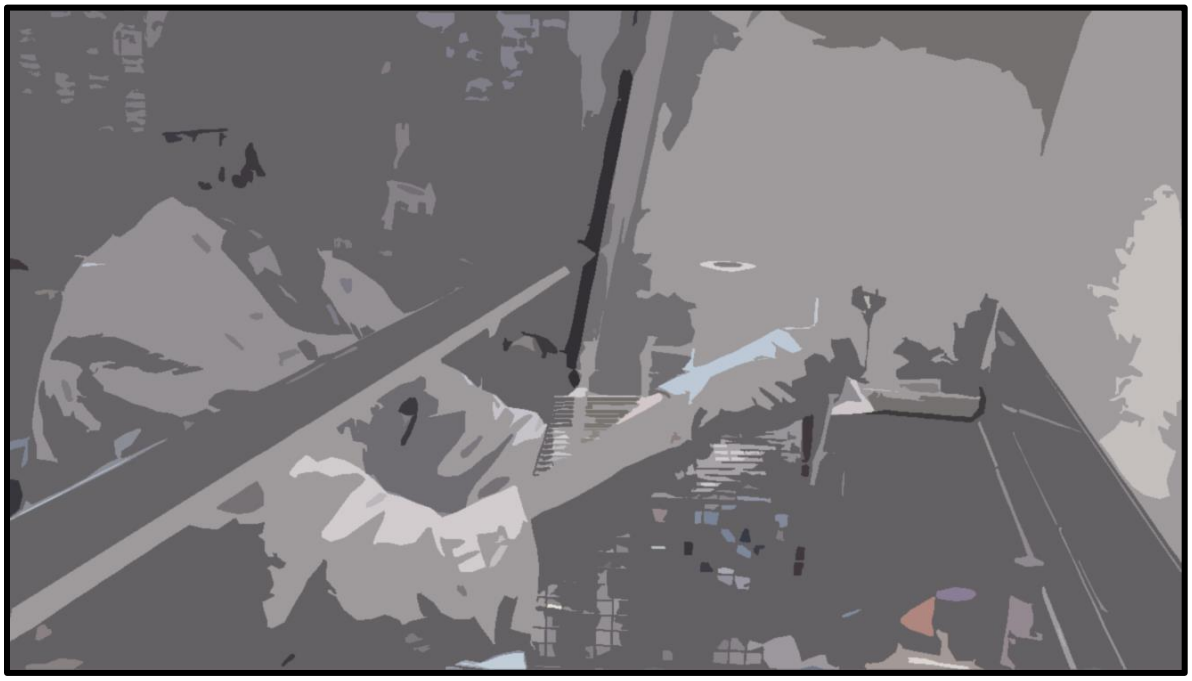

PhD thesis • Sofie Bruun Hartmann • January 2016

DTU Vet
National Veterinary Institute

Supervisors:

Professor Gregers Jungersen (main supervisor)
National Veterinary Institute
Technical University of Denmark
Frederiksberg C, Denmark

Professor Jenny Emnéus
Department of Micro- and Nanotechnology
Technical University of Denmark
Kgs. Lyngby, Denmark

Associate Professor Anders Wolff
Department of Micro- and Nanotechnology
Technical University of Denmark
Kgs. Lyngby, Denmark

Assessment Committee:

Professor Niels Bent Larsen (chairperson)
Department of Micro- and Nanotechnology
Technical University of Denmark
Kgs. Lyngby, Denmark

Senior scientist Jesper Eugen-Olsen
Clinical Research Centre
Copenhagen University Hospital Hvidovre
Hvidovre, Denmark

Professor Mick Bailey
School of Veterinary Science
University of Bristol
Bristol, UK

Table of Contents

Acknowledgements

This PhD project has been a journey for me. A journey full of excitement, frustration, learning, fun, challenges and last but not least, this journey has blessed me with the privileged of working with wonderful colleagues. I could not have completed this PhD without he help from numerous people.

First and foremost I would like to express my deepest gratitude to my supervisor, Gregers Jungersen. Thank you for giving me the opportunity to work on this project and for your always positive inputs and support. I would also like to thank my co-supervisors Jenny Emnéus and Anders Wolff for competent guidance during the project. Also I owe a huge thank to members of the Bioanalytic's and BioLabChip groups, especially to Soumyaranjan Mohanty for providing me with 3D scaffolds and Carl Esben Poulsen for helping me with the chip design. Also a big thank to Claus Højgård Nielsen and Tage A. Larsen from DTU Danchip for expert assistance during the chip manufacture.

I spent most of my time at DTU Vet, where I have been surrounded by the best colleagues one could wish for. I am deeply thankful for the way you have all welcomed me and made it very easy for me to feel at home. Thanks to Jeanne Toft Jakobsen for always being the "go to" person whenever I needed to solve a lab-related question - you are a star. I also owe a big thank to Panchale Olsen and Lien Thi Minh Nguyen for help in the lab and to Ulla Riber for her flow cytometry guidance. A special thank goes to Karin Tarp and Kerstin Skovgaard for their competent help with the PCR work and for always having time for me when needed. I would also like to thank Mette Boye and Martin Weiss Nielsen for help with the confocal microscope.

Thanks to all my fellow (now former) PhD students - Lasse Eggers Pedersen, Aneesh Thakur, Ann Cathrine Findal Støy, Sarah Bøje, Lif Knudsen, and to my office mates - Heidi Mikkelsen Melvang, Maria Rathmann Sørensen and Rikke Birgitte Lyngaa – you have all made it a joy to go work every day.

Last but not least I am grateful for my friends and family who has been patient with me during times of intense workload. Thank you to my parents and mother-in-law for helping taking care of Josephine. Of all the people that have helped me, I owe the biggest thank to my husband, Johan, for his endless support, and for always being there for me whenever I need him.

Preface

The research presented in this thesis was performed under the supervision of Professor Gregers Jungersen, Professor Jenny Emnéus and Associate Professor Anders Wolff. The practical work was performed at the Section for Immunology and Vaccinology, National Veterinary Institute, Technical University of Denmark and at the Department of Micro- and Nanotechnology, Technical University of Denmark from December 2011 to January 2016. The project was financed by DTU.

The original aim of this thesis was to develop a diagnostic chip for detection of CMI responses in a blood sample by recall antigen stimulation and direct IFN-γ detection as readout. This goal was not reached, however, and the focus of the thesis changed into looking at optimization of conditions for *in vitro* culture of primary immune cells. The work included in this thesis is presented in four studies. Study I (chapter 3) looks at the effect of performing interferon-γ release assays using cultures of whole blood or PBMCs and the study is presented in paper I. Study II (chapter 4) presents the results from interferon-γ release assay-optimization by addition of a third dimension to the culture using three dimensional scaffolds. Study III (chapter 5) presents the manufacture of a prototype chip. The last study - study IIII (chapter 6) - looks at the effect of changing the culture environment when studying the differentiation of monocytes to monocyte-derived dendritic cells *in vitro*. This is presented in paper II.

This thesis contains two manuscripts:

Paper I:
Hartmann, S., Emnéus, J., Wolff, A. and Jungersen, G. “Revisiting the IFN-γ release assay: Whole blood or PBMC cultures? - And other factors of influence”. Manuscript ready for submission.

Paper II
Hartmann, S., Mohanty, S., Skovgaard, K., Brogaard, L., Flagstad, F., Emnéus, J., Wolff, A., Summerfield, A. and Jungersen, G. “Investigating the role of surface materials and three dimensional architecture on in vitro differentiation of porcine monocyte-derived dendritic cells”. Manuscript submitted to PLOS ONE.

Abbreviations

2D	Two dimensional
3D	Three dimensional
APC	Antigen presenting cell
BCR	B cell receptor
CMI	Cell-mediated immunity
CTL	Cytotoxic T lymphocyte
ELISA	Enzyme-linked immunosorbent assay
FCS	Fetal calf serum
FRC	Fibroblastic reticular cells
GW	Glass wool
IFN-γ	Interferon gamma
IGRA	Interferon gamma release assay
IL	Interleukin
IP10	Interferon gamma induced protein 10 (or CXCL10)
MAP	*Mycobacterium avium* subsp. *paratuberculosis*
MHC	Major histocompatibility complex
OD	Optical density
PBMC	Peripheral blood mononuclear cells
PBS	Phosphate buffered saline
PCL	polycaprolactone
PDMS	Polydimethylsiloxane
pMHC	Peptide:MHC complex
PP(S)	Polypropylene (shavings)
PPDj	Johnin purified protein derivative (a protein derivative from MAP)
PS	Polystyrene
qRT-PCR	Quantitative real time polymerase chain reaction
RT	Room temperature
RPMI	Roswell Park Memorial Institute (cell culture medium)
SEB	S*taphylococcal* enterotoxin B
TCR	T cell receptor
T_H	T helper cell
WB	Whole blood

Summery

T lymphocytes are key players during the initiation of an adaptive immune response. The activation of these cells *in vivo* requires migration within the lymph nodes until they encounter antigen presenting cells (APCs) that can activate them to secrete IFN-γ which mediates downstream effector functions. The *in vitro* reactivation of antigen-experienced T lymphocytes and detection of IFN-γ from cell cultures can be used in a diagnostic assay to test for disease or vaccine efficacy. Practical procedures of the IFN-γ release assay (IGRA) was investigated using bovine cells and whole blood cultures was found preferable compared to PBMC cultures, partly due to the risk of losing cell subsets after purification of PBMCs.

The development of *in vitro* culture systems for more than 50 years ago revolutionized the biomedical world. It became possible to study cell behavior using cell lines or primary cells in culture and to measure cell activity such as IGRA, as described above. The traditional way of culturing cells are done using polystyrene (PS) plastic ware in flask-, Petri dish- or micro titer plate format. However, these artificial two dimensional (2D) surfaces on which the cells grow, has shown to interfere with cell morphology, gene expression and overall behavior and as such gives a poor reflection of *in vivo* cell behavior. Therefore, it is believed that by mimicking the *in vivo* conditions within the cultures, this would generate "closer-to-*in vivo*" results. For this purpose three dimensional (3D) culture setups have been developed including artificial scaffolds and extracellular matrix gels.

Optimization of IGRA was attempted using solid 3D scaffolds in various formats. The purpose of the 3D scaffolds was to facilitate T lymphocyte migration and subsequently activation due to increased chances of T lymphocyte/APC encounter. However, it turned out that the addition of this extra dimension to the cultures did not translate into increased de novo secretion of IFN-γ in these cultures. Furthermore, we often observed a non-specific effect on the level of IFN-γ when cells were cultures in 3D. This suggested that cells were sensitive to the geometry surrounding them and that this was independent on antigen stimulation.

Based on these findings and a previous discovery that the polymer PDMS, gave rise to increased differentiation of a nerve cell line *in vitro*, we tested the effect of PDMS on the differentiation of porcine monocytes. Monocytes are immune cells of high plasticity, and thus we speculated that they might be sensitive to culture conditions. Indeed, monocytes differentiated into monocyte-derived DC (moDCs) when cultured conventionally (2D PS) in the presence of GM-CSF and IL-4, but adopted a macrophage-like gene expression profile when cultured on PDMS. Further it was found that 3D culturing resulted in increased activation of the monocyte-derived cells.

The work in this thesis covers several aspects within primary cell culture, but central to the work is the investigation of 3D cell culture setups for improved activation/differentiation of immune cells. Conclusively, this work highlights the importance of acknowledging the effect from external factors when analyzing data generated from *in vitro* cultures. This being even more important when working with immune cells since these cells adopt traits and functions simply based on the nature of the culture system.

Sammendrag (Danish summery)

T-lymfocytter er centrale celler i aktiveringen af det adaptive immunrespons. Aktiveringen af disse celler *in vivo* sker i lymfeknuderne og indebærer migration af T lymfocytterne indtil de støder på en relevant antigen-præsenterende celle (APC), som kan aktivere dem. Herved responderer T-lymfocytterne ved at udskille IFN-γ, som er med til at initiere andre dele af immunresponset. *In vitro* reaktivering af primede T-lymfocytter og efterfølgende detektion af IFN-γ fra cellekulturer, kan anvendes i et diagnostisk assay til sygdomsdetektion eller til at teste vaccineeffektivitet. Praktiske procedurer omkring opsætningen af dette assay, kaldet IFN-γ release assay (IGRA), blev undersøgt med immunceller fra kalve. Det viste sig, at fuldblod var bedre egnet end PBMC kulturer, dels på grund af risikoen for at miste specielle celletyper under oprensningen af PBMC'erne.

Udviklingen af metoder til *in vitro*-dyrkning af celler for mere end 50 år siden, revolutionerede den biomedicinske verden. Det blev bl.a. muligt at studere celler og deres adfærd vha. både cellelinjer og primære celler, samt at måle celleaktivitet vha assays såsom IGRA. Den traditionelle måde at dyrke celler på, har været vha. plastikprodukter såsom flasker, skåle eller flerbrøndsplader lavet i polystyren (PS). Disse kunstige todimensionale (2D) overflader, hvorpå cellerne vokser, har dog vist sig at påvirke cellemorfologien, genekspressionen og cellernes generelle opførsel, hvilket resulterer i en dårlig afspejling af cellernes *in vivo*-adfærd. Det antages derfor, at man ville kunne opnå bedre resultater, som i højere grad afspejler *in vivo*-forholdene, hvis der blev optimeret på cellekulturforholdene. Til dette formål er tredimensionelle (3D) kulturer blevet udviklet, herunder kunstige matricer el netværk samt ekstracellulær proteinholdige geler.

I denne afhandling blev IGRA forsøgt optimeret ved at tilføje 3D matricer i forskellige formater til cellekulturerne. Formålet med 3D matricerne var at facilitere effektiv migration af T-lymfocytterne og deres efterfølgende aktivering som følge af øget chancer for T-lymfocyt/APC interaktion. Det viste sig dog, at tilføjelsen af denne ekstra dimension til kulturerne ikke resultere i en øget de novo produktion af IFN-γ i disse kulturer. Vi observerede derimod en uspecifik påvirkning af IFN-γ niveauet når cellerne var i 3D kulturer. Dette antydede, at cellerne var følsomme overfor cellekultur-geometrien, og at dette var uafhængigt af antigenstimuleringen.

På baggrund af disse resultater, samt tidligere studier som viste at polydimethylsiloxane (PDMS) gav anledning til øget *in vitro* differentiering af en nervecellelinje, satte vi os for at teste virkningen af PDMS på differentieringen af monocytter oprenset fra svineblod. Monocytter er immunceller med høj plasticitet, og dermed potentielt følsomme over for dyrkningsbetingelserne. Det viste sig at monocytterne differentierede sig til monocyt-deriverede DCer (moDCer), når de blev dyrket konventionelt (2D PS) med GM-CSF og IL-4, mens de fik en makrofag-lignende genekspressionsprofil når de blev dyrket på PDMS. Yderligere fandt vi, at 3D dyrkning resulterede i øget aktivering af disse monocyt-deriverede celler.

Arbejdet i denne afhandling dækker flere aspekter inden for primær cellekultur, men centralt for arbejdet er undersøgelsen af 3D cellekulturenes effekt på aktiveringen/differentieringen af immunceller. Konklusionsvis fremhæver dette arbejde, hvor vigtigt det er at anerkender virkningen af eksterne faktorer når man analyserer data fra *in vitro* cellekulturer. Dette er især vigtigt, når der arbejdes med immunceller, da disse celler har vist sig at være sensitive overfor ydre ændringer i cellekulturopsættet.

List of figures

Chapter 1 - General background

1.1 The immune system

We live in a world of daily exposure to millions of potential pathogenic microorganism through inhalation, contact and digestion. Yet we manage to stay alive, and the reason for this can be ascribed to our immune system. It consists of a diverse group of cells and molecules specialized in protecting us from pathogens by identifying and targeting them or their products for destruction. The responses carried out by the immune system needs to be tightly regulated in terms of type, intensity and duration to effectively overcome an intruding pathogen, but doing so with minimal collateral tissue destruction and alteration of homeostasis (Goldszmid & Trinchieri 2012). Typically the immune system is divided into innate and adaptive immunity (Figure 1), which serves as a rapid first and a slower second line of defense, respectively. Whereas the adaptive immune system consist of a defined physiologic system that rely on a few subsets of helper and effector cells, the innate system is a product of multiple and diverse defense mechanisms (Medzhitov 2008).

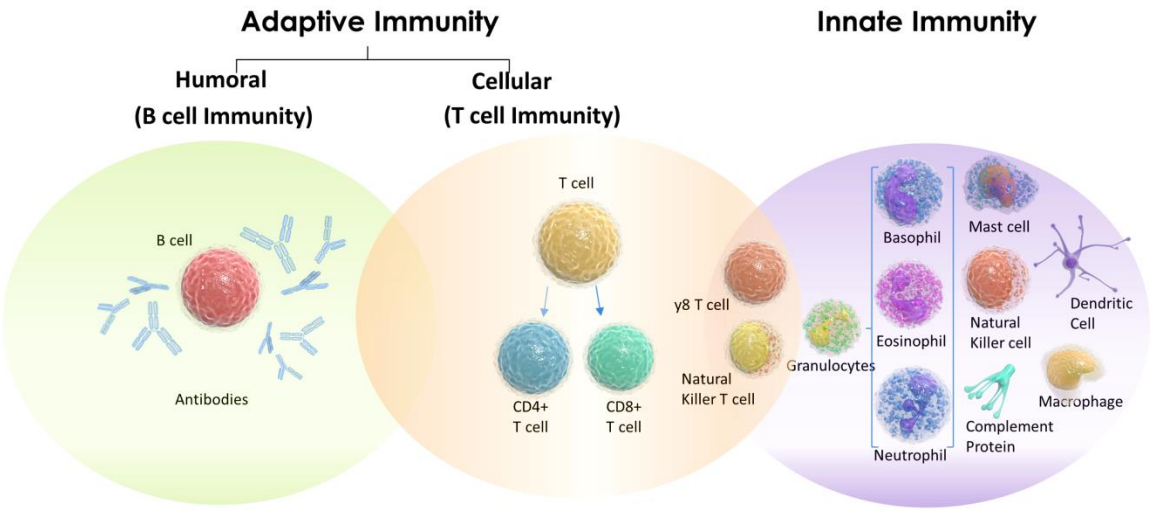

Figure 1: Overview of cells involved in the adaptive and innate immune system. Figure from: http://currentscienceperspectives.com/what-is-immunology/

1.1.1 Innate immunity

The innate immune response is our first line of defense against intruding pathogens. It is characterized as being a fast and non-specific response (though it can discriminate between self and non-self), which is constant over time and does not result in immunological memory. It is comprised of physical barriers, such as skin and mucosal surfaces lining the gastrointestinal, respiratory, and urogenital tracts. Microbes that manage to breach these physical barriers are met by the cells of the innate immune system. These include professional phagocytes such as macrophages, dendritic cells (DC) and neutrophils which exerts phagocytic uptake of both intracellular and extracellular bacterial and fungal pathogens (Savina & Amigorena 2007). The natural killer (NK) cells are specialized in direct killing of virus-infected host cells and also help clearing intracellular infection by production of cytokines, especially interferon (IFN)-γ (Zhang et al. 2006). Finally anti-parasitic cells of the innate immune system consist of mast cells, eosinophils and basophils (Haig & Miller 1990). Apart from the cells listed above, the innate immune system also comprises antimicrobial peptide and secreted proteins of the complement system which functions include opsonization of pathogens for phagocytic uptake. Key factors defining the innate immune system is the recognition of conserved pathogenic structures specific for non-eukaryotic cells, by germline-encoded pattern-recognition receptors (PRRs) as well as the ability to recruit cells of the adaptive immune system by secretion of cytokines (Murphy 2012).

1.1.2 Adaptive immunity

The adaptive immune system takes over as a second line of defense. In contrast to the innate response, the adaptive response is characterized as being slow but specific, it continuously develops during the lifetime of an individual and it provides immunological memory. Cells involved in the adaptive immunity is termed B- and T lymphocytes, referring to the location in which they mature; the primary lymphoid organs, namely bone marrow and thymus, respectively. Once matured these cells initiates their function in the spleen, lymph nodes and mucosal lymphoid tissues, collectively termed secondary lymphoid organs (Murphy 2012). Whereas B lymphocytes produce antibodies and are responsible for the humoral immunity, T lymphocytes constitutes the cell mediated immunity (CMI) involving cytotoxicity and regulatory functions (Danilova 2012). Three major molecules are

central for the adaptive immunity: the T cell receptor (TCR), B cell receptor (BCR) and major histocompatibility complex (MHC). The TCR and BCR are similar in structure; they are both dimers with BCR being composed of a heavy and a light immunoglobulin chain, and TCR being composed of an α and β chain (in αβT lymphocytes) or a γ and δ chain (in γδT lymphocytes) (Murphy 2012). Despite the similarity of their receptors, B and T cells differ functionally in the way they recognize antigens; B cells recognize antigens (non-self) directly via BCR, whereas T cells recognize "non-self" in combination with "self" through antigen:MHC complexes via TCR (Danilova 2012). During the process of maturation, BCR and TCR undergo somatic recombination of gene segments (Schatz 2004; Tonegawa 1983) and through imprecise joining mechanisms a high degree of functionally important for diversity is introduced, creating huge numbers of receptors with unique specificities (Murphy 2012). Through this genomic recombination, the diversity of TCRs with distinctive specificities exceeds 10^{15} (Davis & Bjorkman 1988). The specificities of BCR is even higher due to secondary processes of somatic hypermutation and class switch recombination (Muramatsu et al. 2000; Liu & Schatz 2009) which occur following antigen binding and B lymphocyte activation thus ensuring the production of high affinity antibodies. B lymphocytes with BCRs specific for "self" antigens are negatively selected during development in the bone marrow (Hartley et al. 1993; Gay et al. 1993). In the thymus, T lymphocytes whose receptors interact weakly with antigen:MHC complexes is positively selected for whereas T lymphocytes with strongly self-reactive receptors are negatively selected (Murphy 2012). In this way, autoreactive lymphocytes are eliminated and the remaining pool of naïve (antigen-unexperienced) B and T lymphocytes enter the blood stream and travels to peripheral lymphoid tissues where they, following antigen recognition, become activated and clonally expands and differentiates into antibody-producing plasma cells or cytotoxic/helper T lymphocytes, respectively (Danilova 2012).

1.2 CMI

The immunological response performed by T lymphocytes is the CMI response. During development T lymphocytes commits to expression of either cluster of differentiation (CD)-8 or CD4 co-receptor molecules (Tanaka & Taniuchi 2014). $CD8^+$ T lymphocytes recognize antigen in combination with MHC class I expressed by all nucleated cells, and develops into cytotoxic T lymphocytes (CTLs) following

activation. $CD4^+$ T lymphocytes recognizes antigen bound to MHC class II expressed by professional antigen-presenting cells (APCs) primarily DCs and macrophages, but also B lymphocytes as well as monocytes which are APC precursors (Randolph et al. 2008). Upon activation these lymphocytes develop into cytokine-secreting helper T (T_H) lymphocytes, with T_H1 being key players within the CMI response (Figure 2).

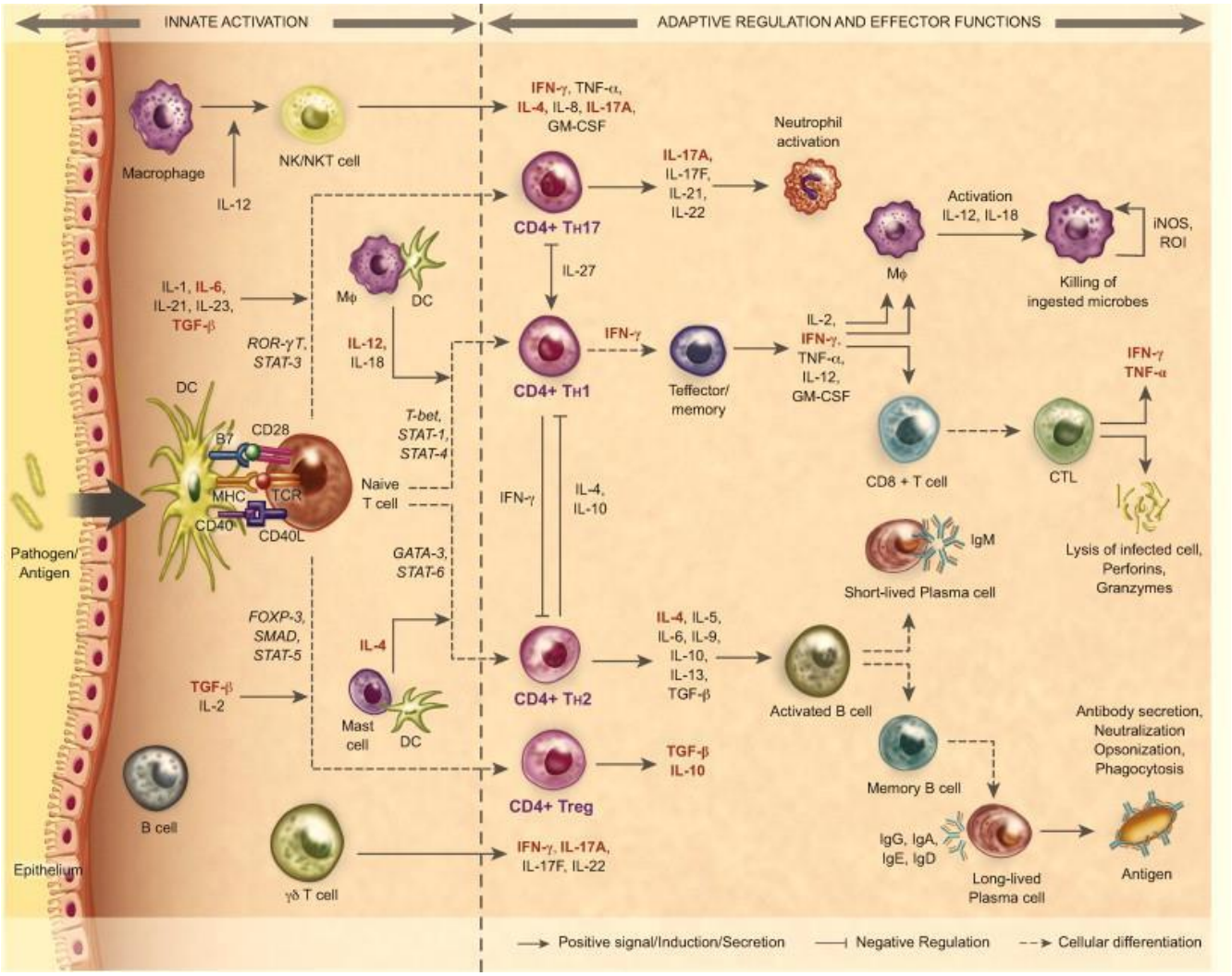

Figure 2: Cells and molecules important for innate and adaptive immune responses. From (Thakur et al. 2012).

Depending on activation factors, including local cytokine milieu, the naïve $CD4^+$ T lymphocyte differentiates into T_H1, T_H2, T_H17 or T regulatory (Treg) lymphocytes. Each of these lymphocytes has specific functions in terms of which cytokines they secrete. T_H1 lymphocytes secretes several

cytokines, but the primary one being IFN-γ (Romagnani 1994) that activates macrophages and CTLs and enabling them to kill pathogens and induce apoptosis in infected cells, respectively. The function of T_H2 lymphocytes is to initiate humoral immunity by B lymphocyte activation, mediated primarily by secretion of interleukin (IL)-4 (Romagnani 1994). T_H17 and Treg lymphocytes are responsible for neutrophils activation and immune regulation through IL-17A and IL-10/transforming growth factor (TGF)-β secretions, respectively (Thakur et al. 2012). Together, these cells orchestrate a complicated network of signals that eventually leads to development of long lived memory cells that due to their antigen-experienced nature, are capable of triggering a strong and fast response upon reencounter with the same antigen.

1.2.1 IFN-γ and IP10

IFN-γ is an 18.8 kD cytokine secreted by T_H1 lymphocytes, however other cells are also capable of producing IFN-γ. These cells includes $CD8^+$ CTLs in the adaptive response as well as NK/NKT cells and γδ T lymphocytes which are cells bridging the innate and adaptive immune system. The latter cells have been shown to be a source of innate IFN-γ production in *in vitro* cultures of bovine cells (Olsen et al. 2005; Kennedy 2002). γδ T lymphocytes have been shown to have immune regulatory functions and are active during the early responses to infection (Hiromatsu et al. 1992; King et al. 1999). Of yet unknown reasons, they are present in much higher numbers in cattle and pigs, especially in young animals where they constitute app. 40% and 23-57% of total circulating T lymphocytes, respectively (Wilson et al. 1996; Yang & Parkhouse 1996; Yang & Parkhouse 2000). IFN-γ has broad biological functions which includes anti-viral activity, enhancement of antigen-presentation via MHC I/II pathways, leucocyte trafficking, antibody isotype switching and immune regulation by means of T_H2 commitment inhibition (Boehm et al. 1997; Schoenborn & Wilson 2007; Schroder et al. 2004).

IP10 (encoded by the *CXCL10* gene) is a 7.4 kD small chemokine secreted by APCs (Moser & Loetscher 2001; Dhillon et al. 2007). It is expressed in pathogen-infected cells, but can also be induced at high levels by cells of the adaptive immune response (Ruhwald et al. 2012). In this case, it is expressed by APC in response to T lymphocyte-derived IFN-γ, but can also be induced by other cytokines. It is thus considered to be a downstream marker to IFN-γ which is the typical CMI readout marker(Chen & Liu

2009; Farrar & Schreiber 1993), and is expressed 100-fold compared to IFN-γ (Aabye et al. 2012). Thus both IFN-γ and IP10 can be used a markers for T_H1 type CMI responses.

1.2.2 Activation of $CD4^+$ T lymphocytes through antigens and superantigens

Once a pathogen or antigen is taken up by an APC, for example a DC, this delivers activating signals via PRR such as toll-like receptors (TLRs). As a downstream process the antigen peptide-processing within the DC accelerates, involving assembling of MHC II dimers in the endoplasmic reticulum, and loading of peptide in the lysosome compartment before being transported to the cell surface as a peptide:MHC complex (Blum et al. 2013). When this complex is presented to naïve CD4+ T lymphocytes, three signals occur eventually leading to T lymphocyte activation and differentiation into effector cells. The activation is initiated by binding of the peptide:MHC complex by the TCR in combination with CD4 co-receptor and results in increased adhesive interactions between the two cells. This represents the first "activating" signal. The second signal comes from binding of co-stimulatory molecules, B7.1/B7.2 (also known as CD80/CD86). These receptors are expressed by the APC and binds to CD28 on the T lymphocyte resulting in a "survival" signal necessary for clonal expansion of the T lymphocyte. This leads to differentiation of the T lymphocyte into various helper cells depending on the nature of the inflammatory cytokines, and the cytokines produced by the APC which represents the third "differentiating" signal (Murphy 2012). Differentiated or antigen-experienced T lymphocytes do not require the same co-stimulatory signals to become activated upon encounter with the same antigen, and can thus be reactivated to induce a fast and strong response.

Superantigens such as the *staphylococcal* enterotoxin B (SEB) differs from "regular" protein antigens in the way they activate T cells; they are not processed and presented via MHC II but instead binds to the MHC II molecules already present at the cell surface. In addition they are able to bind to the β chain of many TCRs and initiate activation of these T lymphocyte by bridging the two cells (Murphy 2012; Pinchuk et al. 2010) (Figure 3). The binding site preferences differ between superantigens, and each superantigen shows specificity towards a few different β chains, and can thus bind to and stimulate up to 20% of all T lymphocytes (Choi et al. 1989). This type of polyclonal stimulation does not result in immunological memory by the adaptive immune system, but mediates

a huge secretion of cytokines including IFN-γ (Assenmacher et al. 1998). Therefore, SEB is frequently used as a positive control within *in vitro* assays to assure viability of T cells.

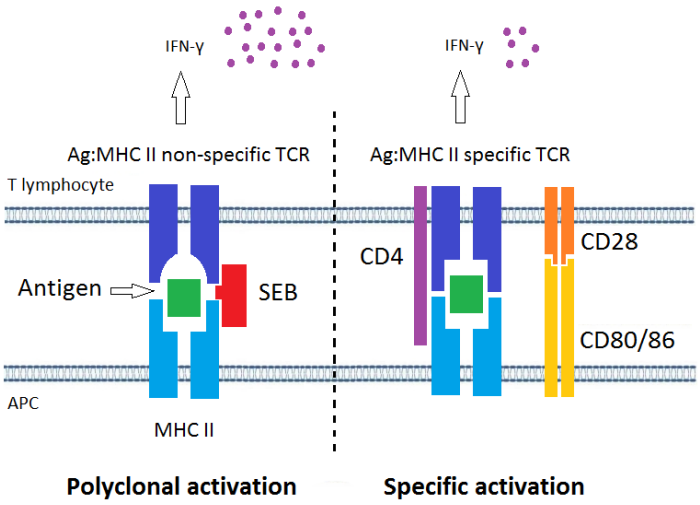

Figure 3: Concept of antigen vs. superantigen activation. SEB binds MHC II on the APC and TCR on the T lymphocyte and initiates a burst in cytokine secretion from the T-lymphocyte, including IFN-γ. During specific T-lymphocyte activation, TCR binds to processed antigen presented by MHC II in combination with CD4 (signal 1). Co-stimulatory receptors CD80/86 binds to CD28 (signal 2) and following cytokines released by the APC (signal 3), this induces T lymphocyte differentiation into T_H1 IFN-γ secreting lymphocytes.

1.3 Lymph nodes

Lymph nodes are essential for the activation of the adaptive immune response by providing an environment that favours the interaction of APC and T lymphocytes. Naïve T lymphocytes constantly patrol our body, trafficking between the vasculature and lymphatic system in search for cognate antigen (Girard et al. 2012). They enter the lymph nodes by the vascular route via high endothelial venules (HEVs). APCs (mainly DCs) that have taken up antigen in the peripheral tissue becomes activated and upregulate the expression of CCR7 (a G protein-coupled receptor), which homes them via the lymphatic system to the nearest lymph node by the chemokines CCL19 and CCL21 expressed in lymphoid tissue by stromal cells termed fibroblastic reticular cells (FRCs) (Worbs et al. 2008; Förster et al. 2012). FRCs produces and ensheaths a reticular network of collagen fibers and extracellular matrix proteins (ECM) which provides a network on which lymphocytes can migrate and DCs settle, ensuring

encounter of the two cell subsets (Bajénoff et al. 2007). T lymphocytes migrate using an 'amoeboid' mode of locomotion in 3D *in vivo* environments (Weninger et al. 2014), and the migration can both be random and directed, depending on the local chemokine milieu (Figure 4).

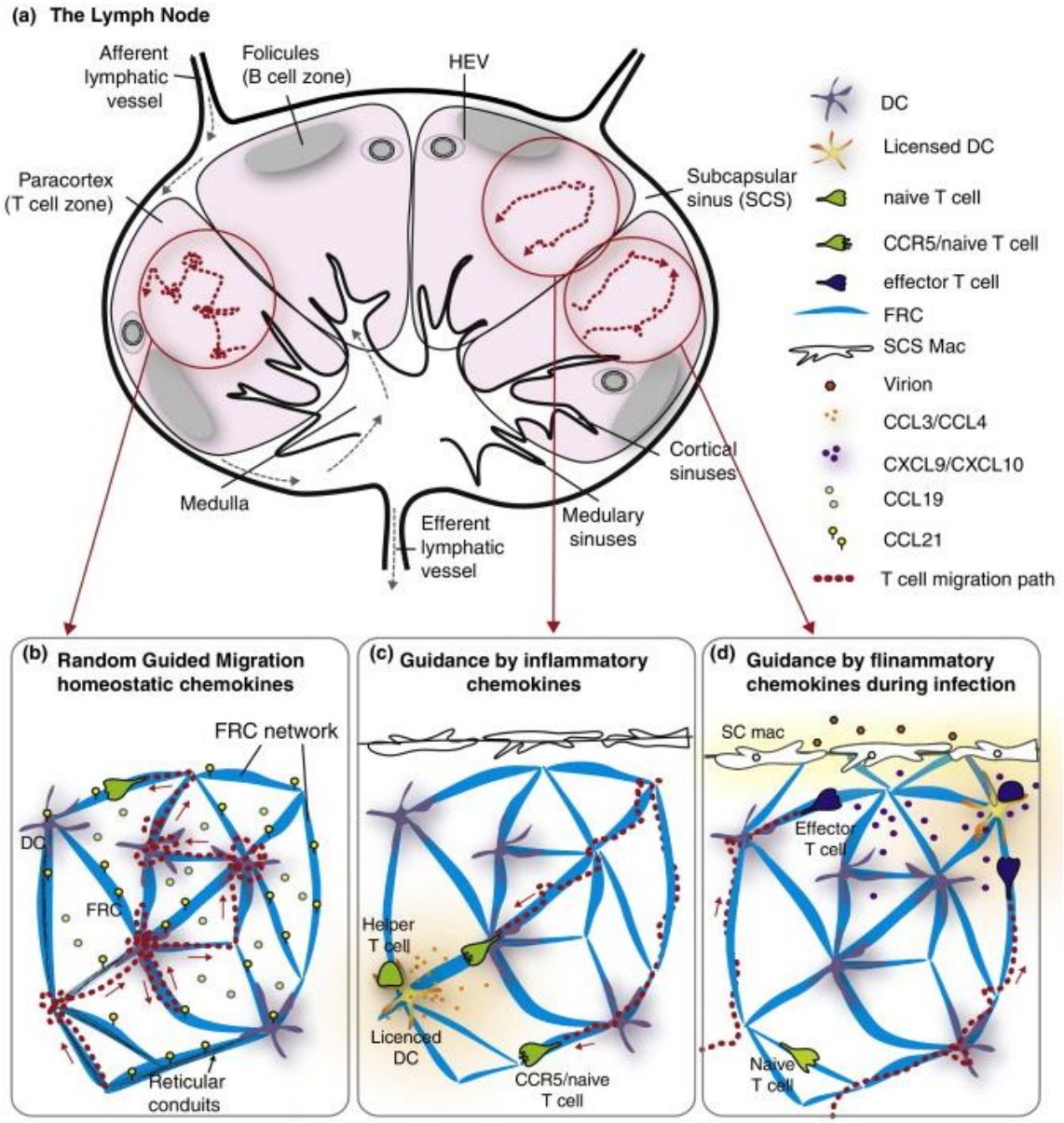

Figure 4: Modes of T lymphocyte migration within the three dimensional network of a lymph node. (a) Overall organisation of a lymph node. DCs enter via afferent lymphatics and T lymphocytes enter via HEVs in the T cell zones. T lymphocyte migration within lymph nodes is guided via the reticular network (FRC network) but can be **(b)** random during homeostatic conditions via constitutively expressed chemokines CCL19 and CCL21, or **(c)** guided by inflammatory chemokines (CCL3/4) expressed by the DCs following activation. This attracts more naïve T lymphocytes bearing the

chemokine receptor CCR5. **(d)** Lymph-born pathogenic particles are captured by resident macrophages that become activated and recruits effector T lymphocytes. From (Munoz et al. 2014).

1.4 In vitro culture

Cell culture became recognized as a research field when the Tissue Culture Commission (now known as The Society for In Vitro Biology) was established in 1946 (Berthier et al. 2012). However, already in 1907 with the demonstration of nerve fiber outgrowth from a frog embryo on a glass dish (Harrison 1911), this marked the beginning of the cell culture discipline. In 1955 Harry Eagle established the first widely used chemically defined medium (Eagle 1955). Glass was the choice for culture ware, but as the field began to expand, glass became a limiting factor and thus alternative materials such as plastic with properties that included reduction of the labor intensive cleaning as well as low production and operational costs, was introduced (Berthier et al. 2012). The plastic industry expanded enormously and companies such as Dow Corning and Falcon Plastics developed techniques decreasing the cost for plastic fabrication, particularly for polystyrene (Teach & Kiessling 1960). Because of its low production costs and other attractive properties such as optical clarity, mechanical strength and durability, polystyrene became the material of choice for disposable cell culture ware. Furthermore, when Falcon Plastics developed the oxygen plasma surface treatment, rendering the polystyrene surfaces more hydrophilic, resulting in improved cell attachment and growth (Barker & LaRocca 1994; Curtis et al. 1983), this cemented the use of polystyrene as *in vitro* culture ware, and from the 1960s it became the dominant material produced by many manufacturers (Curtis et al. 1983). Today many options are available, but the

1.4.1 IFN-γ assay

As a tool to measure CMI *in vitro*, the IFN-γ assay has been available for more than 25 years. Within the field of veterinary medicine, bovine tuberculosis and paratuberculosis were the first infections studied using this method (Wood et al. 1989; Wood et al. 1990; Rothel et al. 1990; Billman-Jacobe et al. 1992). The principle of the test is to measure the level of *de novo* secreted IFN-γ by cells in response to overnight culture with antigen. This is usually done by subtracting the concentrations of IFN-γ obtained in non-stimulated cultures (background) from the concentrations obtained in antigen-stimulated cultures. The assay can be based on whole blood cultures or cultures of purified peripheral

blood mononuclear cells (PBMCs), and following incubation, plasma/supernatant is harvested and used for IFN-γ detection by enzyme-linked immunosorbent assay (ELISA). The assay measures the overall level of IFN-γ upon antigen-recall, with no discrimination of the producing cell subsets. The rationale of using IFN-γ as a diagnostic measure, is that previous sensitized T lymphocytes will, via their TCR, recognize cognate antigen:MHC complexes presented to them by APCs, thus only pre-exposed, or vaccinated individuals will harbor sensitized T cells specific for the antigen and this will translate into *de novo* IFN-γ secretion. QuantiFERON-TB test (QFT) was the first commercial IGRA approved by the Food and Drug Administration (FDA) in 2001 (Mazurek & Villarino 2003).

1.4.2 3D culture

The ability of study cells by *in vitro* cultures has resulted in increased understanding of basic cell biology and behavior, and has proven to be indispensable for a variety of applications from research to industry. However, there is an increasing interest in optimizing the culture format by making 3D *in vitro* cultures for the "closer-to-*in vivo*" investigation of cells using matrices and scaffolds (Ravi et al. 2015). The translation of findings made using 2D cell culture to *in vivo* behavior has proven somewhat challenging and 3D cultures can be used as a bridge between relatively easy-to-use, but inaccurate 2D *in vitro* culture systems and more difficult, but physiologically relevant *in vivo* models (Yamada & Cukierman 2007). Several scaffold-based 3D culture models exist, and they include prefabricated polymer scaffolds where cells attach and migrate within the pores of the scaffold, and biological scaffolds such as hydrogels that trap cells in an artificial ECM environment (Maltman & Przyborski 2010).

1.5 moDCs

The generation of DCs *in vitro* from monocytes harvested from peripheral blood, by using a combination of granulocyte-macrophage colony-stimulating factor (GM-CSF) and Interleukin (IL)-4 was first described in 1994 (Sallusto & Lanzavecchia 1994; Romani et al. 1994). This made it possible to study DCs *in vitro* and has laid the foundation of our present DC knowledge. Most clinical studies using DCs are based on monocyte-derived DCs (moDCs) (Barbuto 2013). Monocytes develop in the bone marrow from hematopoietic stem cells (HSCs) and circulate the blood constituting app. 10% of

total leukocytes in humans. (Italiani & Boraschi 2014). Circulating monocytes have previously been thought to give rise to macrophages and DCs (mononuclear phagocytes) in the tissue (van Furth et al. 1972; van Furth 1980), but the identification of the common DC progenitor (CDP) and pre-conventional DC (pre-cDC) app. 10 years ago (Naik et al. 2007; Naik et al. 2006; Diao et al. 2006), changed the theory of DC development and an updated version on macrophage/DC precursors is presented in Figure 5.

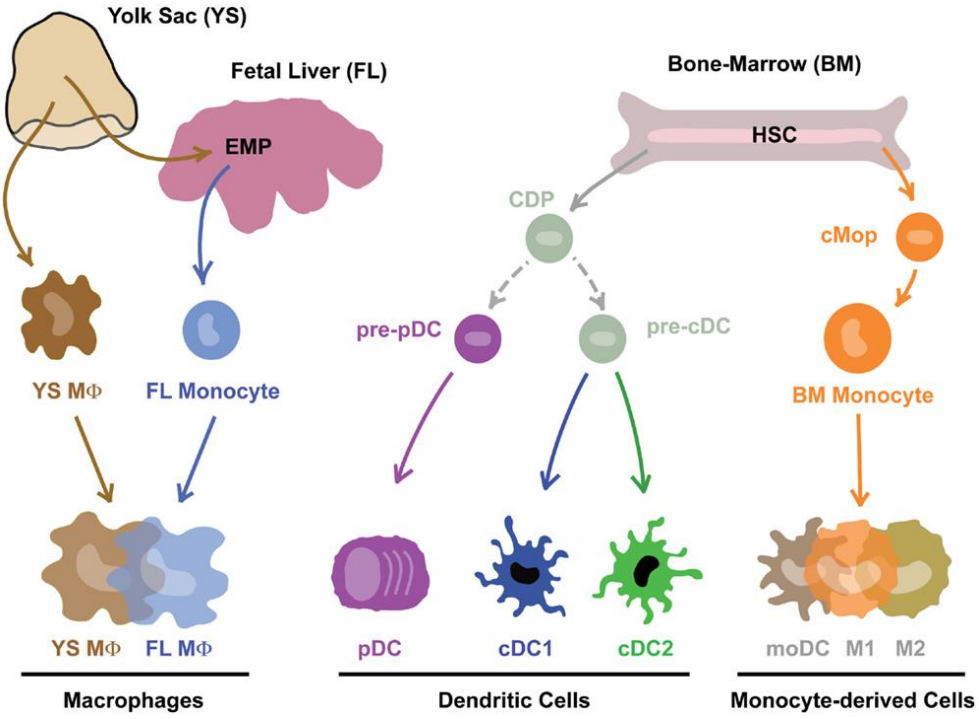

Figure 5: Overview of mononuclear phagocytes and their precursors. Mϕ, macrophage; EMP, embryonic precursor; HSC, hematopoietic stem cells; CDP, common DC progenitor; pDC, plasmacytoid DC; cDC, conventional DC; cMop, monocyte-committed common monocyte progenitor; M1, classically activated Mϕ; M2, alternatively activated Mϕ. From (Guilliams & van de Laar 2015).

Chapter 2 - General methods

In this chapter, methods used during the PhD studies are presented and the protocols described. However, some protocols are described in detail in paper I and II and are therefore not explained in detail in this section.

2.1 Animals

Blood from calves, pigs and goats was used for the experimental studies performed in this thesis. Bovine blood was used for testing and optimization of IGRA (study I and II). For studying the flow and capture of cells within the prototype chip, and for direct one-step blood qRT-PCR reaction optimization (study III), both bovine and goat whole blood was used for practical reasons and since the origin of the cells made no difference to the experiments. For the generation of moDCs (study IIII), porcine cells were chosen over ruminant cells since the research within porcine models for human diseases are expanding and because the DC biology in pigs and humans are similar, making the pig an obvious choice for this particular experiment. All animals were housed at the Veterinary Institute, Technical University of Denmark, except for a few calves (used for testing the effect of microtiter-plates from different suppliers, presented in paper I) housed at a collaborating farm (Freerslev Kotel, Gørløse, Denmark).

Most of the calves were enrolled in preexisting Paratuberculosis vaccine studies, and thus had acquired antigen specific immune responses against *Mycobacterium avium* subsp. *paratuberculosis* (MAP). The presence of an acquired immune response within the calves was exploited in this work. These animals were used to test the effect of culture conditions on specific CMI responses by means of IFN-γ release when restimulated with MAP antigens in the format of single antigen-peptide or crude extract. Polyclonal activation by superantigen stimulation was used with control animals, or animals with no acquired Paratuberculosis responses.

2.2 PBMC purification

Two protocols were applied for purification of PBMCs during the course of work presented in this thesis. The first protocol is described in paper I and II and included a 1:2 dilution of fresh stabilized

whole blood with phosphate buffered saline (PBS) as a first step. The diluted whole blood was then laid on Ficoll-Paque™ Plus (GE Healthcare) with room temperature (RT) in a 2:1 ratio (i.e. 8ml blood/PBS:4ml Ficoll-Paque™ Plus) followed by centrifugation at 2500 rpm (≈1400 x g) for 15 min at RT with low brake. In the second protocol, fresh stabilized whole blood was centrifuged at 2800 rpm (≈1700 x g) for 5 min at RT with low brake. Approximately 2ml of the cloudy middle layer (buffy coat) was harvested and laid on Ficoll-Paque™ Plus (1:2) and centrifuged as described for the first protocol. In both protocols, PBMCs were recovered using Pasteur pipettes and washed twice in RPMI 1640 medium with GlutaMAX™ (Gibco, Life Technologies™) containing 1% heat inactivated fetal calf serum (FCS) (Sigma). Cells were counted manually on a Olympus CH-2 microscope (Olympus Optical Co., Ltd.) using an Improved Neubauer, bright-line hemocytometer chamber (Assistent®) or using an automated cell counter (Nucleocounter® NC-200™, ChemoMetec), and diluted at appropriate concentrations in medium containing 10% FCS. The second protocol (with buffy coat isolation) was used for purifying PBMCs from young animals, since the PBMC fragment in these animals occasionally were difficult to separate from the bottom red blood cell layer.

2.3 Cell culture

For testing the effect of culture conditions on specific responses, whole blood or PBMCs from vaccinated or experimentally infected animals were used. For this purpose, cells were restimulated with either a MAP latency peptide antigen called MAP9436c (herein referred to as MAP antigen) or Johnin purified protein derivative (PPDj) which is a crude extract of undefined MAP antigens, often used for restimulation in IGRAs (Jungersen et al. 2002; Jungersen et al. 2012). SEB stimulation was used for the generation of CMI responses when no animals with specific MAP immune responses were available, or for comparison of specific vs. polyclonal activation. Concentrations of antigens used for stimulations (unless otherwise stated) was 1µg/ml MAP antigen, as well as 10µg/ml PPDj and 1 µg/ml SEB, concentrations that have previously been found to induce optimal responses (Jungersen et al. 2002). Individual culture times, plate formats- and cell concentrations used for the different culture setups, is described in the results sections of chapter 3-6. All 48 well-plates was from Cellstar®, Greiner Bio-One, and 96 well-plates were from Costar, Corning.

The 3D culture setup applied for testing 3D IGRA (presented in chapter 4) consisted of somewhat untraditional 3D scaffolds, including glass wool, small shavings made of polypropylene (PP), filter paper disks and 3D scaffolds made in polydimethylsiloxane (PDMS) polymer using the sugar cube method, as described in paper II (only the scaffold was made from solid sugar cubes and not sugar crystals as described in the paper). Two commercially available 3D scaffolds were tested; 3D polystyrene (PS) and 3D polycaprolactone (PCL) scaffolds. An overview of the different scaffolds and their specifications is listed in Table 1, and images of the scaffolds are presented in appendix 1. Prior to culture, 3D PS scaffolds were treated with 70% ethanol and washed twice in PBS to render the scaffolds hydrophilic.

Table 1: 3D scaffolds used for optimization of IGRA (presented in chapter 4)

Scaffold	Pore size	Source	Supplier
Glass wool	NA	VWR	Glaswarenfabrik Karl Hecht
PP shavings	NA	Prepared for the experiment	-
3D PDMS scaffold	Pore size 300-600µm	Prepared for the experiment[a]	-
3D PS scaffold	Pore size 40µm	Reinnervate	Amsbio
3D PCL scaffold	Pore size 300µm	3D Biotec	Sigma-Aldrich
Filter paper	Pore size 20-25µm	Whatman®	Sigma-Aldrich

[a]Prepared by Soumyaranjan Mohanty, DTU Nanotech, Technical University of Denmark. NA, Not applicable; PP, polypropylene; PDMS, polydimethylsiloxane; PS, polystyrene; PCL, polycaprolactone.

In order to improve cell attachment and migration within the 3D cultures, different types of protein coatings were tested. The first one was MaxGel™ ECM (Sigma), which is a basement membrane extract of human ECM components including collagens, laminin, fibronectin, tenascin, elastin, proteoglycans and glycosaminoglycans. Culture-wells/scaffolds were coated with MaxGel in a 100x dilution for 30 min at 37°C, 5% CO_2 and washed prior to culture. The second ECM mix was Matrigel™ (BD Biosciences), an ECM-based hydrogel extracted from mouse tumor cells rich in laminin, collagen

IV, heparin sulfate proteoglycans, entactin/nidogen including several growth factors. Culture wells/scaffolds were coated with Matrigel in a 2-20x dilution and incubated for app. 1 hour at room temperature (RT) and washed prior to culture. The last protein coating that was tested was recombinant human CCL21 (BioLegend®), a chemokine that is highly expressed in lymph nodes. Culture wells were coated with CCL21 at 0.01µg/well (Figure 13) or 0.02µg/well (Figure 14) and air dried prior to cell culture.

2.4 Flow cytometry

Flow cytometry was used to identify the ratio of cell subpopulations present before and after PBMC purifications (Chapter 3, paper I) and to characterize monocytes before and after culture with differentiating cytokines (Chapter 6, paper II). This was done by staining cells for surface markers using specific antibodies either directly conjugated to a fluorochrome or by the addition of fluorochrome-conjugated secondary antibodies. Different fluorochromes emit light when hit by lasers of particular wavelengths. Stained cells in suspension are led through different lasers one by one and when hit by the laser light, one detector measures the forward scatter (FSC) which is a measure of cell size, and another detector measures the side scatter (SSC) which is the granularity of the cells. Thus, data generated for each cell includes: cell size, granularity and fluorescent labelling. A detailed description on staining protocols is presented in paper I and II. All flow cytometry analysis were performed on a BD FACSCanto™II flow cytometer (BD Biosciences) and the results were analyzed using the BD FACSDiva software version 8.0.1.

2.5 IFN-γ specific ELISA

An in house-developed IFN-γ specific sandwich enzyme-linked immunosorbent assay (sandwich-ELISA) was used to detect and quantify IFN-γ levels in supernatant/plasma harvested from PBMC or whole blood cultures. The protocol is described in detail in paper I and it was slightly modified from the protocol described in (Mikkelsen et al. 2009). In this assay, a monoclonal capture antibody specific against the IFN-γ $F(ab)_2$ fragment was coated in the wells of a micro-well plate. The supernatant/plasma containing IFN-γ to be measured was added and as a following step, a biotinylated anti-IFN-γ monoclonal antibody was added. Finally, enzyme-linked streptavidin was

added and the enzyme was converted to a detectable signal by addition of substrate. Quantity of IFN-γ was measured as optical density (OD) and was calculated using linear regression on log transformed OD values from dilution series of a reference SEB-stimulated plasma standard with known IFN-γ concentrations included on each plate. All samples/standards were added in duplicate, including a blank control.

2.6 Total RNA purification

The RNeasy Mini Kit (Qiagen) was used to purify total RNA from cultured moDCs (chapter 6, study IIII) and purification was performed according to manufacturer's instructions. Briefly, cell lysates were homogenized using a QIAshredder spin column and ethanol was added to bind total RNA to the RNeasy spin column. After a DNase treatment and a following washing step, total RNA could be eluted and stored for cDNA synthesis.

The QIAamp RNA Blood Mini Kit (Qiagen) was used to purify total RNA from 3D-cultured whole blood and PBMCs (chapter 4, study II) and purification was performed according to manufacturer's instructions. Briefly, the steps included lysing of erythrocytes followed by homogenization of cell lysates using the QIAshredder spin column. Ethanol was then added to bind total RNA to the QIAamp membrane and after three washes, total RNA could be eluted and stored for cDNA synthesis.

2.7 cDNA synthesis

QuantiTect® reverse Transcription Kit (Qiagen) was used to reverse transcribe 180-200ng total RNA according to the manufacturer's instructions. Briefly, 2µl gDNA Wipeout Buffer(7X) and various volumes of total RNA and RNase-free water to a total volume of 14ml was mixed in a tube and incubated in a Thermocycler (Qiagen) for 2 min at 42°C. A Mastermix was prepared containing 1µl Reverse Transcriptase (RT), 1µl RT Primer mix and 4µl RT Buffer, and the mix was added to the tube with RNA. Tubes were then incubated in the Thermocycler for 15 min at 42°C allowing the reverse transcription to take place, followed by 3 min at 95°C in order to inactivate the reverse transcriptase. cDNA was stored until qRT-PCR analysis.

2.8 qRT-PCR

Two platforms for detection of specific cDNA were used for the studies performed during the PhD. For detection of *IFNG* (IFN-γ) and *CXCL10* (IP10) in 3D cultures (chapter 4, study II) and for testing the direct one-step blood qRT-PCR reaction (chapter 5, study III), the Rotor-Gene Q (Qiagen) qPCR platform (Corbett research) with Rotor-Gene 4.4.1 software was applied. This platform is convenient when testing the expression of a few genes. Testing the gene expression in moDCs (chapter 6 study IIII) was done in a 96.96 Dynamic Array Integrated Fluidic Circuits (IFC) (Fluidigm) chip, placed in a BioMark real time PCR instrument (Fluidigm) and analysis was done using the Fluidigm Real Time PCR Analysis software 3.0.2 (Fluidigm). This high-throughput BioMark platform is ideal when analyzing multiple genes and samples simultaneously. The protocol used for the BioMark platform, is described in detail in paper II.

For the analysis of *IFNG* and *CXCL10* gene expression in cells from 3D cultures using the Rotor-Gene Q qPCR platform, 24µl reaction mix consisting of 12.5µl 2XMastermix (SYBR Green Jumpstart Taq Readymix without $MgCL_2$, Sigma), 3µl primer mix (5µM of each primer), 3µl $MgCl_2$ and 5.5µl MiliQ water was added in each PCR tube. Then 1µl of cDNA, pre-diluted 10x in miliQ water was added. A non-template control (NTC) was included for each primer pair to test for non-specific amplification. Tubes were placed in the Rotor-Gene Q instrument and the following cycle conditions were applied: 2 min at 50°C and 10 min at 95°C followed by 40 cycles with denaturation for 15 sec at 95° and annealing/elongation for 1 min at 60°C. Melting curves were generated after each run to confirm a single PCR product (from 50°C to 95°C, increasing 1°C/5 sec).

For testing the direct one-step blood qRT-PCR SYBR Green Kit (VitaNavi Technology), stabilized whole blood from bovine or goat was directly added to the reaction mix containing 16µl Blood qRT-PCR mix, 0.75µl Blood qRT-PCR polymerase mix, 0.5µl SYBR Green, 2.5µl primer mix (5µM of each primer) and MiliQ to a final volume of 25µl. Blood concentrations of 2-10% was tested. A non-template control (NTC) was included for each primer pair to test for non-specific amplification. For the detection of *IFNG* and *CXCL10,* blood was pre-incubated with 1µg/ml SEB for two hours prior to qRT-PCR analysis. Tubes were placed in the Rotor-Gene Q instrument and the following cycle

conditions were applied: 58°C for 30 min (reverse transcriptase step), 95°C for 5 min (initial denaturation step), followed by 45 cycles of 94°C for 45 sec (denaturation step) and 63°C (or 60°C) for 90 sec (annealing/extension). A final melting curve analysis was performed to verify a single product, with the temperature rising from 50°C to 99°C, increasing 1°C/5 sec. See appendix 2 for a list of primers used for experiments analyzed on the Rotor-Gene Q qPCR platform.

2.9 Confocal microscopy

For visualization of cells within 3D PS scaffolds or in the prototype chip, bovine PBMCs were purified as described in section 2.2, and cells were stained with Alexa Flour 647 (AF647)-conjugated anti-bovine CD4 monoclonal IgG2a antibody (clone CC8, AbD Serotec) and AF488-conjugated anti-human CD14 IgG2a antibody (cross-reactive to bovine) (clone M5E2, BioLegend®). $1x10^6$ cells in 100 µl were stained with a cocktail of both antibodies in a 40x dilution, washed and resuspended in RPMI medium. 3D PS scaffolds (Alvetex®) were made hydrophilic by addition of 70% ethanol and washed in PBS prior to cell plating/imaging. Scaffolds and cells were imaged on a Zeiss LSM 710 confocal microscope using ZEN 2009 software. The microscope was inverted and equipped with an incubator for temperature control and imaging was performed at 37°C. Prior to plating on the scaffold, cells were mixed with SEB to a final concentration of 1µg/ml. Scaffolds, or scaffolds with SEB-stimulated cells, were placed between two glass microscope slides and imaged. Z-stacks were recorded with (in average) 25 stacks with 10 slices in each, and with app. 20 seconds in between stacks. Maximum projection images were created to show the structure of the autofluorescent scaffold. Movies intending to show cell migration in 2D and 3D surfaces was created using ImageJ/Fiji software.

2.10 Light microscopy

To visualize cell capture on the prototype chip during flow, PBMCs were purified from goat whole blood, and heated to 37°C in an incubator. Using a sp260p syringe pump (WPI, Florida, USA) with a 20ml Luer syringe (Omnifix), elbow Luer connector and silicone tubing (Ibidi GmbH, Germany), cell flow and capture was imaged on an inverted Leica DMIL contrasting microscope equipped with a Leica DFC290 camera (Leica Microsystems).

Chapter 3 - Study I (IGRA)

3.1 Introduction

In vitro cultures of freshly isolated primary cells are being used for cytokine release assays. IGRA is an assay testing the presence of a T_H1-mediated CMI-response by detection of de novo produced IFN-γ by the cultured cells upon antigen recall. In veterinary medicine, IGRA was first used to diagnose infections of bovine tuberculosis and paratuberculosis (Wood et al. 1990; Rothel et al. 1992; Billman-Jacobe et al. 1992). For this type of assay, either whole blood or purified PBMCs are typically used. Cultures of PBMCs consist of a mix of lymphocytes (T lymphocytes, B lymphocytes and NK cells), monocytes and dendritic cells, kept in synthetic media typically with a supplement of bovine serum containing growth factors necessary for cell survival. Apart from the mentioned cell types, whole blood also contains erythrocytes, platelets, and granulocytes (neutrophils, basophils and eosinophils). Several cell types produce IFN-γ, including $CD4^+$ T cells, $CD8^+$ T cells, γδ T cells and NK cells. However, upon antigen recall the major secretion of IFN-γ is believed to come from T_H1 $CD4^+$ T cells.

3.2 Hypothesis

Due to the presence of natural occurring activating and suppressive mediators such as cytokines, hormones and growth factors *in vivo*, it is hypothesized that the activation profile of cells activated in settings close to their natural environment (i.e. whole blood) will differ from the activation profile of cells purified and kept in synthetic media with serum supplement (i.e. PBMCs).

3.3 Results

Paper I

Revisiting the IFN-γ release assay: Whole blood or PBMC cultures? - And other factors of influence

Sofie Bruun Hartmann[a], Jenny Emnéus[b], Anders Wolff[b] and Gregers Jungersen[a]#

[a]National Veterinary Institute, Technical University of Denmark, Frederiksberg C, Denmark

[b]Department of Micro- and Nanotechnology, Technical University of Denmark, Kgs. Lyngby, Denmark

#Corresponding author

Manuscript ready for submission

In this study we investigate factors of influence for the validity of interferon-gamma release assays performed with whole blood or peripheral blood mononuclear cells (PBMC) cultures. We find large differences in the optimal diagnostic conditions with each individual animal and that PBMC cultures are amenable to differences in cellular composition compared to whole blood. Finally, we were able to show effect of culture plates from different suppliers, although this effect was not statistically significant. We believe these studies highlight the need to include detailed descriptions of procedures and warrant that different conditions infer different results in the same animal.

Abstract

The interferon-gamma release assay is a widely used test for the presence of a cell-mediated immune response *in vitro*. Factors potentially influencing the results when performing interferon-gamma release assays in cultures of bovine whole blood and PBMCs, were investigated. It was found that optimal culture conditions varied between individual animals; when polyclonal activated, cells from whole blood cultures were most responsive, but when activated specifically half of the animals had highest responses in whole blood cultures and half of them had highest responses in PBMC cultures. A further investigation of the distribution of cell populations in PBMCs compared to whole blood was conducted, and a significant ($p<0.001$) decrease in the percentage of $CD3^+$ T cells within the PBMCs was found. More specifically, this reduction was due to a significant ($p<0.01$) decrease in the percentage of $\gamma\delta^+$ T cells. Thus measuring immune responses on purified PBMCs might not give a physiologically relevant output. Additionally, it was tested if the choice of incubation plate would interfere with the level of secreted interferon-gamma in whole blood cultures. There was no significant difference in the interferon-gamma levels from the six incubation plates tested, but it was observed that six of eight calves had optimal interferon-gamma production in a flat bottom polystyrene plate from Corning®. Altogether these findings highlight the potential weaknesses of the interferon-gamma release assay in terms of the many variables that can influence the results, and stresses the importance of documenting the precise assay conditions when publishing results of *in vitro* interferon-gamma release assays.

1. Introduction

Cytokines are small signaling proteins produced by various cell types including cells of the immune system. Since specific cytokines are associated with different types of cell-mediated immune (CMI) responses, they can be used to characterize such responses. For example IFN-γ, IL-2, -12, -18, TNF-α, GM-CSF, are all associated with a T helper (T_H) 1 response, IL-4, -5, -6, -10, -13, and TGF-β with a T_H2 response, IL-17, -21, -22 with T_H17, and IL-10 and TGF-β with a T regulatory (Treg) response (1).

Cytokines usually act in a paracrine or autocrine manner, thus being produced and taken up at local sites where immune reactions take place. Therefore, most cytokine levels are too low for direct detection in peripheral blood. Instead CMI can be analyzed *in vitro* by measuring the function of T cells in terms of their ability to proliferate and to produce cytokines in response to antigen. The IFN-γ release assay (IGRA) is based on the detection of *de novo* produced IFN-γ by cultured immune cells including T_H1 cells. This is used to measure the efficacy of a vaccine or as a diagnostic measure to test if a subject is suffering from a specific intracellular pathogen, for example *Mycobacterium bovis* or *M. avian* subsp. *paratuberculosis* (MAP) in cattle or *Mycobacterium tuberculosis* in humans. In the latter case two FDA approved IGRAs exists (QuantiFERON-TB Gold in-Tube, Cellestis, Austria and T-Spot.TB, Oxford Immunotec, UK). IGRAs (and cytokine release assays in general) can be performed using cultures of whole blood or purified peripheral blood mononuclear cells (PBMCs). In the present study, an investigation and discussion of the different factors potentially influencing the results when testing CMI *in vitro* by means of IFN-γ secretion in cultures of whole blood or PBMCs is presented.

2. Materials and methods

2.1. Animals

For the purpose of this study, blood was drawn using heparinized vacutainer tubes from sixteen Danish Jersey calves (#1-16) aged 16-22 weeks. The calves were enrolled in three preexisting Paratuberculosis vaccine programs, and thus had obtained different levels of antigen-specific immunity against a MAP peptide-antigen. The different vaccination regimes used were irrelevant for the present study since immunological responses were merely used to test if assay conditions/cell concentrations had an influence on the specific responses within each individual animal. The calves were housed at the animal facility at the Veterinary Institute, Technical University of Denmark, or at a collaborating farm and were, apart from the vaccinations, handled the same way. Not all calves were used for all experiments and the numbering of the calves used for the individual experiments appears on the figures/tables. All animals were handled in accordance with the Danish animal experiments

legislation and registered in studies approved by the Danish Animal Experiments Inspectorate, license number 2012-15-2934-00269.

2.2. Isolation of PBMCs

Fresh, heparinized whole blood was diluted 1:2 with PBS, laid on Ficoll-Paque™Plus (GE Healthcare) and centrifuged 2500 rpm (≈1400 x g) for 15 min at room temperature (RT) with low brake. PBMCs were recovered and washed twice in RPMI 1640 medium with GlutaMAX™ (Gibco, Life Technologies™) containing 1% heat inactivated fetal bovine serum (FCS) (Sigma). Cells were counted using Improved Neubauer, bright-line hemocytometer chamber (Assistent®) and diluted at different concentrations in medium containing 10% FCS.

2.3. Stimulation and incubation of whole blood and PBMCs for comparison of IFN-γ-release

Fresh stabilized whole blood was drawn from eight vaccinated calves (#1-8) aged 16-22 weeks. Samples were split in two; one half was used for PBMC purification (see above), the other half was used for whole blood cultures. Non-diluted whole blood and whole blood diluted 1:2 with PBS was plated in triplicates of 500µl in 48-well plates (Cellstar®, Greiner Bio-One). Prior to cell-plating, 50µl of either PBS, the superantigen Staphylococcal enterotoxin B (SEB) (Sigma), or vaccine MAP antigen (Statens Serum Institute) plus co-stimulatory antibodies anti-CD28 and anti-CD49d (clone TE1A and FW3-218, respectively, Monoclonal Antibody Center, Washington State University) (2), all at a final concentration of 1µg/ml, was added to the wells. Cultures were incubated for 20 hours at 37°C, 5% CO_2. PBMCs were purified from the other half using density gradient centrifugation, and cells were diluted in media with 10% FCS to obtain final concentrations of 10, 5, 2.5, 1.25 and $0.625x10^6$ cells/ml. PBMCs were stimulated and incubated the same way as whole blood samples. Plates were centrifuged and approximately 350µl supernatant/plasma was harvested and stored at -20°C until further analysis. The quantity of IFN-γ in the plasma and supernatant was measured by ELISA

2.4. Stimulation and incubation of whole blood for testing the effect of micro-well plates

Fresh, heparinized whole blood from eight calves (#9-16) aged 18-22 weeks, was plated in double triplicates of 200µl in the following six different 96-well plates: a) Nunc™, clear, flat-bottom, Nunclon™ Delta surface, polystyrene, cat# 167008; b) Corning®, clear, flat-bottom, tissue culture treated, polystyrene, cat# 3596; c) BD Falcon® Optilux, black, clear flat-bottom, tissue culture surface, polystyrene, cat# 353948; d) Corning®, clear, flat-bottom, tissue culture treated, polystyrene, low evaporation lid, cat# 3595; e) Corning®, clear, round-bottom, tissue culture treated, polystyrene, cat# 3799 and f) Cellstar® Greiner bio-one, clear, round bottom, tissue culture treated, polystyrene, cat# 650108. Prior to cell-plating, 20µl of PBS, SEB or vaccine MAP antigen (both at a final concentration of 1µg/ml) was added to the wells. Cultures were incubated for 20 hours at 37°C, 5% CO_2. Plates were centrifuged following the addition of 55µl heparin solution (at a final concentration of 10 IU/ml) to avoid clotting when freezing. Approximately 140µl plasma was harvested from each well and double triplicates were pooled resulting in 280µl plasma in triplicates from each calf and stimulus. Plasma was stored at -20°C until further analysis.

2.5. Measurement of IFN-γ production by ELISA

The IFN-γ-secretion in plasma and supernatant was determined using an in-house developed monoclonal sandwich ELISA, as described elsewhere (3), with a few modifications. Briefly, MaxiSorp™ microtiter plates (Nunc) were coated overnight with 100µl anti-bovine IFN-γ $F(ab)_2$ monoclonal antibody (clone 6.19) (National Veterinary Institute, Technical University of Denmark) at 0.49µg/ml. After a one-hour blocking with 200 µl blocking buffer (PBS, 0.05% Tween 20, 0.1% Casein) followed by 5 washes with washing buffer (PBS, 0.05% Tween 20), 50µl blocking buffer and 50µl thawed supernatant/plasma was added to the wells in duplicate. A two/three-fold standard dilution series prepared from calf plasma stimulated with 0.2µg/ml SEB and with previously determined concentrations of IFN-γ was also added in duplicate to each plate in order to generate a standard curve used for quantification of IFN-γ levels after log-log transformation. The plates were incubated for 1 hour at room temperature with gentle agitation followed by 5 washes. 100µl biotinylated secondary anti-bovine IFN-γ monoclonal antibody (clone 6.22) (National Veterinary Institute,

Technical University of Denmark) was added in final concentrations of 0.95µg/ml and 0.087µg/ml (different batches for the ELISA used in the experiment comparing PBMC and whole blood cultures (figure 1) and for the experiment testing different microwell plates (figure 3)) and incubated for 1 hour at room temperature with gentle agitation followed by 5 washes. Next, 100µl streptavidin-horseradish peroxidase conjugate (Invitrogen) was added at a final concentration of 0.125µg/ml and incubated for 1 hour at room temperature with gentle agitation followed by 5 washes. Finally, 100µl TMB-Plus ready-to-use substrate (Kem-En-Tec Diagnostics) was added and the plates were incubated at room temperature in the dark for app. 10-20 minutes. The enzyme reaction was stopped by adding 100µl 0.5 M H_2SO_4 and the optical density (OD) measured at 450 nm with 650 nm as a reference using a Multiscan® EX reader (Thermo Scientific). The level of IFN-γ (pg/ml) was calculated by inserting the log-transformed OD values in the equation obtained from linear regression of the log-transformed OD values from the dilution series of a reference SEB stimulated plasma standard with known IFN-γ concentrations.

2.6. Flow cytometry

For determination of the cell distribution before and after PBMC purification, cells were stained and analyzed by flow cytometry. Tubes containing 100µl whole blood or PBMC ($1x10^7$cells/ml) were incubated with 20µl primary antibodies in the four cocktails as summarized in Table 1 for 30 minutes in the dark at 5°C. One ml 1X BD FACS lysis solution was added to the whole blood tubes which were incubated for ten minutes at room temperature in order to lyse the red blood cells. All cells were washed in wash buffer (PBS, 0.1% sodium azide, 1% FCS) and incubated with a 20µl secondary antibody cocktail (see Table 1) for 30 minutes in the dark at 5°C. Cells were washed twice in wash buffer and resuspended in FACS sheath fluid containing 0.5% paraformaldehyde. For compensation adjustments, pooled lysed whole blood cells were stained with primary staining cocktail 1 plus either anti-mouse IgG1-PE or anti-mouse IgG2a-AF647 (Table 1). Cells were acquired on a BD FACSCanto™II flow cytometer (BD Biosciences) with a lymphocyte gate based on FSC SSC profile and the results were analyzed using the BD FACSDiva software version 8.0.1.

2.7. Statistics

When analyzing the level of IFN-γ production, one way analysis of variance in combination with Bonferroni´s Multiple Comparison test was used. Two-way analysis of variance and Bonferroni´s posttest was used when analyzing the cell distribution in whole blood compared to PBMCs.. All statistical analyses were done using GraphPad Prism version 5.02.

Table 1: Staining overview

	Primary staining			**Secondary staining**		
Cocktail	**Monoclonal Abs**[a]	**Isotype**	**Clone (Company)**	**Secondary Abs**[c]	**Fluoro-chrome**	**Company**
1	Anti-bovine CD3 Anti-bovine CD4	IgG1 IgG2a	MM1A (VMRD) IL-A11 (VMRD)	Anti-IgG1 Anti-IgG2a	PE AF647	Southern Biotechn. Invitrogen
2	Anti-bovine CD3 Anti-bovine CD8	IgG1 IgG2a	MM1A (VMRD) CC63 (AbD Serotec)	Anti-IgG1 Anti-IgG2a	PE AF647	Southern Biotechn. Invitrogen
3	Anti-bovine CD3 Anti-bovine WC1	IgG1 IgG2a	MM1A (VMRD) CC15 (AbD Serotec)	Anti-IgG1 Anti-IgG2a	PE AF647	Southern Biotechn. Invitrogen
4	Anti-bovine NKp46 Anti-human CD14	IgG1 IgG2a	AKS1[b] Tük4 (DAKO)	Anti-IgG1 Anti-IgG2a	PE AF647	Southern Biotechn. Invitrogen
For compensation (pool of lysed whole blood cells)						
A	Anti-bovine CD3 Anti-bovine CD4	IgG1 IgG2a	MM1A (VMRD) IL-A11 (VMRD)	Anti-IgG1	PE	Southern Biotechn.
B	Anti-bovine CD3 Anti-bovine CD4	IgG1 IgG2a	MM1A (VMRD) IL-A11 (VMRD)	Anti-IgG2a	AF647	Invitrogen

[a]All antibodies were generated in mouse and directed against bovine (except for CD14 which is directed against human but is cross-reactive against bovine. [b] A kind gift from Anne K Storset, Norway. [c]Both antibodies were generated in goats and directed against mouse. PE, phycoerythrin; AF647, Alexa Fluor® 647

3. Results

3.1. Culture conditions for optimal IFN-γ production varies from individual to individual

Using ELISA, quantity of IFN-γ was measured from overnight cultures of whole blood, diluted whole blood or PBMCs at various cell concentrations (i.e. 10, 5, 2.5, 1.25, and $0.623x10^6$ cells/ml) from eight calves (#1-8). Cells were incubated with MAP antigen+ co-stimulation, SEB or PBS (background).. In the MAP antigen-stimulated samples (Ag-specific activation) four of eight tested calves had highest IFN-γ production in non-diluted whole blood (calf # 2, 4, 5 and 7), two in PBMC cultures with $10x10^6$ cells/ml (calf # 1 and 6) and finally two calves had highest production in PBMC cultures with $5x10^6$ cells/ml (calf # 3 and 8) (figure 1 A). Some of the calves had very low IFN-γ levels in all incubation settings but they did show high levels when stimulated with SEB (polyclonal non-specific activation). In this case, six of eight calves had highest IFN-γ levels in non-diluted whole blood (calf # 1, 2, 3, 4, 5 and 7), one in the diluted whole blood culture (calf # 6), and one had highest level in PBMC cultures with $10x10^6$ cells/ml (calf # 8) (figure 1 B). In general, the background concentration of IFN-γ was low but there was a tendency of higher levels in whole blood cultures compared to PBMC cultures (figure 1 C).

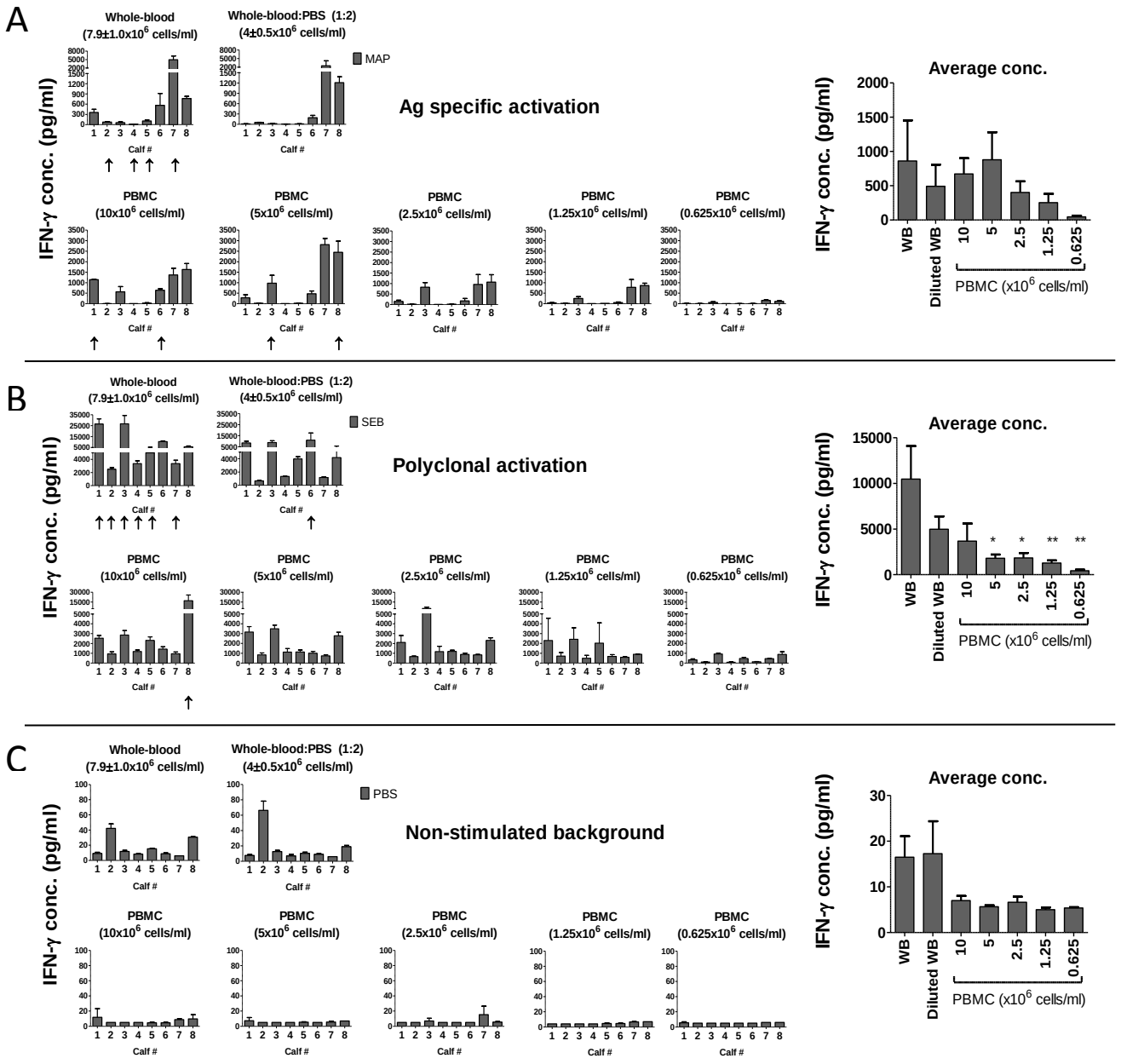

Figure 1) Mode of activation and type of cell culture population influences the IFN-γ release

Stabilized fresh whole blood, diluted whole blood and titrations of purified PBMCs from eight vaccinated calves (#1-8) were stimulated with MAP antigen + co-stimulation (A), SEB (B) or PBS as a negative control (C) and incubated 20 hours at 37°C and 5% CO_2. Plasma and supernatant was analyzed for IFN-γ levels by ELISA. Left graphs: shows the mean + SD of three technical replicates from each calf. Arrows indicate individual IFN-γ level optima. Right graphs: shows the mean + SEM of all eight calves. A statistical difference in IFN-γ levels was observed for whole blood (WB) cultures compared to PBMC cultures with concentrations equal to or less than $5x10^6$ cells/ml in polyclonal activated cultures. Statistics: One way ANOVA and Bonferroni's Multiple Comparison test (n=8), ** = $p<0.01$, * = $p<0.05$.

3.2. Selective cell loss of γδ-T cells during PBMC purification

In order to investigate if isolation of PBMCs by density gradient centrifugation had an influence on cell distribution, unstimulated whole blood and PBMCs from seven calves (same animals as above, only samples from one animal (#4) was discarded due to technical errors) were stained for selected surface markers and analyzed by flow cytometry (figure 2). A significant decrease in the percentage of $CD3^+$ T cells was observed within the mononuclear leukocyte population from PBMCs compared to whole blood (from 64.5% to 55.3%). No difference in the distribution of NK cells and monocytes was detected. Since the cells were gated on the mononuclear leukocytes the granulocytes present in whole blood samples did not influence the relative levels. Further gating on the $CD3^+$ T cells showed a significant loss of $\gamma\delta^+$ T cells in the PBMCs (from 28.8% to 22.9%) while no significant difference was seen for the $CD4^+$ - and $CD8^+$ T cells.

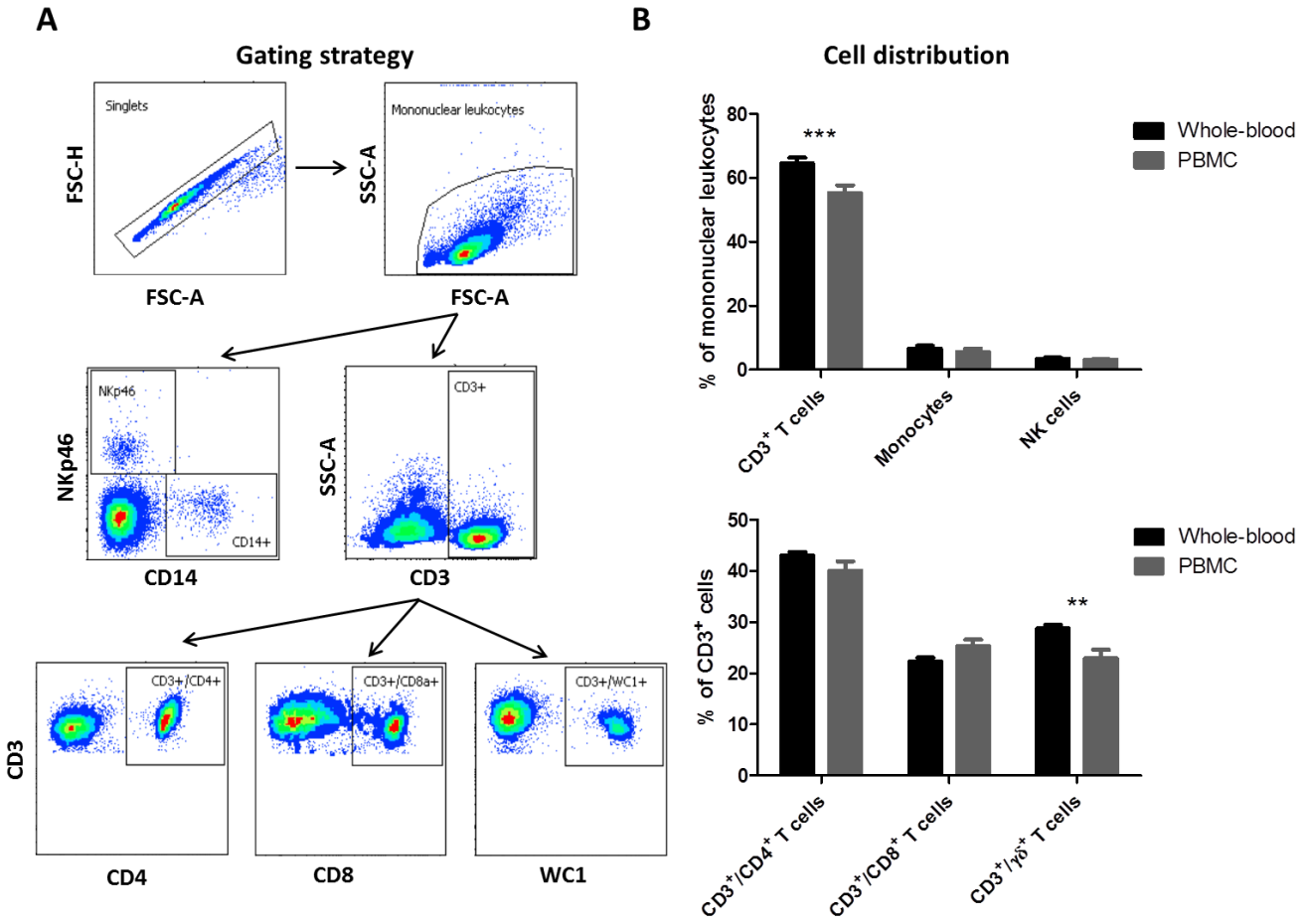

Figure 2) Selective loss of γδ T cells after PBMC purification

Stabilized fresh whole blood and purified PBMCs from seven calves (#1, 2, 3, 5, 6, 7, and 8) were stained for surface markers and analyzed by flow cytometry in parallel. A) Gating strategy. $Nkp46^+$ = NK cells, $CD14^+$ = monocytes, $CD3^+/CD4^+$ = $CD4^+$ T cells, $CD3^+/CD8^+$ = $CD8^+$ T cells, $CD3^+/WC1^+$ = γδ T cells. B) Bar graph showing the distribution of cell subpopulations within whole blood and PBMCs. Top graph: percent of total mononuclear leukocytes, bottom graph: percent of total $CD3^+$ cells. Statistics: Two way ANOVA and Bonferroni posttest (n=7), *** = $p<0.001$, ** = $p<0.01$.

3.3. No significant effect of incubation plate on whole blood IGRA performance

When cells are incubated for *in vitro* stimulation assays, it is typically done in micro-well plates. These are commercially available from several companies and are often tissue culture treated for optimal cell performance. It could be speculated if choice of incubation plate would influence the levels of IFN-γ since the surface-treatment and shape of the micro wells differ between brands. To clarify this, a whole blood stimulation assay using stabilized blood from eight vaccinated 18-22 weeks old calves (#9-16) was conducted in 6 different culture plates. Two of the animals (#12 and 15) belonged to a

non-vaccinated control group, but were included in order to cover all ranges of activation. Stimulation was done with MAP antigen, SEB or PBS (background) and after 20 hours of incubation at 37°C, 5% CO_2 plasma was harvested and used for IFN-γ quantification by ELISA. No significant difference was found between the six plates tested when looking at IFN-γ levels after both polyclonal and Ag-specific activation (figure 3). However, 5 out of 6 animals had their highest IFN-γ concentrations following Ag-specific activation when incubated on plate b, and the relative-to-maximum concentration showed that plate b had significantly higher relative concentration compared to plate a and e (Table 2).

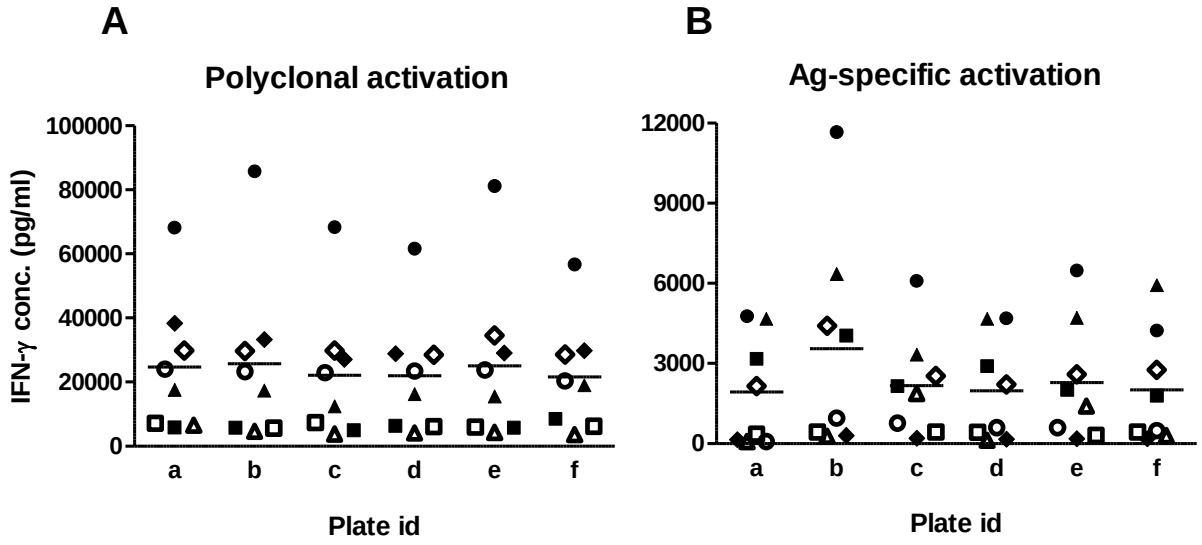

Figure 3) Effect of incubation plate on level of IFN-γ production

Stabilized whole blood from eight calves (#9-16) was stimulated with SEB (1µg/ml) or MAP antigen (1µg/ml) for 20 hours at 37°C and 5% CO_2 in six different 96 well-microtiter plates. Plasma was harvested and analyzed for IFN-γ by ELISA. The plates tested were: a) Nunc™, clear, flat-bottom, Nunclon™ Delta surface, polystyrene, cat# 167008; b) Corning®, clear, flat-bottom, tissue culture treated, polystyrene, cat# 3596: c) BD Falcon® Optilux, black, clear flat-bottom, tissue culture surface, polystyrene, cat# 353948: d) Corning®, clear, flat-bottom, tissue culture treated, polystyrene, cat# 3595; e) Corning®, clear, round-bottom, tissue culture treated, polystyrene, cat# 3799 and f) Cellstar® Greiner bio-one, clear, round bottom, tissue culture treated, polystyrene, cat# 650108. Shown is the IFN-γ concentration (pg/ml) of SEB-stimulated whole blood (polyclonal activation) and MAP antigen-stimulated whole blood (Ag-specific activation). Background levels of IFN-γ (PBS) have been subtracted and each value represents the mean of three technical replicates.

Table 2: Relative-to-maximum IFN-γ concentration (%)

	Polyclonal activation						Ag-specific activation					
Animal #	**a**	**b**	**c**	**d**	**e**	**f**	**a**	**b**[a]	**c**	**d**	**e**	**f**
9	80	**100**	80	72	95	66	41	**100**	52	40	56	36
10	69	69	58	75	68	**100**	79	**100**	53	72	50	44
11	92	91	65	85	82	**100**	74	**100**	52	74	74	93
12	**100**	87	71	75	76	78	51	**100**	66	52	62	62
13	**100**	97	95	97	99	85	8	**100**	80	62	63	50
14	97	76	**100**	83	81	84	81	99	98	98	68	**100**
15	**100**	70	58	63	65	56	4	15	**100**	7	75	16
16	86	86	87	83	**100**	83	49	**100**	57	50	59	63
Average	90	84	77	79	83	81	48	77	70	57	63	58

Relative IFN-γ concentration within each calf (#9-16) on the different incubation plates (a-f). Highest concentration is set to 100%. [a] The average relative concentration on plate b is significant compared to plate a ($p>0.05$). Statistics = One way ANOVA and Bonferroni's Multiple Comparison test

4. Discussion

In vitro measurement of CMI responses is an important tool for vaccine evaluation and disease detection. When performing this type of assay, one question is whether to use whole blood- or PBMC cultures for the basis of CMI response detection. This study compares IFN-γ levels upon antigen recall (i.e. Ag-specific activation), superantigen stimulation (i.e. polyclonal non-specific activation) and background levels in cultures of both whole blood and PBMCs (figure 1). The optimal culture conditions varied between animals; when activated specifically via recall MAP antigen, half of the animals showed highest IFN-γ production in whole blood cultures with an average cell concentration of $7.9x10^6$ cells/ml, and half of them had optimal conditions in PBMC cultures with the two highest cell concentrations (i.e. 10- and $5x10^6$ cells/ml). When averaging the response from the eight calves, $5x10^6$cells/ml seemed to be the optimal PBMC concentration with a response similar to the non-diluted whole blood samples. The individual cell concentration-, and maybe more important, the individual cell population optima (i.e. whole blood or PBMC), makes it difficult to choose the best assay conditions. Calf # 3 is a disturbing example of an animal that only shows high IFN-γ levels in the PBMC but not in whole blood cultures during Ag-specific activation.

In the polyclonal activated cultures, numerous $CD4^+$ T cells are able to become activated since SEB, as a superantigen, non-specifically cross-binds the variable part of the β-chain (Vβ) of the T cell receptor and the MHC class II on the antigen presenting cell, resulting in activation and cytokine release, especially IFN-γ (4, 5). Thus, higher cell concentration theoretically equals higher IFN-γ release. In the present study the highest response was seen in the whole blood cultures, with the exception of one calf which had optimum IFN-γ levels in the PBMC $10x10^6$ cells/ml culture. On average the PBMC did not have an optimal concentration comparable to whole blood samples as was the case with the Ag-specific activation. Following the polyclonal activation, the whole blood assay resulted in more than twice the amount of IFN-γ compared to the optimal PBMC assay (with $10x10^6$ cells/ml). This indicates that factors other than the total cell number influence the IFN-γ production. This could be due to granulocytes and platelets present in whole blood cultures but absent in PBMC cultures, and studies have shown that both granulocytes and platelets are able to produce cytokines (6–8). Other factors possibly present in the autologous plasma of the whole blood cultures include cytokines, soluble cytokine receptors and antagonists and growth factors – elements that potentially are important regulators of cell viability (9). In a study of apoptosis, Hodge and colleagues found a greater level of leukocyte apoptosis in human PBMC cultures compared to whole blood cultures following stimulation (9). Maybe not surprisingly they observed a decreased percentage of IFN-γ-producing T cells in the Annexin V-positive apoptotic cells population compared to the viable population. Thus, if the PBMCs have an increased tendency to become apoptotic during culture, this may explain the lower levels of IFN-γ in cultures of PBMC compared to whole blood cultures seen in the polyclonal non-specific activation assays.

This phenomenon of lower IFN-γ levels in cultures of PBMC, however, does not apply to the assays of specific activation. One explanation could be that when cells are non-specifically stimulated with a superantigen such as SEB they will be more prone to apoptosis as a result of exhaustion due to the massive activation as compared to PBMCs that have undergone Ag-specific activation. Interestingly, Hodge and colleagues found that the addition of plasma could protect PBMCs from apoptosis (9). It is therefore likely that survival factors present in whole blood contribute to the higher IFN-γ levels observed in these cultures.

A concern when using PBMC cultures is the risk of losing cells during the purification process. This could affect the overall distribution of cells in the sample, thus introducing a bias in the cell-mediated response observed after *in vitro* stimulation. Therefore, the distribution of cells in PBMCs and whole blood was compared, and a significant decrease in the percentage of γδ-T cells was found. Since this cell type is an important early contributor to the IFN-γ production during a CMI response after stimulation (10), the results obtained from *in vitro*-stimulated PBMC cultures may be somewhat misleading. Other groups have also found selective cell loss after PBMC purification. De Groote et al. describes a decreased ratio of monocytes:lymphocytes (monocytes concentrations being reduced) after PBMC purification using ready-to-use leukoprep tubes (Becton Dickinson) (11). They speculate that monocytes disappear due to adsorption to structures such as glass and gels used during the purification process. Their isolation system is different from the one used in the present study (Ficoll-Paque™Plus, GE Healthcare) which might explain the discrepancy in the type of cell-loss. Also they look at human, not bovine cells. Another study by Hokland and Heron on purification of human PBMCs reports selective cell loss of T cells when using Isopaque-Ficoll with a density of 1.076 g/ml (12). They found that the cell-loss was due to autorosette formation in which some cells, primarily T cells, were binding to red blood cells and were lost due to the higher density of the rosettes. Numerous studies of bovine PBMCs have used Ficoll for separation with a density of 1.077 g/ml, as in the present study (2, 13–16).

To our knowledge this is the first study reporting selective cell loss of bovine T cell subsets during PBMC purification. It is a possibility, however, that the actual number of $CD3^+/\gamma\delta^+$ T cells present after PBMC purification is not detected due to surface marker internalization. This has been described in mice by Koenecke and colleagues who found that mAbs targeting the $\gamma\delta^+$ T cells used in a depletion model, actually did not result in $\gamma\delta^+$ T cell depletion, but instead induced γδ T cell receptor (TCR) internalization generating “invisible” cells (17). If the anti-$\gamma\delta^+$ T cell antibody used in the present study should result in internalization of the receptor, this does not explain the difference in the two cell populations though. The internalization would have to happen after PBMC purification but before staining in order to explain the difference. The same applies for the CD3 marker. If the decrease in γδ TCR and CD3 is caused by internalization of multiple surface markers due to PBMC purification or in

fact caused by loss of a cell subset during the purification process, can only be speculated. If the former is the case, then the presence of cells being CD3 negative and γδ TCR positive (i.e. cells that have internalized CD3 but not γδ TCR) would be expected, but this is not the case (data not shown). The observation of selective cell loss during purification deserves attention and should be taken into account when PBMC assays are used for measurement of CMI responses.

The variety of culture plates available for cell-incubation assays are plenty and the choice of plate used in published studies is rarely described nor elaborated on. Therefore, a comparison of the IFN-γ levels in antigen-specific and polyclonal activated whole blood cultures incubated in six commercially available cell-incubation plates was performed. Even though the overall level of IFN-γ did not differ significantly across the different plates in both cultures, it was observed that six out of eight calves had highest specific IFN-γ levels when incubated on plate b (Corning®, clear, flat-bottom, tissue culture treated, polystyrene, cat# 3596), and that this relative level was significant compared to plate a, which was from Nunc™. Based on the present experiment it seems that flat bottom plates from Corning® was the optimal plate, although it remains unresolved why polyclonal SEB stimulation was less responsive than antigen-specific stimulation to the type of culture plate.

Choosing whether to use whole blood and PBMC assays or choosing which PBMC concentration to use for *in vitro* stimulation experiments is complex due to individual cell concentration optima. A number of studies have focused on comparing cytokine levels in cultures of human whole blood and PBMCs measured by ELISA (18–20), cytokine arrays (11, 21, 22) or by measuring the intracellular cytokine concentration using flow cytometry (9, 23). Most of these studies come to the conclusion that whole blood assays correlates well with PBMC cultures and are even preferable since this type of assay require no complex cell separation steps which saves both time and money and only requires small amounts of blood. On the contrary, Silberer and colleagues who compared cytokine release from cultures of diluted (1:5) whole blood and PBMCs (10^6 cells/well) in 25 human volunteers found no correlation of the IFN-γ levels in the two culture systems (24). Additionally they observed a significant increase in IFN-γ levels in serum-free PBMC cultures compared to PBMCs cultured in medium containing fetal bovine serum (FBS). Altogether they

conclude that a standardized approach with clearly defined culture conditions is needed for better comparability of cytokine data in the literature. The relevance of this request is further emphasized with the data presented here. Table 3 summarizes the advantages and disadvantages of using whole blood compared to PBMC cultures for IFN-γ release assays. If the purpose of the assay is to measure CMI responses against e.g. vaccine antigens in order to assess the quality of a vaccine or for diagnostic purposes, then whole blood cultures is preferable since the physiological conditions (such as cell-cell communications, cell ratios, growth factors, cytokines and other regulators) are preserved. This can be important since some cells rely on the presence of IL-2 for survival, and when removed they undergo apoptosis (25). In respect to this, the whole blood assay thus reflects the *in vivo* milieu in the most appropriate way. If long term incubation is needed, or if the purpose of the assay is to compare the in vitro-effect of different drugs on an exact number of cells, then PBMC cultures could be preferable.

In conclusion, this study shows the potential weaknesses of IFN-γ release assays in terms of the many variables that can influence the results. A difference in the response when comparing whole blood assays with PBMC assays was observed. The highest IFN-γ levels was found in a plate from Corning® (cat# 3596) following specific activation in 6 out of 8 calves tested. Last but most importantly, it was shown that purification of PBMC using Ficoll-Paque™Plus resulted in selective loss of γδ T cells. This highlights the limitations of the assay and stresses the importance of documenting the precise assay conditions when publishing results of *in vitro* IFN-γ release assays, or cytokine release assays in general.

Table 3: Advantages and disadvantages of whole blood compared to PBMC cultures for cytokine release assays

Characteristic	Whole blood cultures		PBMC cultures	
Ease of performing	Immediate culture		Time-consuming cell separation necessary	
Sample volume	Small blood sample		Require larger blood volumes due to the purification process	
Cell environment	Cells are kept in their natural environment and physiological proportions of blood-borne regulatory mediators are present		Cells are kept in synthetic media containing serum containing hormones and nutrients that can influence the immunological responsiveness of the cells	(26)
Cell number	Cell number is unknown and may vary from donor to donor		Cell number is controlled, helping standardizing the assay	
Culture period	Only suited for short term culture due to granulocyte lysis in cultures beyond 48 hours, but most cytokines are produced within this time frame	(9) (11) (27)	Long term culture possible due to sufficient nutrient supply within the media	
Cell loss	No cell loss		Risk of selective cell loss during purification potentially resulting in skewed cell ratios	(11)
Apoptosis	No apoptosis in short term culture		Increased apoptosis which may mask the intensity of immunological responses due to lower levels of produced cytokines	(9)

Funding information

This research received no specific grant from any funding agency in the public, commercial, or not-for-profit sectors.

Acknowledgement

A thank to Ulla Riber for assistance with the flow cytometry and to Jeanne Toft Jakobsen for assistance in the lab.

References

1. **Thakur A, Pedersen LE, Jungersen G**. 2012. Immune markers and correlates of protection for vaccine induced immune responses. Vaccine **30**:4907–20.

2. **Thakur A, Riber U, Davis WC, Jungersen G**. 2013. Increasing the ex vivo antigen-specific IFN-γ production in subpopulations of T cells and NKp46+ cells by anti-CD28, anti-CD49d and recombinant IL-12 costimulation in cattle vaccinated with recombinant proteins from Mycobacterium avium subspecies paratube. Vet Immunol Immunopathol **155**:276–83.

3. **Mikkelsen H, Jungersen G, Nielsen SS**. 2009. Association between milk antibody and interferon-gamma responses in cattle from Mycobacterium avium subsp. paratuberculosis infected herds. Vet Immunol Immunopathol **127**:235–241.

4. **Schmaltz R, Bhogal B, Wang Y-Y, Petro T, Chen S-S**. 1995. Staphylococcal Enterotoxin is a Bovine T Cell Superantigen. Immunol Invest.

5. **Schlievert PM**. 1993. Role of Superantigens in Human Disease. J Infect Dis **167**:997–1002.

6. **Weyrich AS, Zimmerman GA**. 2004. Platelets: signaling cells in the immune continuum. Trends Immunol **25**:489–95.

7. **Allam O, Samarani S, Marzouk R, Ahmad A**. 2012. Human platelets produce and constitute the main source of IL-18 in the circulation. J Immunol **188**:44.25.

8. **Cassatella MA**. 1995. The production of cytokines by polymorphonuclear neutrophils. Immunol Today **16**:21–26.

9. **Hodge G, Hodge S, Han P**. 2000. Increased levels of apoptosis of leukocyte subsets in cultured PBMCs compared to whole blood as shown by Annexin V binding: relevance to cytokine production. Cytokine **12**:1763–8.

10. **Baldwin C., Sathiyaseelan T, Naiman B, White A., Brown R, Blumerman S, Rogers A, Black S.** 2002. Activation of bovine peripheral blood γδ T cells for cell division and IFN-γ production. Vet Immunol Immunopathol **87**:251–259.

11. **De Groote D, Zangerle PF, Gevaert Y, Fassotte MF, Beguin Y, Noizat-Pirenne F, Pirenne J, Gathy R, Lopez M, Dehart I, Igot D, Baudrihaye M, Delacroix D, Franchimont P**. 1992. Direct stimulation of cytokines (IL-1β, TNF-α, IL-6, IL-2, IFN-γ and GM-CSF) in whole blood. I. Comparison with isolated PBMC stimulation. Cytokine **4**:239–248.

12. **Hokland P, Heron I**. 1980. The Isopaque-Ficoll Method Re-evaluated: Selective Loss of Autologous Rosette-forming Lymphocytes during Isolation of Mononuclear Cells from Human Peripheral Blood. Scand J Immunol **11**:353–356.

13. **Pearson TW, Roelants GE, Lundin LB, Mayor-Withey KS**. 1979. The bovine lymphoid system: Binding and stimulation of peripheral blood lymphocytes by lectins. J Immunol Methods **26**:271–282.

14. **Yang TJ, Jantzen PA, Williams LF**. 1979. Acid alpha-naphthyl acetate esterase: presence of activity in bovine and human T and B lymphocytes. Immunology **38**:85–93.

15. **Ioannou XP, Griebel P, Hecker R, Babiuk LA, van Drunen Littel-van den Hurk S**. 2002. The Immunogenicity and Protective Efficacy of Bovine Herpesvirus 1 Glycoprotein D plus Emulsigen Are Increased by Formulation with CpG Oligodeoxynucleotides. J Virol **76**:9002–9010.

16. **Rankin R**. 2002. CpG-containing oligodeoxynucleotides augment and switch the immune responses of cattle to bovine herpesvirus-1 glycoprotein D*1. Vaccine **20**:3014–3022.

17. **Koenecke C, Chennupati V, Schmitz S, Malissen B, Förster R, Prinz I**. 2009. In vivo application of mAb directed against the γδ TCR does not deplete but generates “invisible” γδ T cells. Eur J Immunol **39**:372–379.

18. **Antas PR, Cardoso FL, Oliveira EB, Gomes PK, Cunha KS, Sarno EN, Sampaio EP**. 2004. Whole blood assay to access T cell-immune responses to Mycobacterium tuberculosis antigens in healthy Brazilian individuals. Mem Inst Oswaldo Cruz **99**:53–55.

19. **Deenadayalan A, Maddineni P, Raja A**. 2013. Comparison of whole blood and PBMC assays for T-cell functional analysis. BMC Res Notes **6**:120.

20. **Damsgaard CT, Lauritzen L, Calder PC, Kjaer TMR, Frøkiaer H**. 2009. Whole-blood culture is a valid low-cost method to measure monocytic cytokines - a comparison of cytokine production in cultures of human whole-blood, mononuclear cells and monocytes. J Immunol Methods **340**:95–101.

21. **Silva D, Ponte CGG, Hacker MA, Antas PRZ**. 2013. A whole blood assay as a simple, broad assessment of cytokines and chemokines to evaluate human immune responses to Mycobacterium tuberculosis antigens. Acta Trop **127**:75–81.

22. **Stoddard MB, Pinto V, Keiser PB, Zollinger W**. 2010. Evaluation of a whole-blood cytokine release assay for use in measuring endotoxin activity of group B Neisseria meningitidis vaccines made from lipid A acylation mutants. Clin Vaccine Immunol **17**:98–107.

23. **Godoy-Ramirez K, Franck K, Mahdavifar S, Andersson L, Gaines H**. 2004. Optimum culture conditions for specific and nonspecific activation of whole blood and PBMC for intracellular cytokine assessment by flow cytometry. J Immunol Methods **292**:1–15.

24. **Silberer J, Ihorst G, Kopp MV**. 2008. Cytokine levels in supernatants of whole blood and mononuclear cell cultures in adults and neonates reveal significant differences with respect to interleukin-13 and interferon-gamma. Pediatr Allergy Immunol **19**:140–7.

25. **Cohen JJ, Duke RC, Fadok VA, Sellins KS**. 1992. Apoptosis and programmed cell death in immunity. Annu Rev Immunol **10**:267–93.

26. **Albers R, Antoine J-M, Bourdet-Sicard R, Calder PC, Gleeson M, Lesourd B, Samartín S, Sanderson IR, Van Loo J, Vas Dias FW, Watzl B**. 2007. Markers to measure immunomodulation in human nutrition intervention studies. Br J Nutr **94**:452.

27. **Sautois B, Fillet G, Beguin Y**. 1997. Comparative cytokine production by in vitro stimulated mononucleated cells from cord blood and adult blood. Exp Hematol **25**:103–8.

Chapter 4 - Study II (3D IGRA)

4.1 Introduction

The initiation of CMI responses requires the presentation of antigen peptides by APCs to rare T lymphocytes having TCRs specific for the unique antigen:MHC complex. This compares to finding a needle in a haystack with frequencies of naïve epitope specific T lymphocytes ranging from 0.2-10 per million naïve $CD4^+$ T lymphocytes in humans (Kwok et al. 2012; Jenkins & Moon 2012). This challenge is solved *in vivo* by the internal structures of lymph nodes. Lymphoid tissues consist of a scaffold of fibers (or reticular network) enwrapped by fibroblastic reticular cells (FRC). The tissue contains ECM proteins such as collagens, laminin, fibronectin, and tenascin, and enables T lymphocytes to migrate whereas APCs settle within the network (Sobocinski et al. 2010). It has been estimated that DCs can scan $0.5\text{-}5x10^3$ T lymphocytes per hour within the lymph node and thus the reticular network constitutes an optimal structural geometry that promote APC/T lymphocytes contact (Bousso & Robey 2003; Miller et al. 2004; Gretz et al. 1996).

When measuring CMI responses *in vitro* by IGRA it is not a primary activation that takes place in the culture well, but a re-activation of memory cells. Thus the number of cognate T lymphocytes with specificities toward the antigen:MHC complex presented by APCs is higher by around two orders of magnitude (Kwok et al. 2012). Nevertheless, the cell-cell contact is essential and no special measures are done to facilitate this contact in a conventional 2D culture setup.

4.2 Hypothesis

Cells cultured *in vitro* are placed in an environment that is very far from their natural milieu and thus might behave somewhat different compared to *in vivo*. It is hypothesized that when measuring cytokine responses from cells cultured on a 2D surface, the full potential of these cells is not obtained as they are not able to migrate and engage in cell-cell contact in an optimal way. Therefore, we speculated if culturing cells on a 3D surface would facilitate structured cell migration thus facilitating

contact between T lymphocytes and their cognate antigen presented by non-migrating monocytes, resulting in increased IFN-γ levels.

4.3 Results

In this section the results from several studies of IGRA-optimization in the form of 3D culture is presented. In an attempt to mimic the structural network of a lymph node in a simplified version, a culture setup was developed that included a scaffold made of glass wool coated with a mix of ECM proteins and which made use of gravity as a means of generating a flow of cells through the coated glass wool fibers. Glass wool fibers were placed in thin 1 ml syringes and bovine whole blood or PBMCs from two previously MAP infected animals was added together with antigen (Figure 6). Following overnight culture total RNA was purified and used for detection of *IFNG* and *CXCL10* cDNA (coding for IFN-γ and IP10 protein, respectively) using qRT-PCR. Both *IFNG* and *CXCL10* was expressed at higher levels in both PPDj-stimulated whole blood and PBMC cultures containing glass wool compared to control cultures (with no glass wool) (Figure 7). Coating the glass wool with ECM proteins did not seem to have a positive effect on the expression levels of *IFNG* and *CXCL10*. An overall trend was increased non-specific activation within the 3D cultures as seen by elevated background expression levels in non-stimulated cultures.

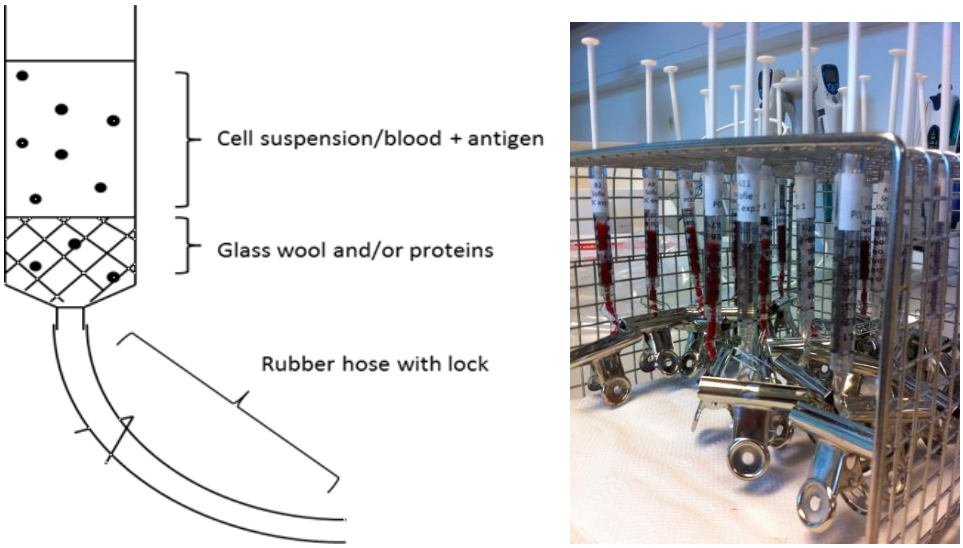

Figure 6: Glass wool-mediated gravity flow culture setup. Left: Illustration showing the culture setup, right: photograph of the setup.

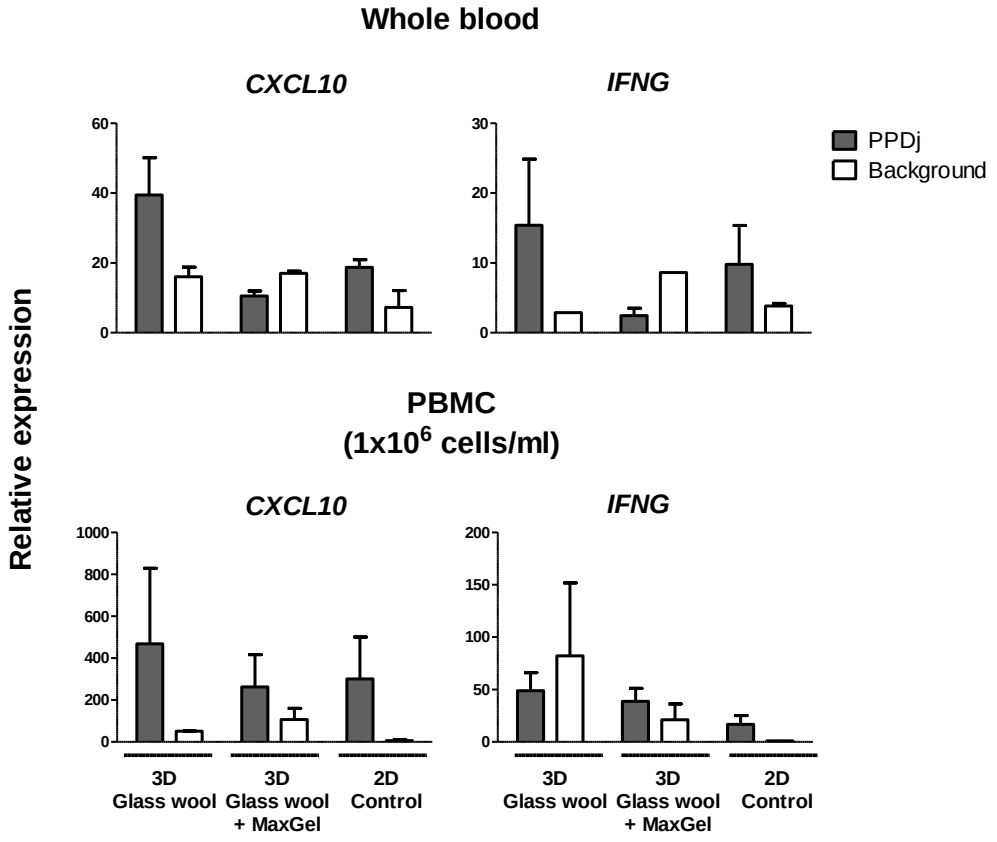

Figure 7: Glass wool-mediated gravity flow experiment. App. 1 ml of Whole blood or PBMCs from two calves were added to 1ml syringes and incubated for 22 hours with or without addition of PPDj (10µg/ml). Prior to addition of cells, the syringes were filled with glass wool, MaxGel-coated glass wool or kept empty as control. After incubation, cells from flow through were saved and used for *IFNG* and *CXCL10* gene expression analysis using qRT-PCR. Shown is mean+SEM of relative expression from the two calves where least expression (highest Cq) is set to 1. Data were normalized to *peptidylprolyl isomerase A (PPIA).*

When looking at expression on RNA levels, the incubation time necessary for mRNA detection is shorter than when looking at protein level. Therefore a new experiment was set up with incubation times of 1.5, 5 and 22 hours (Figure 8). In this experiment, stabilized whole blood from two previously MAP infected calves were stimulated with PPDj for the given time intervals followed by RNA isolation, cDNA synthesis and qRT-PCR analysis. This time cells were cultured in 48 well plates, thus no extra "gravity" element was included in the setup. Again glass wool was used as 3D scaffold in an ECM-coated and non-coated version. In addition also shavings made of polypropylene (PPS) were included in the experiment as an additional 3D scaffold to be tested.

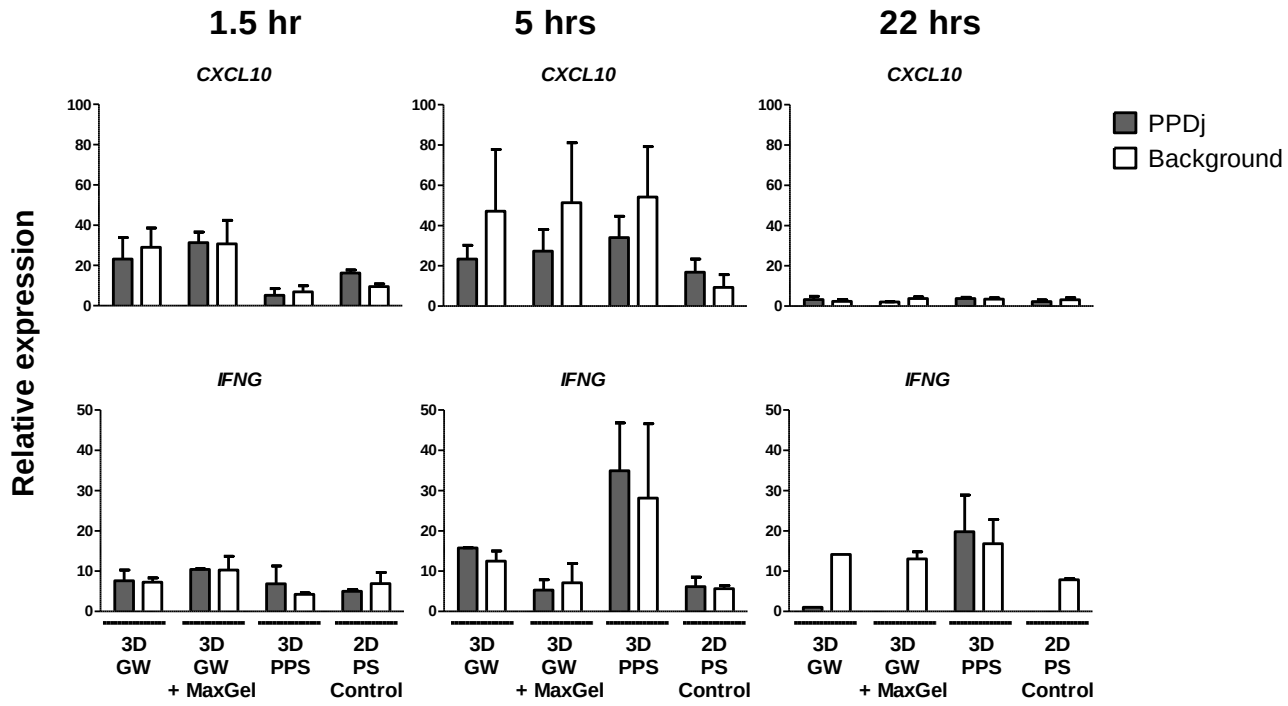

Figure 8: Kinetics of *IFNG* and *CXCL10* gene expression in 3D cultures. Whole blood from two calves was incubated in duplicate for 1.5, 5, or 20 hours in 48-well plates with or without the addition of PPDj (10µg/ml). The cell cultures consisted of (from left): Three-dimensional glass wool, MaxGel-coated three-dimensional glass wool, three dimensional polypropylene shavings and two-dimensional polystyrene (control). After incubation, cells were saved and used for *IFNG* and *CXCL10* gene expression analysis by qRT-PCR. Shown is mean+SEM of relative expression from the two calves where least expression (highest Cq) is set to 1. Data were normalized to *hypoxanthine phosphoribosyltransferase 1 (HPRT1)* and *glyceraldehyde 3-phosphate dehydrogenase (GAPDH).*

Peak expression of both *CXCL10* and *IFNG* was measured after 5 hours of incubation. Surprisingly the background level of expression was equal to, or higher than, the expression from the PPDj-stimulated cells. This was seen for both *CXCL10* and *IFNG*. Since the high background levels was observed in both 3D glass wool and PPS samples as well as the 2D control, this indicated that the cells must have been activated prior to culture but as the background expression was found to be higher in 3D cultures this suggest an additional 3D effect on the non-specific activation of the cells.

Glass wool fibers are an untraditional choice of 3D scaffold usually used for filtering purposes and there are only a few publications reporting its use for cell culture (Snapka 1979; Korohoda 1972).

However the well-known ability of monocytic cells to adhere to glass combined with the increased surface area provided by the fibers while allowing medium exchange, in theory makes glass wool an attractive 3D scaffold. When harvesting cells for RNA purification, a bias may be introduced if some cell subsets within the blood preferably stick to the glass wool compared to other subsets, resulting in an unrepresentative cell pool used for analysis. To avoid this, the expression of IFN-γ on protein level was analyzed on whole blood from two previously MAP infected calves (Figure 9). In this procedure cells were not isolated but plasma was harvested and tested for IFN-γ protein using ELISA, thus the potential difference in stickiness of cell subsets had no effect on the results.

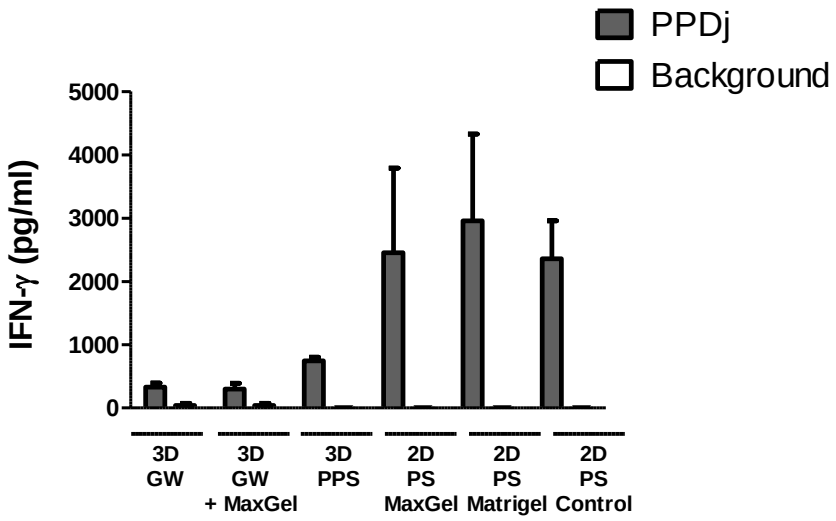

Figure 9: IFN-γ protein expression in 3D cultures. Whole blood from two calves was incubated in duplicate for 22 hours in 48 well plates with or without the addition of PPDj (10µg/ml). The cell cultures consisted of (from left): three dimensional glass wool, MaxGel-Coated three dimensional glass wool, three dimensional polypropylene shavings, two dimensional polystyrene coated with MaxGel, two dimensional polystyrene coated with Matrigel and two dimensional polystyrene (control). After incubation, plasma was harvested and used for IFN-γ detection by ELISA. Each bar represents the mean+SEM of the two calves.

The IFN-γ protein levels were decreased in 3D cultures of glass wool, ECM-coated glass wool and PPS cultures compared to conventional 2D culture. Coating the culture surface with either of two commercial available ECM protein mixes resulted in the same level of expression as the control culture.

One of the advantages of using 3D scaffolds is the number of cells that can be cultured. Due to increased surface areas, a larger number of cells can be plated without the risk of apoptosis due to insufficient nutrient supply. In fact having the right cell concentration might be crucial when testing immunological responses using IGRA. This also relates to the size of the culture wells used; a large well size with a low cell concentration may not facilitate cell encounter and thus result in IFN-γ levels below the detection limit, whereas a high cell concentration in a small well size may result in cell crowding and apoptosis. The effect of well size when performing IGRA in a 2D culture setup was tested using freshly isolated PBMCs from one previously vaccinated calf (Figure 10). Cells were cultured in two concentrations; $1x10^6$ and $1x10^7$ cells/ml, corresponding to $2x10^5$ and $2x10^6$ cells/well, in both 12- and 48-well plates (with wells having surface areas of approximately 3.8 cm^2 and 0.95cm^2, respectively).

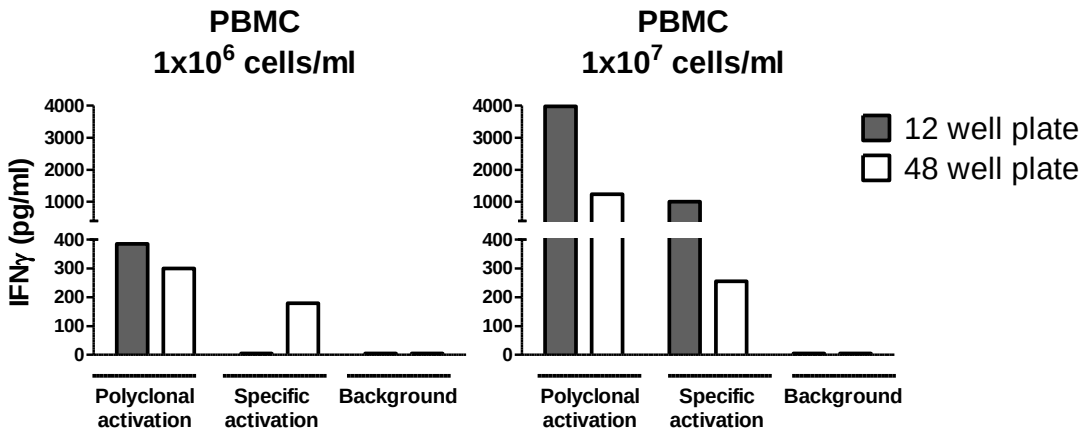

Figure 10: Effect of well size and cell concentration on IFN-γ protein secretion. PBMCs from one calf was incubated for 20 hours in 12 or 48 well plates in concentrations corresponding to $2x10^5$cells/well and $2x10^6$cells/well, with the addition of either 1µg/ml SEB (polyclonal activation), 1µg/ml MAP antigen (specific activation) or PBS (background). After incubation, supernatant was harvested and used for IFN-γ detection by ELISA.

Background levels of IFN-γ were low in cultures of both cell concentrations and well sizes. Cells were activated with MAP antigen (specific activation) and with SEB (polyclonal activation). A higher response was detected from cultures with the high cell concentration. For the polyclonal activated cells, IFN-γ secretion levels were ten and three times higher in the high cell concentration cultures compared to the low cell concentration cultures in the 12- and 48-well plates cultures, respectively.

For the specifically activated cells, the same level of IFN-γ secretion was detected in the 48-well plate cultures of both cell concentrations. However the secretion of IFN-γ from specifically activated cells in the low cell concentration, was below the limits of detection (5 pg/ml) when cultured in 12-well plates. Increasing the cell concentration or reducing the culture area resulted in detectable levels of IFN-γ (1002 and 179 pg/ml, respectively). When both reducing the culture area and increasing the cell concentration, this did not have a synergistic effect on the level of IFN-γ, suggesting that adding $2x10^6$ cells in $0.95cm^2$ (48-well plate) exceeds the optimal cell density.

To test if the addition of a 3D scaffold made of the same material (PS) had an effect on the optimal cell density used for IGRA cultures, a commercial available 3D PS scaffold fitting into the well of a 12-well plate was tested on PBMCs from the same calf as the previous experiment (Figure 11).

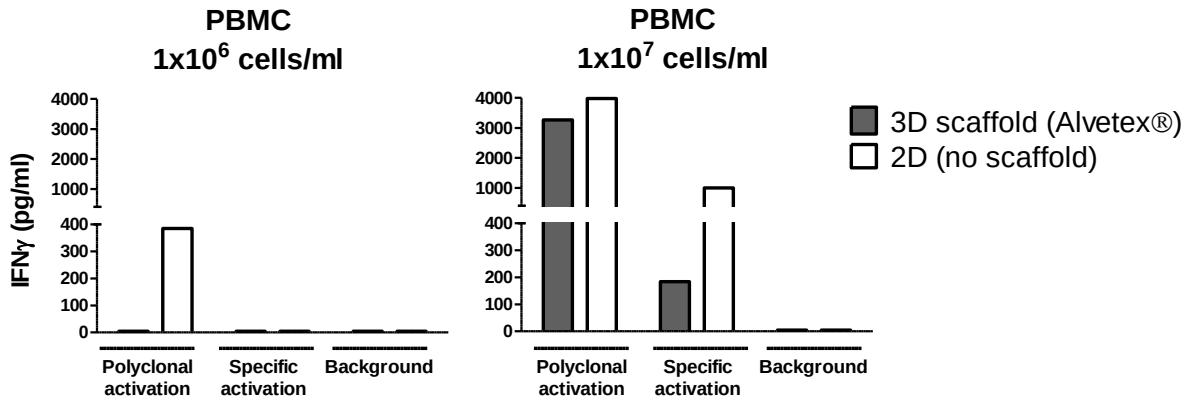

Figure 11: Effect of 3D culture and cell concentration on IFN-γ protein secretion. PBMCs from one calf were incubated for 20 hours in 48 well plates in concentrations corresponding to $2x10^5$cells/well and $2x10^6$cells/well, with the addition of either 1µg/ml SEB (polyclonal activation), 1µg/ml MAP antigen (specific activation) or PBS (background). The cell cultures consisted of either three dimensional polystyrene scaffolds (3D scaffold, Alvetex®) or two dimensional polystyrene (2D, no scaffold). After incubation, supernatant was harvested and used for IFN-γ detection by ELISA.

When cells were cultured on the 3D scaffold in a low cell concentration, secreted IFN-γ was below detection limit in both cultures of polyclonal and specifically activated cells. When culturing cells at the high cell concentration, 3D cultures resulted in detectable IFN-γ levels (3263 pg/ml and 184 pg/ml for polyclonal and specifically activated cells, respectively), but they did not exceed the levels detected in 2D cultures (3975 pg/ml and 1002 pg/ml for polyclonal and specifically activated cells,

respectively). This indicated that the surface area in wells of 12-well plates were large enough to avoid crowding of cells when $2x10^6$ cells were added, and the addition of a 3D scaffold did not increase the activation of cells probably due to too low cell density within the scaffold. Therefore the following experiments were done using 48- or 96-well plates in order to minimise the number of cells plated in each well.

Results so far indicated that changing the culture setup from 2D to 3D did not improve cell migration and activation in IGRA. Glass wool, PP shavings and 3D PS scaffolds did either not result in increased IFN-γ levels compared to 2D cultures, or gave rise to elevated background activation. Therefore a new 3D scaffold was tested. This time the 3D scaffold was made of PDMS polymer fabricated using sugar cubes resulting in square scaffolds with pore sizes ranging from 300-600µm and fitting into wells of 48-well plates. Stabilised whole blood and PBMCs from two calves were cultured overnight with or without the addition of a polyclonal activator (SEB) and the level of IFN-γ in plasma was measured by ELISA (Figure 12).

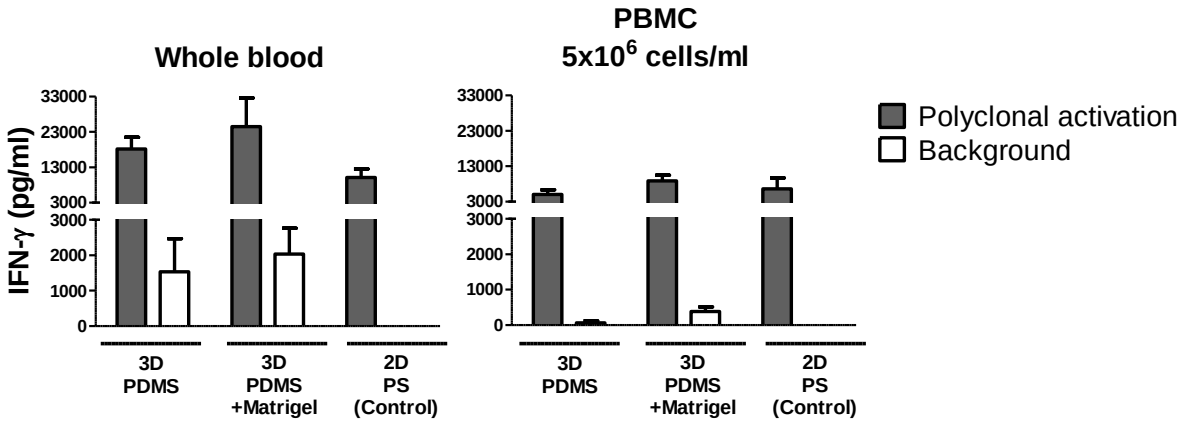

Figure 12: 3D cultures in PDMS sugar cubes. Whole blood and PBMCs from two calves were incubated for 22 hours in a 48 well plate (PBMC = $2.5x10^6$cells/well) with or without the addition of SEB (1µg/ml). The cell cultures consisted of (from left): three dimensional polydimethylsiloxane scaffolds, Matrigel-coated three dimensional polydimethylsiloxane scaffolds and two dimensional polystyrene (control). After incubation, plasma/supernatant was harvested and used for IFN-γ detection by ELISA. Each bar represents the mean+SEM of the two calves.

The same level of IFN-γ could be detected in polyclonal activated cultures with 3D PDMS scaffolds, ECM-coated 3D PDMS scaffolds and 2D PS cultures with PBMCs. Whole blood cultures resulted in

increased IFN-γ levels compared to PBMC cultures, and 3D cultures had a slightly positive effect on the IFN-γ levels. However, once again there was a noticeable increase in non-specific activation of cells cultured in 3D compared to 2D.

For routine testing, the costs of IGRAs will have to be kept low as there is no point in developing an improved 3D assay if the expense for performing the test makes it unattractive. With that in mind, 3D scaffolds made of filter paper disks punched to fit into the wells of 96-well plates were prepared. To increase the T cell motility and thus the chance of activation, disks were coated with CCL21 chemokine. When coated onto culture surfaces, CCL21 have previously shown to trigger T cell locomotion *in vitro* (Woolf et al. 2007), as well as being responsible for increased *in vitro* T cell proliferation and activation after TCR stimulation (Gollmer et al. 2009). Therefore, an experiment was set up testing the effect of 3D scaffolds made of filter paper combined with CCL21 in a coated and soluble form, using stabilized whole blood or PBMCs from two calves (Figure 13).

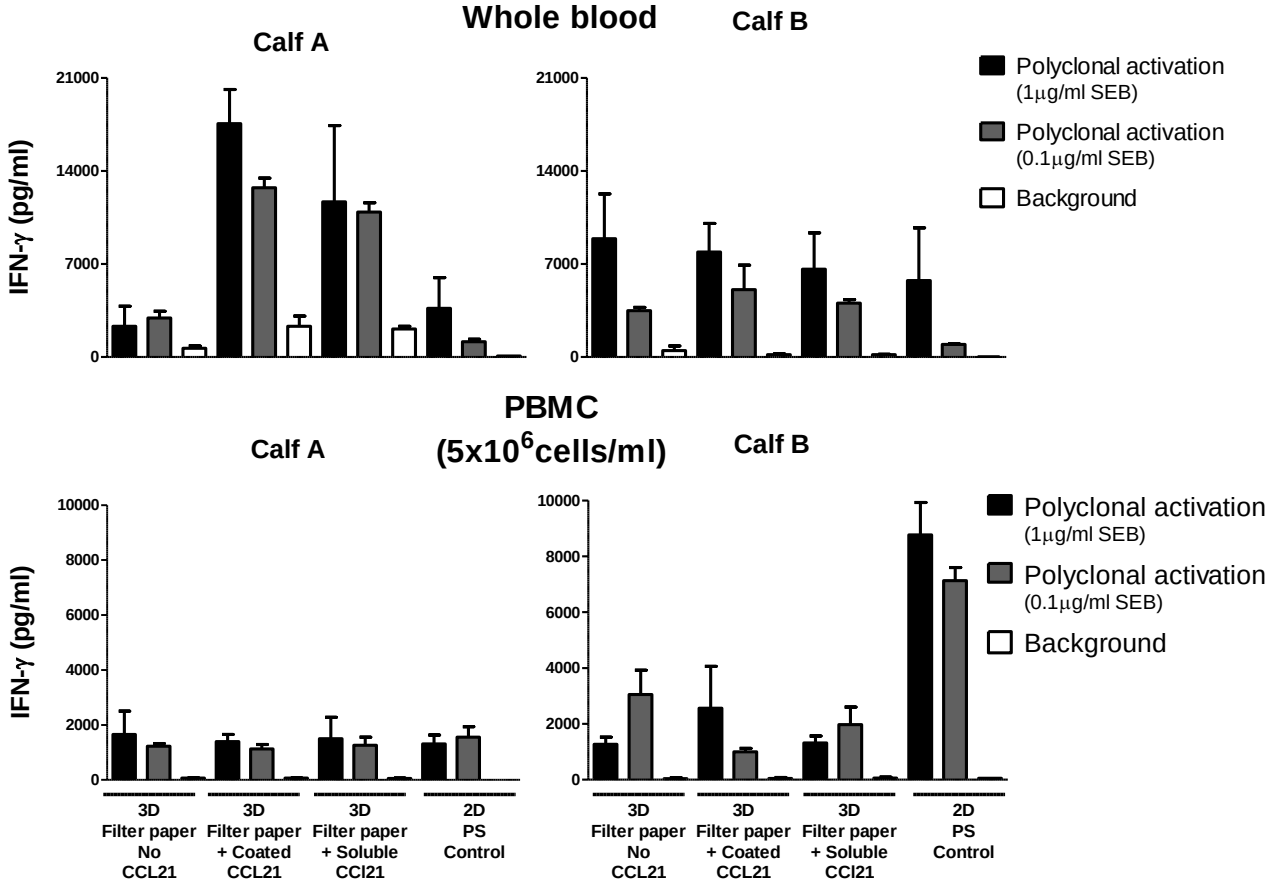

Figure 13: 3D cultures using filter paper. Whole blood and PBMCs from two calves were incubated in triplicate for 20 hours in 96-well plates (PBMCs = $1x10^6$ cells/well) with or without the addition of SEB (1 or 0.1 µg/ml). The cell cultures consisted of (from left): three dimensional filter paper grade 4, CCL21-coated three dimensional filter paper grade 4, three dimensional filter paper grade 4 with soluble CCL21 and 2D polystyrene (control). After incubation, plasma/supernatant was harvested and used for IFN-γ detection by ELISA. Each bar represents the mean + SD of three technical replicates.

Highest responses were observed in cultures of whole blood. Whereas no difference in the IFN-γ levels were detectable in whole blood from calf B in the different culture setups stimulated with 1µg/ml SEB, a slight increase in IFN-γ concentrations was detected when stimulated with 0.1µg/ml SEB in filter paper-cultures compared to control. In calf A, a more profound difference in IFN-γ levels in filter paper cultures with CCL21 compared to control was observed in whole blood stimulated with both concentrations of SEB. However, the 3D cultures gave once again rise to non-specific activation as opposed to conventional 2D culture. For the PBMC cultures, no difference in IFN-γ concentrations

was observed in the different culture setups in calf A, whereas a three-fold decrease in IFN-γ concentrations was detected in 3D cultures from calf B.

The few number of animals used in the previous experiments, makes it difficult to conclude on the results. Therefore, to sum up the results in one final experiment, PBMCs from six calves were polyclonal activated in conventional 2D cultures (tissue culture treated and non-tissue culture treated) as well as 3D cultures consisting of 3D PS scaffolds, 3D PCL scaffolds and filter paper disks, all either coated with CCL21 or non-coated (Figure 14).

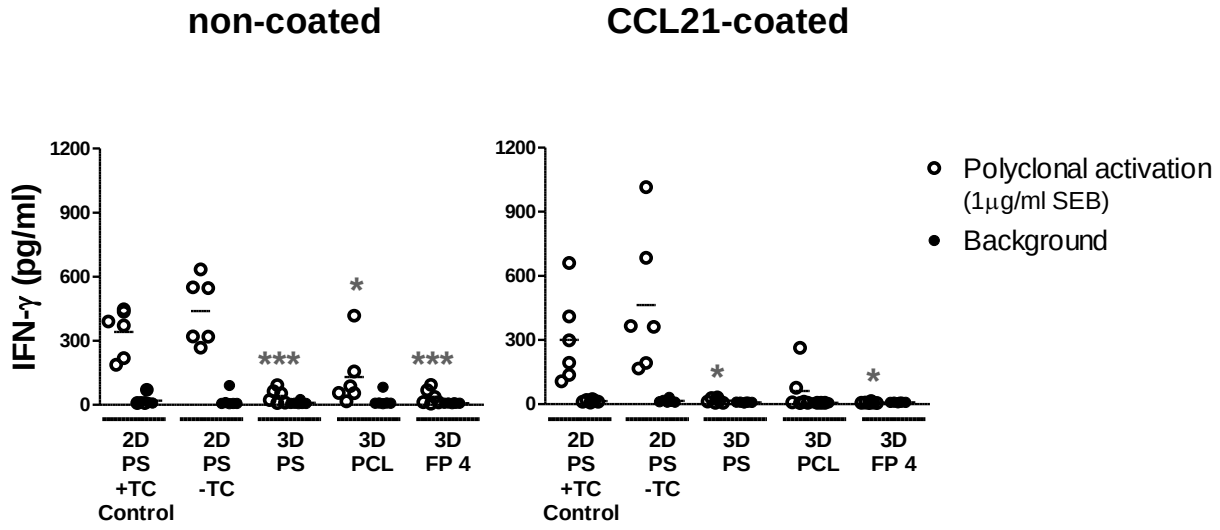

Figure 14: 3D cultures coated with CCL21. PBMCs from six calves were incubated in triplicate for 21 hours in 96-well plates (1x10^5 cells/well) with or without the addition of SEB (1μg/ml). Half of the wells/scaffolds were coated with CCL21 chemokine (1μg/ml) prior to cell plating. The cell cultures consisted of (from left): tissue culture treated two dimensional polystyrene (control), non-treated two dimensional polystyrene, three dimensional polystyrene scaffolds, three dimensional polycaprolactone scaffolds and three dimensional filter paper grade 4. After incubation, supernatant was harvested and used for IFN-γ detection by ELISA. Each dot represents the mean of three technical replicates and the horizontal line represents the mean of six calves. Statistics = One way ANOVA + Dunnett´s Multiple Comparison Test. (n=6), ***p≤ 0.001, *P≤0.5.

Common for all 3D cultures was a decreased concentration of IFN-γ compared to control, and this decrease was significant in all but CCL21-coated 3D PCL cultures. Non-specific activation was not detected and CCL21 did not seem to have a positive effect on T cell activation and thus IFN-γ levels.

There was no significant difference in tissue culture-treated and non-tissue culture-treated 2D cultures.

In conclusion, the attempt to improve IGRAs by introducing a 3D scaffold to the cultures did not succeed. Several scaffolds resulted in non-specific activation. When using scaffolds of different material than the control surface made of PS, it can be difficult to elucidate whether the effect came from the 3D architecture or from properties caused by the shift in material. To this end, the 3D PS scaffold makes a good candidate for narrowing the change in parameters to only apply to architecture and not material. Confocal microscopy was used to visualize the architecture of the 3D PS scaffold (Figure 15).

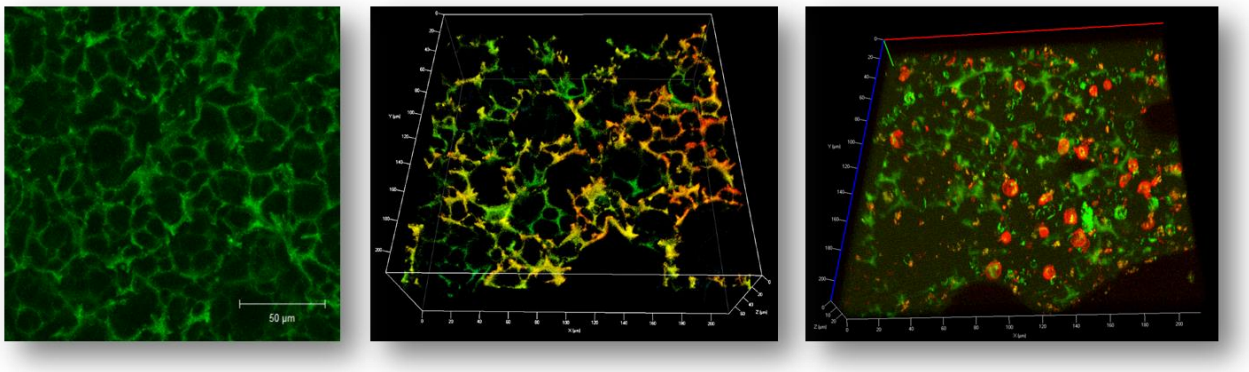

Figure 15: Confocal Images of 3D PS scaffold (Alvetex®). Z-stack images were recorded on a Zeiss LSM710 confocal microscope with ZEN 2009 software. Left: maximum projection image of the 3D PS scaffold, middle: topography of 3D PS scaffold, right: 3D PS scaffold with incubated PBMCs stained for $CD4^+$ T (red) and $CD14^+$ monocytes (green) using fluorophore-conjugated antibodies. The 3D PS scaffold was autofluorescent and could therefore be visualized without staining the scaffold.

Left image illustrate the architecture of the 3D PS scaffold by autoflorescence and the middle image show the topography of the scaffold. Right image illustrates the scaffold with cultured PBMCs stained for CD4 (red) and CD14 (green), to show CD4+ T lymphocytes and monocytes, respectively. Due to bleaching it was not possible to obtain good-quality images/movies for visualization of possible T lymphocyte migration within the 3D scaffolds. Migration on 2D surfaces (glass slide) was visualized and an example is shown in Figure 16.

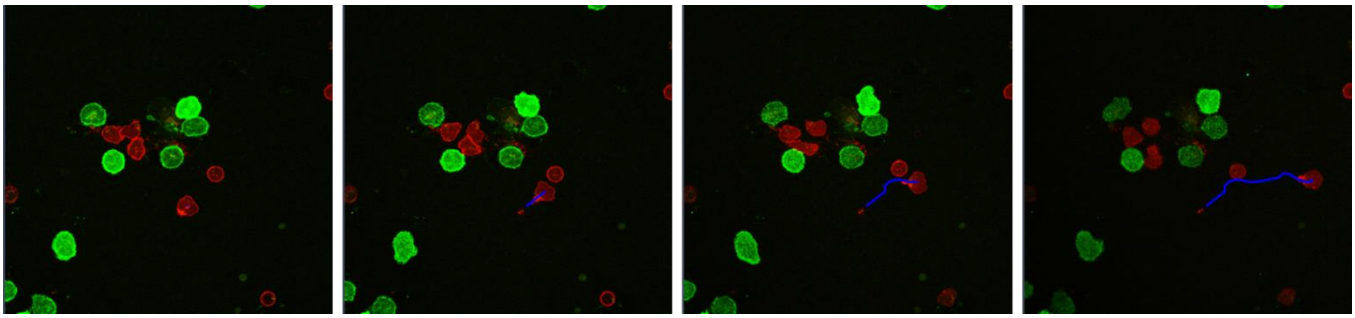

Figure 16: CD4$^+$ T lymphocyte migration on 2D surface. SEB-stimulated, stained cells were imaged by time-lapse on a 2D surface (glass slide) using Zeiss LSM710 confocal microscope, ZEN 2009 software. Migration was tracked using Fiji software, manual tracking.

Chapter 5 - Study III (chip prototype)

5.1 Introduction

The miniaturization of tests and assays usually performed in the lab was first described in 1975 when C.S Terry designed a miniaturized analytical device for gas chromatography as part of his PhD dissertation (Terry 1975). Fifteen years later, in 1990, Manz and colleagues created the term "micro total analysis system" or "μTAS" (Manz et al. 1990) and this was the beginning of the lab-on-a-chip renaissance (Berthier et al. 2012). The idea with lab-on-a-chip is the integration of one or several laboratory functions on a single chip. This has several advantages such as reduced sample and reagent consumption, less sample handling and shorter analysis time (Menegatti et al. 2013). Developing a fast and low-cost method for detection of diseases (or indirectly by detection of immune responses against certain pathogenic microorganisms) would be desirable for the diagnostic of diseases in low-income countries or where a one-time visit to the medical clinic would ease the logistics and result in higher treatment rates and thus prevention of disease spreading.

5.2 Hypothesis

In this study, a low-cost microfluidic diagnostic chip was sought developed. The chip would combine an optimized 3D cell chamber, facilitating cell migration and thus cell-cell contact and activation with detection of IFN-γ or IP10 mRNA by direct blood qRT-PCR as a readout. The idea was that this lab-on-a-chip device could diagnose the presence of a CMI response against intracellular pathogens (such as *Mycobacterium tuberculosis* in humans) within the same day of blood sampling. It would thus be a fast and cheap diagnostic solution ideal for developing countries where tuberculosis represents a major cause of death.

5.3 Results

A thorough novelty search was conducted at the beginning of the study, concluding that no similar invention had previously been described (as per February 2012); see the Novelty Search Report in appendix 3. The practical work was split into three parts: (1) chip design and fabrication, involving the

manufacturing of a prototype chip, (2) optimization of the direct one-step blood PCR reaction, and (3) optimization of cell culture with facilitated cell migration by 3D incubation. The 3D incubation-part was optimized off-chip and has been described in chapter 4 - Study II.

Chip design and fabrication

A prototype chip with micro slide format (75 mm x 25 mm x 1 mm) containing eight cell incubation chambers with different microstructures was designed using AutoCAD® 2013 (Autodesk Inc.) and CimatronE10 (Cimatron Ltd.) software. A mold was made in aluminum (MetalCentret) using computer numerical control (CNC) micro milling (Folken Ind) followed by polishing (metal polish, Autosol). Using this mold, microchips made of cyclic olefin copolymer (COC) (TOPAS grade 5013L-10, Tg =135°C) (TOPAS Advanced Polymers GmbH) were produced by polymer injection molding (Engel). To close the chambers, chips were sealed by another piece of COC with same dimensions as the chips, containing holes above the inlets and outlets, using a thermal bonding press (P/O/Weber) set to 115-120°C and 9.5-10 kN for 5-10 minutes. Prior to bonding, the chips and lids were UV treated for app. 30 sec. to activate the surfaces and improve the bonding process. Alternatively the chambers were sealed using Microseal® B Adhesive Sealer (Bio-Rad). Finally, Luer ports (provided by Carl Esben Poulsen, Department of Micro- and Nanotechnology, Technical University of Denmark) produced using the same methods as for the micro slide chips, were attached above inlets and outlets using double adhesive tape. The processes involved in the fabrication are shown in Figure 17.

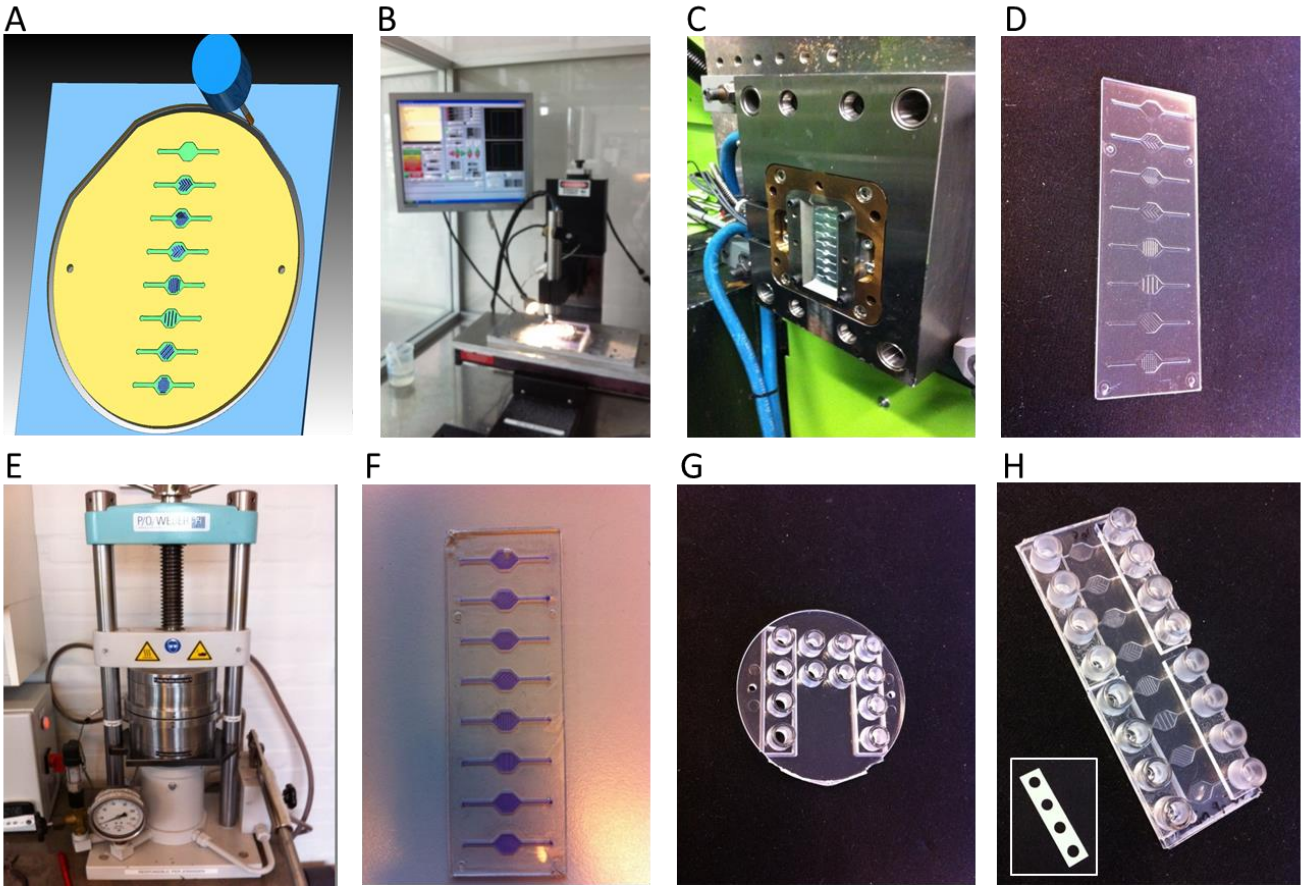

Figure 17: Chip design and fabrication. A mold was designed using 3D drawing programs (A) and cut in aluminum using CNC micro milling (B). Injection molding (C) was used to fabricate COC polymer chips (D), which were sealed by thermal bonding (E). The sealing was successful (F), and to ease liquid loading, Luer ports (G) was attached to the bonded prototype chip (H) by double adhesive tape (H insert).

The microstructures in the chambers of the chip prototype are shown in Table 2. The first chamber was an "empty" cell incubation chamber with space for a 3D scaffold/protein matrix in case such structures were found to be favourable for cell-activation. The remaining seven chambers contained additional microstructures at the bottom surface, each with different designs. The idea was that these microstructures would capture cells passing by, when the chamber was connected to a fluidic circuit. This would make it possible to retain cells of interest while changing the liquid within the chamber, for example changing to PCR reagents for direct PCR reaction on the chip.

Table 2: Overview of microstructures in the chambers of the prototype chip

Chamber	Microstructure	Dimension (mm) (depth)x(width) x(length)	Chamber	Microstructure	Dimension (mm) (depth)x(width) x(length)
1	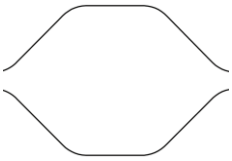	-	5	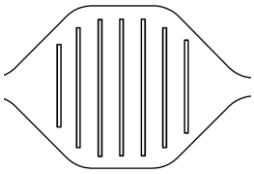	(0.100) x (0.101) x (2.285-3.788)
2	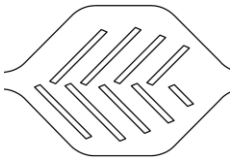	(0.100) x (0.171-0.175) x (0.813-2.341)	6	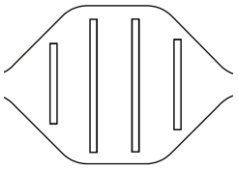	(0.100) x (0.204) x (2.285-3.788)
3	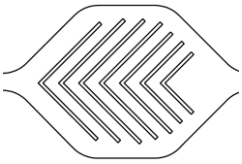	(0.100) x (0.100) x (2.592-5.213)	7	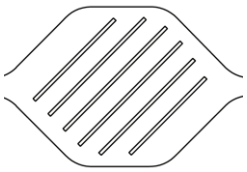	(0.100) x (0.097) x (3.023-4.091)
4	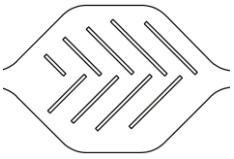	(0.100) x (0.101) x (0.838-2.341)	8	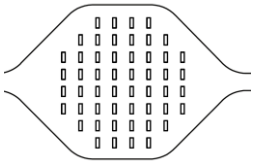	(0.100) x (0.101) x (0.295)

For visualization purposes, and to find out if relevant cells could be captured within the microstructures, PBMCs purified from goat blood was used as test-material. PBMCs ($5x10^6$ cells/ml) were preheated in an incubator (37°C, 5% CO_2) for one hour prior to flow test. Using a syringe pump, a cells-flow through the chambers on the chip was generated, and images of the cell capture by selected microstructures are shown in Figure 18.

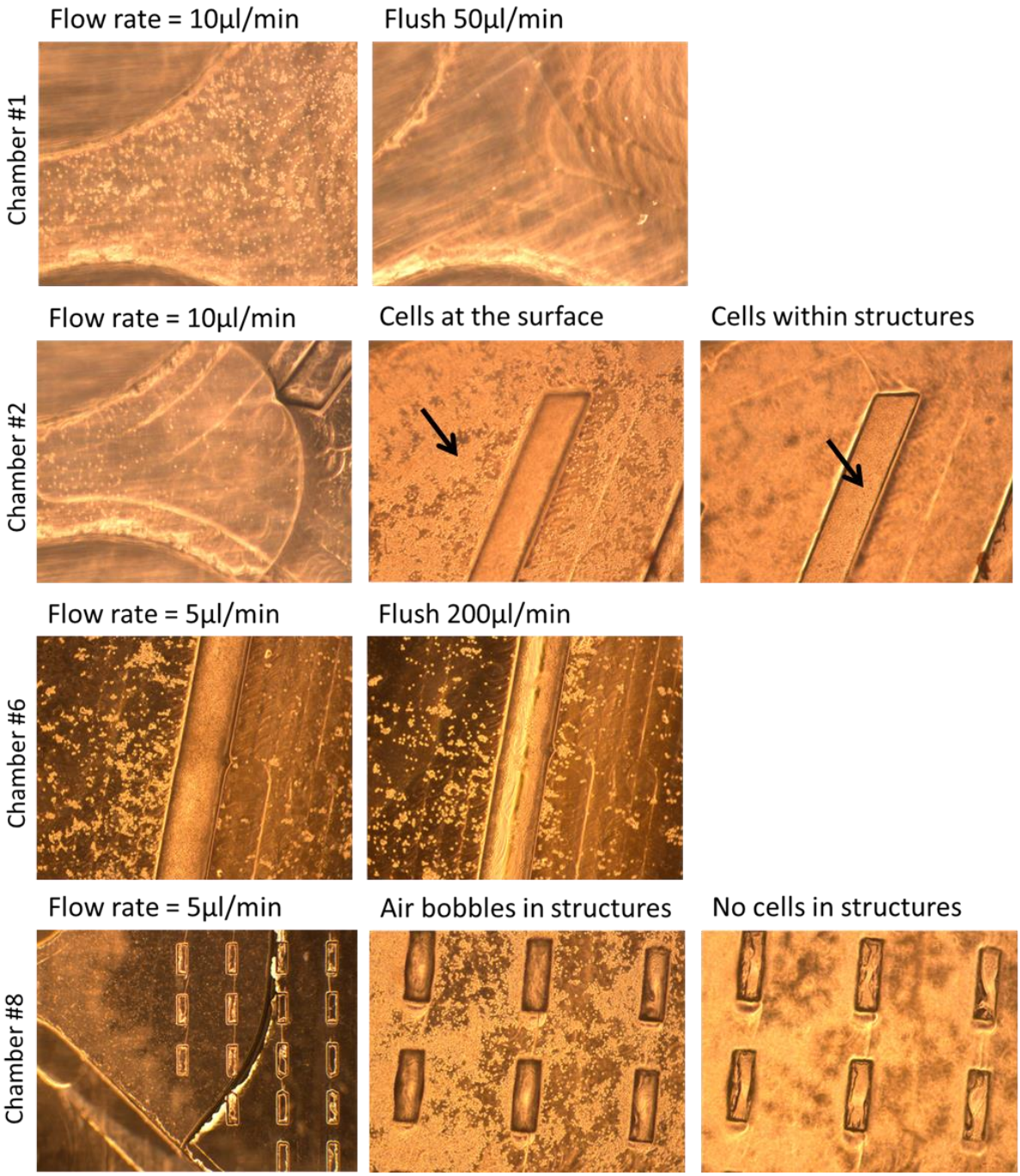

Figure 18: Cell flow and capture by microstructures on the chip prototype. Images were recorded using an inverted Leica DMIL contrasting microscope equipped with a Leica DFC290 camera.

In chamber 1, cells distributed evenly across the chamber surface when applied at a flow rate of 10µl/min, and could be flushed away when changing to cell-free medium at a flow rate of 50µl/min. In chamber 2, cells were detectable both at the surface and within the microstructures when applied at

a flow rate of 10µl/min. Increasing the flow rate by flushing with medium at 200µl/min resulted in disruption of cells settled within the microstructures (chamber 6), thus the structures could not retain trapped cells at high flow rates. There was an overall problem with air bobbles being trapped in the microstructures, especially the structures in chamber 8. These structures were very small (app. 100x100x300µm) and not suited for trapping cells, at least not with the conditions used for this experiment (PBMCs, room temperature and no degas of medium prior to experiment).

To verify that the cells of interest, i.e. $CD4^+$ T cells and monocytes, were present among the cells trapped within the microstructures, bovine PBMC were stained for CD4 and CD14 using fluorescently labeled antibodies and loaded into chambers on the chip, and imaged using a confocal microscope, Figure 19. Both types of cells were detectable within the microstructures of analyzed chambers (chamber 2 and 3), representing a wide and a narrow structure, respectively.

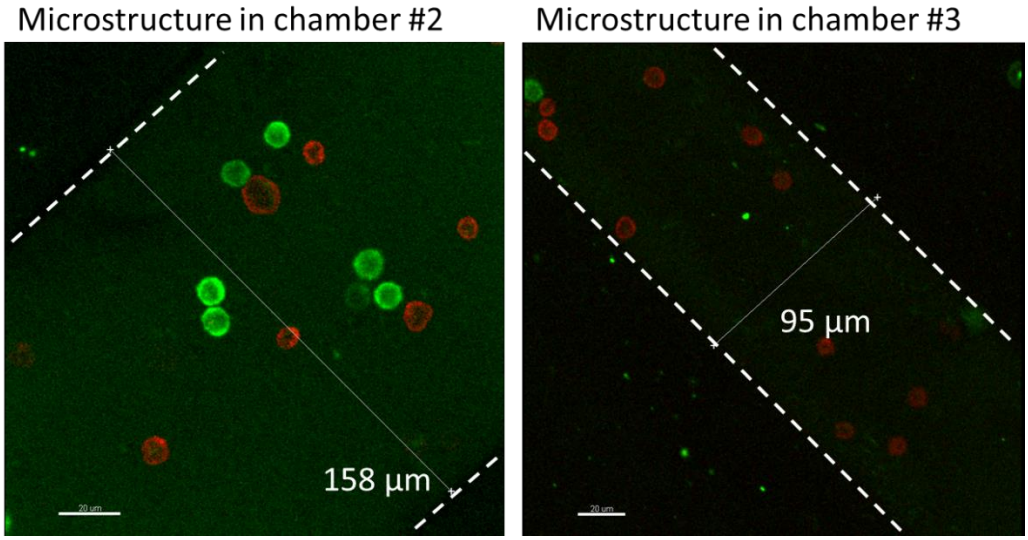

Figure 19: Images of T cells and monocytes within microstructures from the chip prototype. Fluorescence images were taken using a Zeiss LSM710 confocal microscope with ZEN 2009 software. Bovine PBMCs were purified and stained for $CD4^+$ T (red) and $CD14^+$ monocytes (green) using fluorophore-conjugated antibodies. Cells were loaded into the chambers on the chip and images were taken to document the capture of relevant cells within the microstructures.

Direct one step blood PCR

The readout for the diagnostic chip was intended to be on-chip qRT-PCR performed directly in the blood, detecting *IFNG* and/or *CXCL10* mRNA. For this purpose, a direct one-step blood qRT-PCR SYBR Green Kit was tested. This was done off-chip on the Rotor-Gene Q qPCR platform. Numerous optimization experiments was performed using both goat- and bovine whole blood, including titrations of the percentages of whole blood used in the final reaction (10%, 8%, 6%, 5% and 2%), use of stabilizing agent (EDTA or heparin), titrations of SYBR Green concentrations (20x, 10x, 5x) and the annealing temperature (63°C and 60°C). *IFNG* and *CXCL10* as well as reference genes could all be detected when 2% blood was used in the reaction. To be able to determine a coefficient of determination (R^2) and PCR amplification efficiency, standard curves were generated using a dilution of template material (blood). The best results were obtained using 2% EDTA-stabilized whole blood, 5x SYBR Green and an annealing temperature of 60°C when testing for the *ACTB* reference gene (Figure 20).

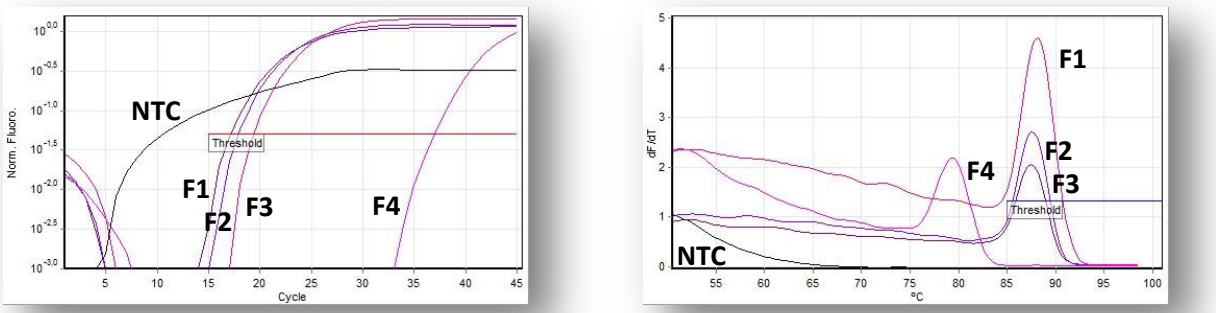

Figure 20: Quantitation- and melting curve analysis of *ACTB* in titrated samples of goat blood. Quantitation analysis (left) of four 4-fold dilutions (F1-F4, start concentration F1 = 2% blood) of EDTA-stabilized goat whole blood. Threshold of fluorescence detection set to 0.05. Melting curve analysis (right) with a threshold temperature set to 85°C. NTC = no template control.

With the above settings, and using results from F1-F3 depicted in Figure 20 (F4 contained no product, and the misplaced melting curve is a sign of primer-dimer), the *ACTB* primers had a coefficient of determination of 0.96 and an efficiency of 2.44, which was not acceptable (coefficient of determination should preferable be 0.98 or above and the efficiency should be between 0.90 and

1.10). Therefore, additional optimization was necessary, but due to time limitations this was not pursued.

Chapter 6 - Study IIII (differentiation of moDC)

6.1 Introduction

The use of monocytes as DC precursors has been an attractive approach in the attempt to generate competent APCs able to induce anti-cancer responses via immunotherapy. Immunotherapy has advantages over traditional cancer treatments such as chemotherapy, including no or few side effects (Janikashvili et al. 2010) and the treatment is personalized (DCs are loaded with antigens originating from the patient's own tumor). It is known that during cancer, DCs are negatively influenced by the microenvironment and are not able to mature properly, resulting in poor induction of tumor-targeting T lymphocytes (Barbuto 2013). Therefore, it is believed that the generation of DCs outside this environment (i.e. by *in vitro* culture) would increase the functionality of the cells. A large number of monocytes can be obtained relatively easy via blood and they can be loaded with tumor antigen (Barbuto 2013). Despite this, the generation of effective immunotherapy for the treatment of cancer patients using moDCs has not been very successful as moDC-based vaccines have not been able to induce durable anti-cancer immunity, reviewed in (Wimmers et al. 2014). In addition, functionally biased moDCs generating regulatory T cell responses *in vitro* has been reported (Ramos et al. 2012). Therefore, optimization of the moDC differentiation protocol is needed.

6.2 Hypothesis

DCs act as cellular sensors and are able to respond to external stimuli coming from complex cellular and molecular signals from their surroundings (Palucka & Banchereau 2012). In relation to this, it was hypothesized that changing the surface material and architecture of cultures used for porcine moDC differentiation would influence the gene expression profile of the cells, as the cell-to-surface and cell-to-cell contact would be changed.

6.3 Results

Enrichment of monocytes was performed by positive selection of CD172a+ cells from PBMC using magnetic separation technology (Miltenyi Biotec). The purity of the monocytes was measured by flow

cytometry by staining the positive selected cells with phycoerythrin (PE)-conjugated goat anti-mouse IgG1 secondary antibody. PBMC (pre-stained with anti CD172a antibody) were likewise stained with the secondary PE-conjugated antibody and the two cell populations were analyzed on a BD FACSCanto™ II flow cytometer (BD Biosciences) Figure 21A.

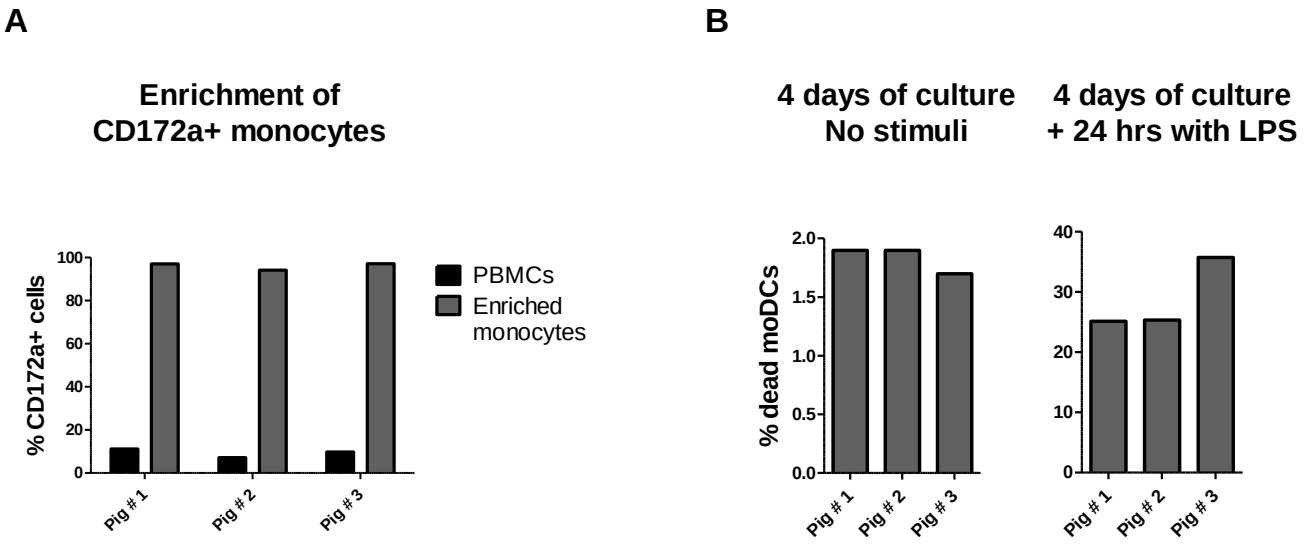

Figure 21: Purification of CD172a+ monocytes (A) and viability check of moDCs before and after LPS (B). Viability was checked on cells cultured conventionally (on 2D polystyrene surfaces) using the live/dead stain 7-amino-actinomycin D (7-AAD). LPS, lipopolysaccharide.

Prior to enrichment, monocytes constituted app. 10% of total PBMCs. After enrichment the percentages of monocytes exceeded 94% for all three pigs, so the purification was successful. Monocytes were then cultured using different culture setups as described in paper II, with addition of GM-CSF and IL-4 for the generation of moDCs. After 4 days of culture, monocytes cultured conventionally in wells of polystyrene plates, had differentiated into moDCs based on morphology and surface marker expression (presented in paper II). A viability check showed that cultured moDC were viable, with only 1-2% dead cells, Figure 21B. After additional 24 hrs stimulation with lipopolysaccharide (LPS), this resulted in an increased proportion of dead cells, which were between app. 25-35%. This did not seem to affect the RNA quality when purified from cell lysates though, since

this was found to be very high. The effect of culturing monocytes using different culture setups are presented in paper II.

Paper II

Investigating the role of surface materials and three dimensional architecture on in vitro differentiation of porcine monocyte-derived dendritic cells

Sofie Bruun Hartmann[a], Soumyaranjan Mohanty[b], Kerstin Skovgaard[a], Louise Brogaard[a], Frederikke Bjergvang Flagstad[a], Jenny Emnéus[b], Anders Wolff[b], Artur Summerfield[c] and Gregers Jungersen[a]#

[a] National Veterinary Institute, Technical University of Denmark, Frederiksberg C, Denmark,

[b] Department of Micro- and Nanotechnology, Technical University of Denmark, Kgs. Lyngby, Denmark,

[c] Institute of Virology and Immunology (IVI), Mittelhäusern, Switzerland

Corresponding author

Manuscript submitted to PLOS ONE

In this study we investigate the effect of culture conditions when generating porcine monocyte-derived dendritic cells (moDC) *in vitro*. We compare traditional polystyrene (PS) culture surface material with an untraditional culture surface made from polydimethylsiloxane (PDMS), a material frequently used for lab-on-a-chip device fabrication. Additionally, we examine the effect on moDC when cultured on three-dimensional scaffolds compared to two dimensional surfaces. Interestingly, we were able to show that both the culture surface material (PS vs. PDMS) as well as the dimension (2D vs. 3D) resulted in changes in gene expression. PDMS generated cells with a macrophage-like phenotype and 3D cultures had a positive effect on the activation profile of the cells. With this study, we show how sensitive moDCs are to their surrounding environment and that it is possible to modulate the gene expression of these cells simply by changing the culture material and architecture.

Abstract

In vitro generation of dendritic-like cells through differentiation of peripheral blood monocytes is typically done using two-dimensional polystyrene culture plates. In the process of optimizing cell culture techniques, engineers have developed fluidic micro-devises usually manufactured in materials other than polystyrene and applying three-dimensional structures more similar to the *in vivo* environment. Polydimethylsiloxane (PDMS) is an often used polymer for lab-on-a-chip devices but not much is known about the effect of changing the culture surface material from polystyrene to PDMS. In the present study the differentiation of porcine monocytes to monocyte-derived dendritic cells (moDCs) was investigated using CD172a^{pos} pig blood monocytes stimulated with GM-CSF and IL-4. Monocytes were cultured on surfaces made of two- and three-dimensional polystyrene as well as two- and three-dimensional PDMS and carbonized three-dimensional PDMS. Cells cultured conventionally (on two-dimensional polystyrene) differentiated into moDCs as expected. Interestingly, gene expression of a wide range of cytokines, chemokines, and pattern recognition receptors was influenced by culture surface material and architecture. Distinct clustering of cells, based on similar expression patterns of 46 genes of interest, was seen for cells isolated from two- and three-dimensional polystyrene as well as two- and three-dimensional PDMS. Changing the material from polystyrene to PDMS resulted in cells with macrophage-like characteristics. When changing to three-dimensional culture the cells became more activated in terms of *IL6, IL8, IL10* and *CCR5* gene expression. Further stimulation with LPS resulted in a slight increase in the expression of maturation markers (*SLA-DRB1, CD86* and *CD40*) as well as cytokines (*IL6, IL8, IL10* and *IL23A*) but the influence of the surfaces was unchanged. These findings highlights future challenges of combining and comparing data generated from microfluidic cell culture-devices made using alternative materials to data generated using conventional polystyrene plates used by most laboratories today.

1. Introduction

Dendritic cells (DCs) are a heterogenic group of antigen presenting cells important for induction of immunological responses. *In vitro* generation of DCs is a technique that has been practiced for decades (1). It can be difficult to harvest sufficient quantities of DCs for characterization and study,

and therefore *in vitro* generated monocyte-derived dendritic cells (moDCs) have been used as an alternative. With this technique peripheral blood mononuclear cells (PBMCs) are harvested, and monocytes isolated and cultured with growth factors, such as granulocyte macrophage colony-stimulating factor (GM-CSF) and interleukin 4 (IL-4) (2). With the central role of DCs as immune modulators and with the observation that cancer patients have DCs with reduced capacity to initiate efficient Th1 immune responses (3,4), controlling the differentiation of DCs may result in generation of cells able to activate *in vivo* immune responses against antigenic targets that otherwise are not recognized as immunogenic. An example of this is Provenge® (Sipuleucel-T), an FDA registered immunotherapy treatment for prostate cancer (5). Thus, *in vitro* culture systems for controlled DC maturation, differentiation and immune priming hold promise for activation or deactivation of the immune system against antigenic targets which are inaccessible with current immunization protocols.

In the present study, the pig was used as monocyte donor. The reason this animal was chosen was because of the increasing interest in using porcine models for human diseases. The number of research groups working with the porcine model has been steadily expanding for the last 50 years as judged by the number of publications in PubMed within this area. Advantages using the pig over rodents as animal models for human diseases have been summarized in (6) and includes comparable organ size, large number of cells that can be harvested repeatedly, and blood physiology being similar to humans. The porcine immune system also resembles the human immune system with respect to toll-like receptors (TLR) and DC biology (7). Porcine DCs have been characterized in several studies (8–14), and much information is already available making the use of this animal as a model for *in vitro* DC differentiation more attractive.

Today most *in vitro* cell studies and cultures are performed using standard flat-bottom polystyrene (PS) culture plates/flasks. This however, constitutes a very non-physiological environment for the cells to grow in and therefore new three dimensional (3D) culture-systems for mammalian cells are gaining increasing interest. Cells cultured in a 3D environment, are largely thought to behave more like *in vivo* compared to cells cultured on a two dimensional (2D) surface, thus making data on

gene expression, motility and activity more reliable and comparable to *in vivo* settings (reviewed in (15,16)).

An emerging field within the cell culture area is the use of fabricated micro devices for the study of cells or tissues. By the use of microfluidics, these lab-on-a-chip devices allows for the study of cells using only a small fraction of reagents, and cell analysis can be performed directly in the chip (17). However, these devises are typically not produced in PS due to difficulties of production, including challenges associated with bonding of thermoplastic materials and production of molds capable of resisting high temperatures and pressures used in hot embossing processes (18). Alternative polymers with properties suitable for e.g. soft lithography are preferably used. One of these polymers often used is polydimethylsiloxane (PDMS) (19). Since most reported *in vitro* results on cell activity/behavior originates from cells cultured on PS surfaces, not much is known about the effect of changing the culture surface material from PS to other materials more frequently used within micro devise fabrication.

However, a few studies do exist, and it has previously been reported that PDMS affects the gene expression of adrenal phaeochromocytoma (PC12) cells (20). The authors found that when cells were cultured on polymethyl methacrylate (PMMA) 6 genes were up-regulated and 35 were down-regulated compared to cells cultured on a PS surface. By contrast, when cells were cultured on a perforated PMMA surface with a PDMS layer underneath 642 genes were up-regulated and 35 were down-regulated compared to cells cultured on PS. They conclude that PDMS opposed to PMMA has a major impact on the gene expression of PC12 cells. Many of the genes differently expressed in the PC12 cells were involved in neuronal cell development and function and so it would be interesting to find out if PDMS had a similar effect on the differentiation of porcine dendritic cells, thus giving rise to cells with a more differentiated and activated phenotype. Therefore, in the present study the differentiation of monocytes to moDCs was investigated using CD172a^{pos} pig blood monocytes stimulated 4 days with GM-CSF and IL-4 followed by 24 hr activation with lipopolysaccharide (LPS). Monocytes were cultured on PS, PDMS and a pyrolysed (carbonized) form of PDMS (21). Additionally, 2D culture surfaces were compared with 3D scaffolding variants. The purpose of this study was to

explore possible changes in gene expression of moDCs when generated on alternative culture surfaces, including materials preferably used for fabrication of micro devices, and 3D vs. 2D architecture.

2. Materials and methods

2.1. Isolation of PBMCs

Fresh, heparinized whole blood was collected from three 7-8 weeks old pigs (Yorkshire-Landrace x Duroc crossing) housed at the animal facility at The Veterinary Institute, Technical University of Denmark. PBMCs were isolated using Ficoll-Paque™ Plus (GE Healthcare) and following two washes, cells were counted using an automated cell counter (Nucleocounter® NC-200™, ChemoMetec) and diluted in RPMI 1640 medium with GlutaMAX™ (Gibco, Life Technologies™) containing 10% heat inactivated fetal calf serum (FCS). Animals were kept and sampled under approval by The National Animal Experiments Inspectorate.

2.2. Monocyte enrichment

Enrichment of CD172a (SWC3) positive monocytes was done using the MACS magnetic separation technology (Miltenyi Biotec). Briefly, PBMCs were resuspended in MACS buffer (PBS/5xEDTA/1%FCS) and labelled with mouse anti-porcine CD172a IgG1 (clone 74-22-15) at 5.5 µg/10^6 target cells. After 20 min incubation on ice followed by two washes, MACS magnetic anti-mouse IgG microbeads was added (2 µl/10^6 target cells) and cells were incubated on ice for 15 min and washed twice. The CD172a positive cells were purified using equilibrated LS columns placed in a magnet on a MACS multistand. The positive fraction was collected, washed, counted and resuspended in complete cell culture medium (see below). The purity was confirmed by incubating with phycoerythrin (PE)-conjugated goat anti-mouse IgG1 secondary antibody (Southern Biotechnology) followed by analysis on a BD FACSCanto™ II flow cytometer (BD Biosciences, USA) and was found to be above 94% (data not shown).

2.3. Preparation of cell culture surfaces

The five different surfaces tested in the present experiment are listed in table 1. Microtiter plates were from Corning Scientific and were either in 6-well (cat# 3516) or 24-well (cat# 3526) format for the 2D and 3D incubations, respectively. They were made in polystyrene, thus empty well on the 6-well plates represented 2D PS surfaces (control). The 3D PS surfaces were made by placing a porous polystyrene 3D scaffold, Alvetex® (Reinnervate) in the bottom of the wells in 24-well plates. For the 2D PDMS surface, PDMS pre-polymer was mixed with a curing agent (10:1, w/w) according to the manufacturer's instructions (Sylgard® 184, Dow Corning Corporation) and poured in a thin layer into the wells of 6 well plates followed by curing in an oven at 60°C for 4 hours.

The random pore 3D PDMS scaffolds were fabricated using particle leaching technique as described previously (22,23) (Fig. 1). Briefly, 10 gram of sugar crystals of size ranging from 300-600µm (Sigma-Aldrich) was mixed with 1ml of water on a 100 mm Petri dish. The mixture was placed in an oven at 60°C to generate interconnections between the sugar crystals and to evaporate the excess water. The hardened sugar cube was cooled at room temperature. The PDMS pre-polymer was mixed with a curing agent (10:1, w/w) and poured into the Petri dish containing the sugar cube. The PDMS covered sugar cube was placed in a vacuum desiccator for one hour to let the PDMS infiltrate into the pores of the sugar cube. The PDMS was cured in an oven at 60 °C for 4-6 hours. The sugar particles were then dissolved by soaking in water for 4 hours. After dissolving, random micro-porous 3D PDMS scaffolds were cut to cylinders having a diameter of 6 mm and a height of 5 mm, fitting into wells of 24-well plates, using biopsy punches. Both the 2D PDMS surface and the 3D PDMS scaffolds were treated with oxygen plasma (125 W, 13.5 MHz, 50 sccm, and 40 millitorr) to render their surface hydrophilic and sterilized by autoclaving.

The pyrolysed 3D PDMS scaffolds were made by pyrolysing the 3D PDMS scaffolds made by square sugar cubes in a furnace at 900°C for one hour in N_2 atmosphere, resulting in highly porous and hydrophilic square 3D carbonized scaffolds (21). The morphology and microstructure of PDMS and carbonized PDMS porous scaffolds were examined using scanning electron microscopy (SEM) (JEOL Ltd.). Prior to SEM analysis scaffolds were dried in an oven at 60°C overnight and sputter coated

with gold. Samples were then analyzed using 12 kV of accelerating voltage. Pore sizes of the molds and scaffolds were evaluated from SEM micrographs using Image J software.

Table 1: Overview of culture surfaces tested

Surface		Description
2D PS	Two-dimensional polystyrene	6-well plate with no insert (Corning Scientific)
2D PDMS	Two-dimensional polydimethylsiloxane	PDMS moulded in the wells of 6-well plates creating a thin surface layer
3D PS	Three-dimensional polystyrene	Alvetex® discs inserted into wells of 24-well plates (Reinnervate)
3D PDMS	Three-dimensional polydimethylsiloxane	Random micro-porous scaffolds inserted into wells of 24-well plates (22,23)
Pyrolysed 3D PDMS	Pyrolysed three-dimensional polydimethylsiloxane	Carbonised random micro-porous scaffolds inserted into wells of 24-well plates (21)

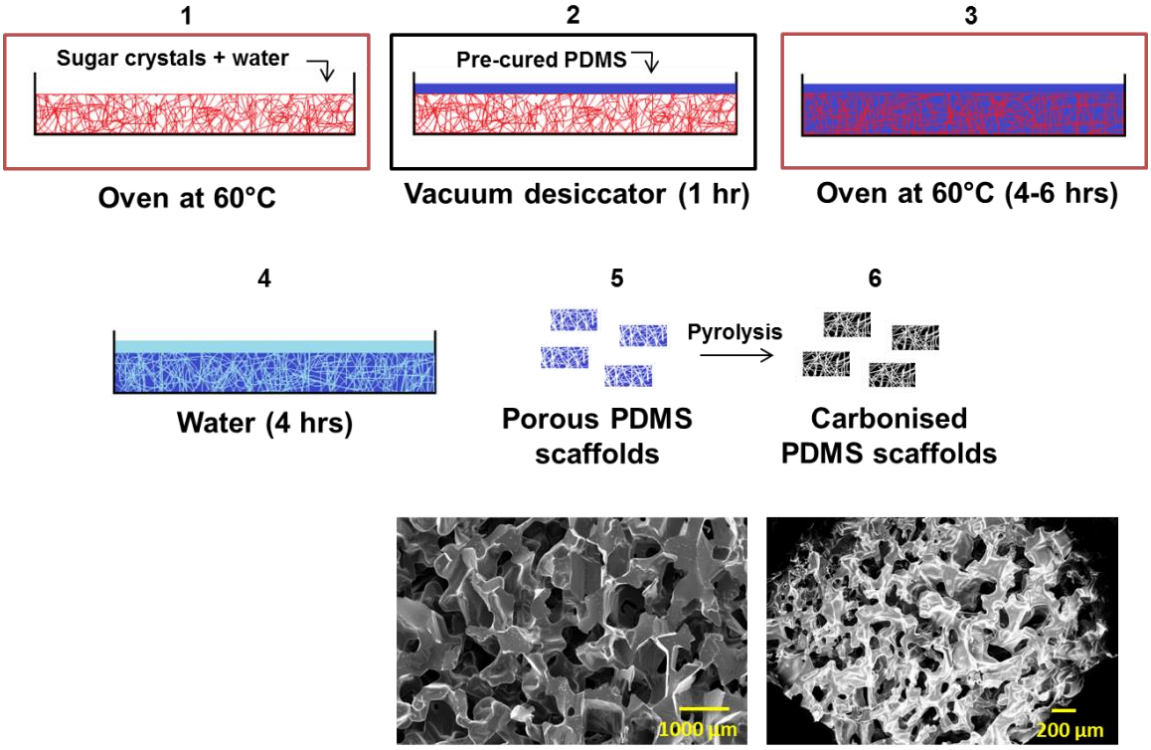

Fig. 1: 3D PDMS and pyrolysed 3D PDMS scaffold manufacturing. Sugar crystals mixed with water was incubated at 60°C to interconnect the sugar crystals (1), pre-cured PDMS was poured on top of the sugar and placed in a vacuum desiccator (2) to let the PDMS infiltrate the sugar. After an additional incubation at 60°C (3) the PDMS/sugar cube was soaked in water (4) to dissolve the sugar. Disks of random micro-porous PDMS were cut to fit the wells of a 24 well-plate (5). 3D PDMS scaffolds made from square sugar cubes were incubated at 900°C in N_2 atmosphere resulting in carbonised 3D random micro-porous PDMS (6). Bottom photographs are SEM images showing a 3D PDMS scaffold (left) and pyrolysed 3D PDMS scaffold (right).

2.4. Cell culture and harvesting

Cells were kept in culture medium (DMEM minus phenol red, high glucose containing 1xNEAA, 1xsodium pyruvate, 1xGlutaMax™ supplement, penicillin/streptomycin (100 U/ml and 100 µg/ml, respectively), Fungizone (2µg/ml) (all from Gibco/Life Technologies) and 10% porcine serum (Biochrom)). Prior to cell plating the 3D PS surface was made hydrophilic by adding 70% ethanol followed by two washes with PBS. The 3D PDMS and pyrolysed 3D PDMS surfaces were prepared by washing them twice in PBS. For the 3D surfaces, 1 or 2 $x10^6$ cells (for flow cytometry or gene expression analysis, respectively) in a 100-300µl volume was carefully placed on top of the scaffolds, and the plates were pre-incubated at 37°C, 5% CO^2 for 1 hour in order for the cells to settle within the

scaffold. Media containing recombinant porcine GM-CSF and IL-4 (R&D Systems) at a final concentration of 100 and 25ng/ml, respectively, was added to reach a final volume of 2ml per well. Plating of cells on 2D surfaces was done similarly except for the 1 hour pre-incubation step. After three days of incubation, additional 500µl of fresh medium containing GM-CSF and IL-4 was added to all cultures. On day four, half of the cultures received 50µl of LPS (Sigma) at a final concentration of 1µg/ml and were incubated for additional 24 hours. After four days of incubation (five days for the LPS stimulated cultures) cells were harvested by collecting the supernatant and adding ice-cold PBS/5xEDTA to the wells followed by 15 min incubation on ice, shaking. The scaffolds from the 3D cultures were placed in 15 ml tubes (the 3D PS scaffolds were placed in a pipette tip in a 15 ml tube), 1 ml ice-cold PBS/5xEDTA was added and tubes were centrifuged (5 min, 5°C, 500 x g). The cell solution was pooled with the supernatant, centrifuged (5 min, 5°C, 500 x g) and resuspended in RLT buffer (Qiagen) and stored at -80°C for later gene expression analysis or resuspended in FACS buffer (see below) for characterization using flow cytometry. For visualization of cell morphology, moDCs and monocytes (cultured in media with or without differentiating cytokines, respectively) cultured on 2D PS surfaces were inspected using an inverted Leica DMIL contrasting microscope equipped with a Leica DFC290 camera (Leica Microsystems) at day 1, 4, and 5.

2.5. Flow cytometry

For characterization of surface marker expression, cells were stained and analyzed by flow cytometry. Cells were distributed in 96-well plates and washed once in FACS buffer (PBS, 0.1% sodium azide, 1% FCS) and incubated 20 min in the dark with 20µl primary antibodies or isotype controls in four antibody cocktails, see table 2. Following three washes, cells were incubated 20 min in the dark with 20µl secondary antibodies, as listed in table 2. For compensation adjustments and viability check, pooled cells were stained with either mouse anti-porcine CD172a IgG1 in combination with PE-, APC- or FITC-conjugated anti-mouse IgG1 antibodies, biotin-conjugated CD152 (CTLA-4)-muIg in combination with V450-conjugated streptavidin or the dead cell marker 7-aminoactinomycin D (7-AAD) (Sigma-Aldrich). Cells were washed three times and resuspended in FACS sheath fluid containing

0.5% paraformaldehyde. Cells were loaded on a BD FACSCanto™ II flow cytometer (BD Biosciences, USA) and the results were analyzed using BD FACSDiva software version 8.0.1.

Table 2: Staining overview

Primary staining

Cocktail #	Primary antibody	Conjugate	Isotype	Clone	Company
1	Mouse anti-porcine CD172a	-	IgG1	74-22-15	DTU Vet[a]
	Mouse anti-porcine SLA class II DR	FITC	IgG2b	2E9/13	AbD Serotec
	CD152(CTLA-4)-muIg (fusion protein)	Biotin	IgG2a	-	Ancell
2	Mouse anti-porcine CD1	-	IgG2a	76-7-4	VMRD
	Mouse anti-porcine CD14	-	IgG1	CAM36A	VMRD
3	Anti-mouse IgG2b (isotype control)	FITC	-	-	AbD Serotec
	Anti-mouse IgG1 (isotype control)	-	-	-	DAKO
	Anti-mouse IgG2a (isotype control)	-	-	-	DAKO
4	muIgFc control (fusion protein)	Biotin	-	-	Ancell

Secondary staining

Cocktail #	Secondary antibody	Conjugate	Isotype	Clone	Company
1	Goat anti-mouse IgG1	PE	-	-	Southern Biotechnology
	Streptavidin	V450	-	-	BD Biosciences
2	Goat anti-mouse IgG2a	FITC	-	-	Southern Biotechnology
	Goat anti-mouse IgG1	APC	-	-	Southern Biotechnology
3	Goat anti-mouse IgG1	APC	-	-	Southern Biotechnology
	Goat anti-mouse IgG1	PE	-	-	Southern Biotechnology
	Goat anti-mouse IgG2a	FITC	-	-	Southern Biotechnology
4	Streptavidin	V450	-	-	BD Biosciences

[a]Produced at The Veterinary Institute, Technical University of Denmark. FITC, Fluorescein isothiocyanate; PE, Phycoerythrin; APC, Allophycocyanin.

2.6. RNA extraction

Total RNA was purified from RLT-buffered cell lysates using the RNeasy Mini kit (Qiagen) including an on-column DNase treatment (Qiagen) according to the manufacturer's instructions. The RNA quantity and quality was measured using a NanoDrop ND-1000 spectrophotometer (Saveen Biotech) and the Agilent 2100 Bioanalyzer (Agilent Technologies), respectively. The average yield of total RNA was (in nanogram ± SD): 2D PS (3698 ± 734); 2D PDMS (5724 ± 785); 3D PS (275 ± 273); 3D PDMS (1340 ± 238) and pyrolysed 3D PDMS (1096 ± 381). The RNA integrity number (RIN) was determined using the Agilent RNA 6000 Nano Kit (Agilent Technologies) according to the manufacturer's instructions. All RIN numbers were between 8.1 and 10.

2.7. cDNA synthesis and pre-amplification

QuantiTect® reverse Transcription Kit (Qiagen) was used to reverse transcribe 180ng total RNA in duplicate according to the manufacturer's instructions. For the pre-amplification, cDNA was diluted 1:5 in low EDTA Tris-EDTA (TE)-buffer (VWR-Bie & Berntsen). TagMan PreAmp Master mix (1µl) (Applied Biosystems) was mixed with 2.5µl of a 200nM primer mix (containing all primer pairs used in this study) and 2.5µl diluted cDNA. Using a Thermocycler (Biometra), samples were incubated at 95°C for 10 min followed by 18 cycles of 95°C for 15 sec and 60°C for 4 min. For removal of excess primers, exonuclease I (New England Biolabs) (4U/µl) was added to the pre-amplified cDNA and samples were incubated at 37°C for 30 min and 80°C for 15 min. Pre-amplified, exonuclease-treated cDNA was diluted 1:5 in low EDTA TE-buffer and stored at -20°C until quantitative real time PCR (RT-qPCR) analysis.

2.8. Primer design and validation

Primers targeting genes involved in differentiation and activation were designed using the free software Primer3 (http://bioinfo.ut.ee/primer3-0.4.0/primer3/) as described previously (24) and synthesized at TAG Copenhagen (Copenhagen, Denmark) or Sigma-Aldrich (Denmark). All primers, primer sequences and amplicon length are listed in suppl. table S1. If possible, primers were designed to span introns to prevent amplification of genomic DNA, and BLAST searches were performed to

ensure primer specificity and absence of intraspecies polymorphisms at the primer site. For several genes, two primer pairs, annealing at different sites at the mRNA transcript, were designed. Primer amplification efficiencies and correlation coefficients were obtained by standard curves constructed from four separate dilution series of pooled pre-amplified, exonucleated cDNA. To ensure primer specificity, melting curves were visually inspected for all primer assays.

2.9 Quantitative real-time PCR

qRT-PCR was performed in 96.96 Dynamic Array Integrated Fluidic Circuits (IFC) (Fluidigm), combining 54 samples, 38 dilution curve samples, three minus reverse transcriptase controls and one non-template control, all pre-amplified (96 samples in total) with 96 primer sets for 9216 individual and simultaneous qPCR reactions. Reaction mix was prepared using the following reagents for each of the 96 reactions: 3µl TaqMan Gene Expression Master Mix (Applied Biosystems), 0.3µl 20XDNA Binding Dye Sample Loading Reagent (Fluidigm), 0.3µl 20X EvaGreen (Biotium, VWR-Bie & Berntsen) and 0.9µl low EDTA TE buffer. Reaction mix (4.5µl) was mixed with 1.5µl pre-amplified, diluted cDNA. Primer mix was prepared for each of the 96 primer sets using 3µl of 20µM primer (forward and reverse) and 3µl of 2X Assay loading Reagent (Fluidigm). The 96.96 Dynamic Array was primed in the IFC Controller (Fluidigm), and reaction mix including cDNA (5µl) and primer mix (5µl) was loaded into appropriate inlets on the chip, and again placed in the IFC controller to ensure equal distribution of cDNA and primer in the 9216 reaction chambers. The chip was then placed in the BioMark real time PCR instrument (Fluidigm), and the following cycle conditions were used: a thermal mix consisting of 2 min at 50°C, 30 min at 70°C and 10 min at 25°C, then an uracil-N-glycosylase (UNG) phase with 2 min at 50 and a hot start phase with 10 min at 95°, followed by 35 cycles with denaturation for 15 sec at 95° and annealing/elongation for 1 min at 60°C. Melting curves were generated after each run to confirm a single PCR product (from 60°C to 95°C, increasing 1°C/3 sec). Reactions were performed in duplicate (cDNA replicates). Minus RT controls (samples generated without reverse transcriptase enzyme) and non-template controls (NTC) were included to check for genomic DNA contamination and non-specific amplification, respectively. Expression data (Cq values) was acquired using the Fluidigm Real Time PCR Analysis software 3.0.2 (Fluidigm).

2.10. Data pre-processing and analysis

Data pre-processing, normalization and relative quantification was done using GenEx5 (MultiD). Data were corrected for primer efficiency for each individual assay. If primer efficiency was below 0.85 or above 1.15, a default efficiency of 0.90 was assigned and differential expression was later validated using the Rotor-Gene Q (Qiagen) qPCR platform. Normalization was done using the geometric mean of four reference genes: *hypoxanthine phosphoribosyl-transferase 1 (HPRT1), tyrosine 3-monooxygenase/tryptophan 5-monooxygenase (YWHAE), β-actin (ACTB)* and *β-2-microglobulin (B2M*), found to be the most stably expressed ones out of eight reference genes tested using both GeNorm (25) and NormFinder (26). Data from the two technical cDNA replicates were averaged, and for each specific primer set and sample, a maximum of 10% samples/primer sets with a ΔCq above ±1.5 for the two cDNA replicates was accepted. To visualize differential gene expression, expression was calculated relative to the sample with the lowest expression (highest Cq) within each primer assay. Finally the data was $\log_2$ transformed and autoscaled before principal component analysis (PCA). No statistical analyses were attempted since only three pigs were analysed in the present study. For comparison of the effect of the different culture surfaces the expression was set relative to the control surface (2D PS) and a fold change of ±2 was arbitrarily defined as the cut-off for biologically significant changes.

3. Results

3.1. Monocytes cultured conventionally with differentiating cytokines have moDC morphology and surface marker expression

In the present study, the effect of culture surface architecture and material on the *in vitro* differentiation of porcine moDC was investigated. For this purpose three pigs were used as donors. Purified CD172a positive monocytes were cultured with medium containing GM-CSF and IL-4 on surfaces that differed in material; PS, PDMS or carbonized (pyrolysed) PDMS, and dimension; 2D or 3D. After four days of culture on 2D PS in the presence of differentiating cytokines, monocytes differentiated into elongated cells with dendrites – a morphology characteristic of moDC (Fig. 2). This

was even more profound after 24 hours of activation with LPS. To confirm the differentiation into moDCs the expression of surface markers was analysed by flow cytometry. Prior to culture, monocytes were CD1 negative, CD80/86$^{negative/low}$ and MHCII^{low} (Fig. 3). After conventional (2D PS) culture with differentiating cytokines, cells were CD1^{pos}, CD80/86^{high} (especially after activation by LPS) and MHCII^{high} which further confirmed their differentiation into moDCs (9,11,12). When cultured on 3D surfaces of both materials however, cells were CD1^{neg}, CD80/86^{low} and MHCII^{low}, a phenotype resembling monocytes more than moDCs. Cells cultured on 2D PDMS had an intermediate phenotype; CD1^{low}, CD80/86^{high} and MHCII^{high}. CD14 was equally expressed by cells cultured on all five surfaces.

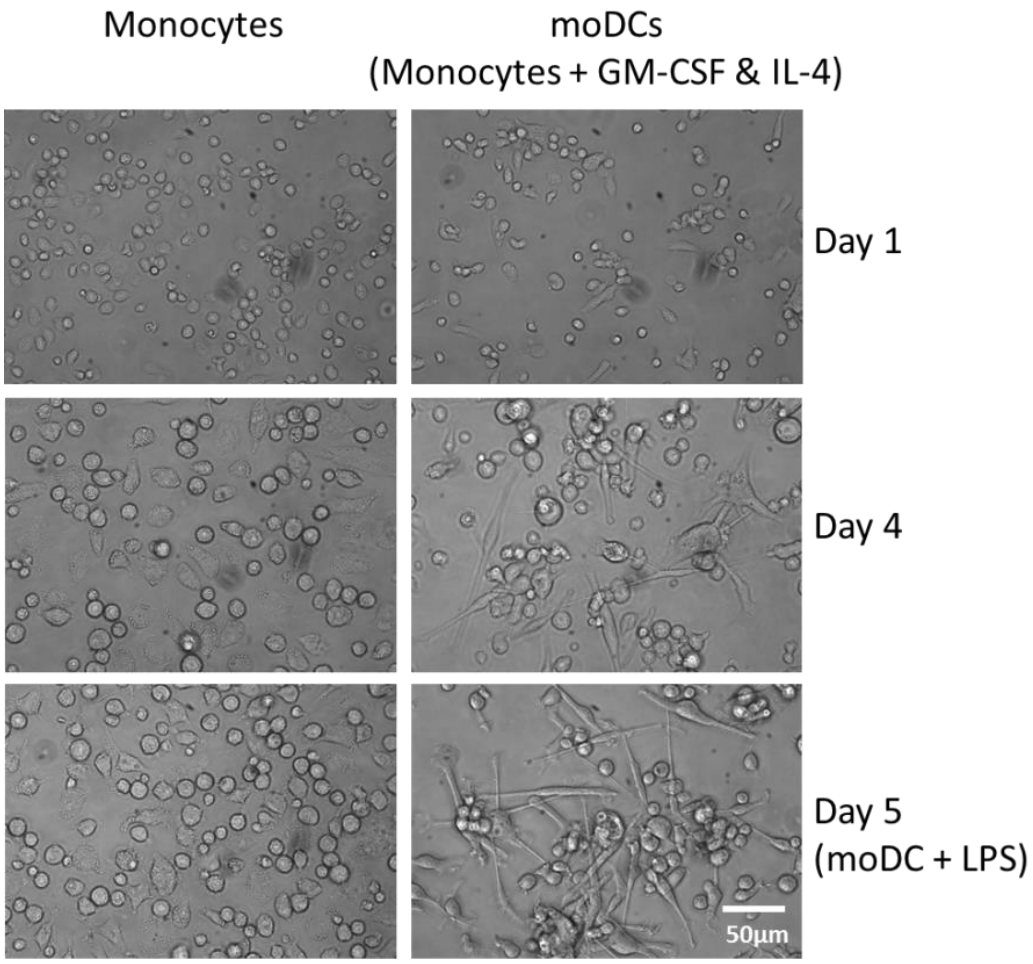

Fig. 2: Light microscopy images of monocytes and moDCs after 1, 4 and 5 days of incubation on a 2D PS surface. At day 5 the moDCs had been stimulated with LPS for 24 hours. MoDCs were generated by addition of differentiating cytokines GM-CSF and IL-4. MoDC, monocyte-derived dendritic cells; LPS, lipopolysaccharide; GM-CSF, Granulocyte-macrophage colony-stimulating factor; IL-4, interleukin 4.

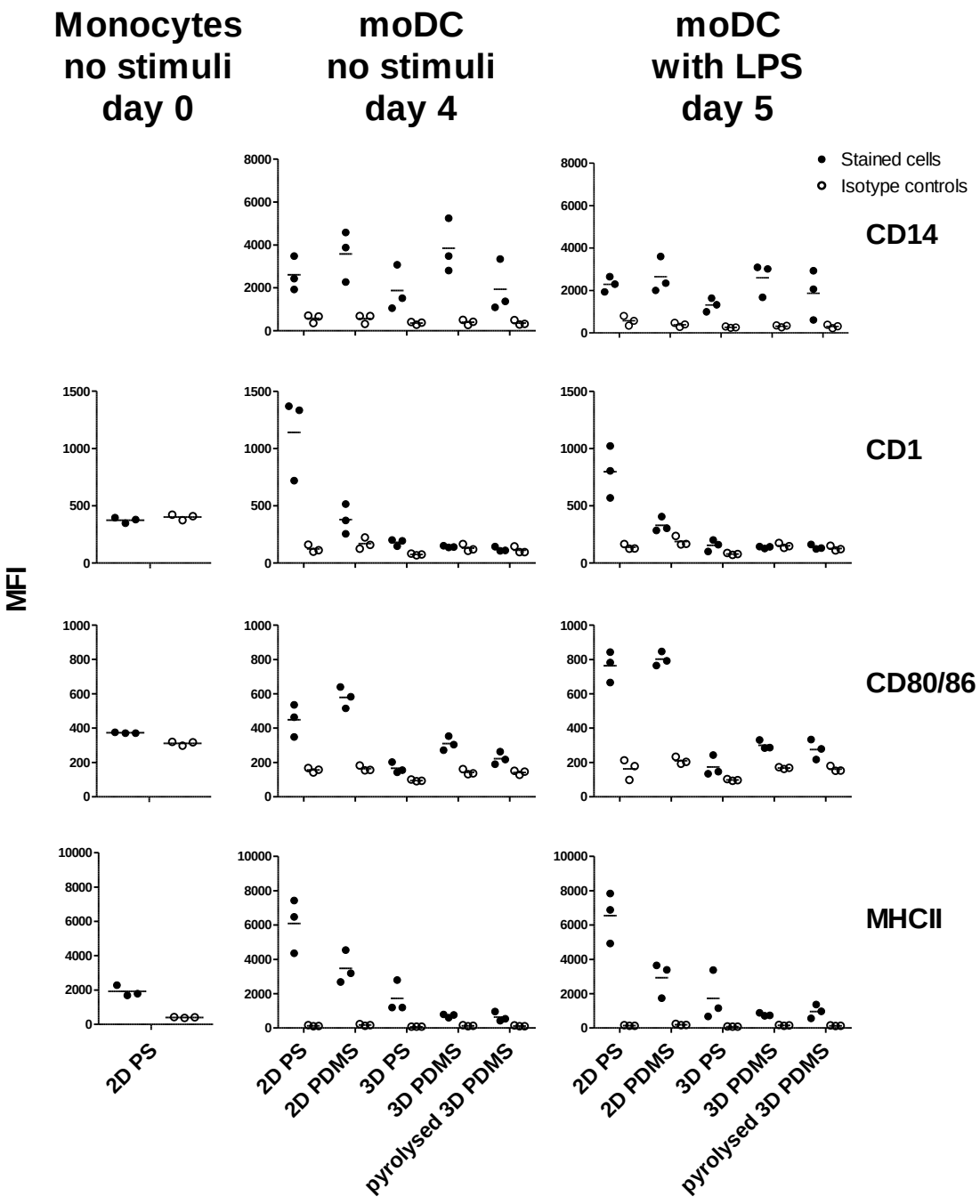

Fig. 3: Surface marker expression of porcine monocytes compared to non-stimulated (day 4) and LPS-stimulated (day 5) moDCs cultured on different surfaces. Shown is the median fluorescence intensity (MFI) of individual surface markers (n=3). Filled circles represent relevant antibody-stained samples, open circles represents isotype controls. It was not possible to detect CD14 on monocytes as this antibody had same isotype (IgG1) as the antibody used to purify the monocytes thus giving rise to false positives. PS, polystyrene; PDMS, polydimethylsiloxane; LPS, lipopolysaccharide.

3.2. Gene expression

The expression of 96 genes - 88 genes of interest and 8 reference genes was examined. Genes were selected to cover transcription factors, cytokines, maturation markers and phenotypic markers. The following genes were excluded due to expression levels below limits of detections or variable cDNA replicates: *IL12(p35), IL12(p40), IFN-β, IFN-γ, ITGAM(a), ITGAM(b), CXCL10, IL1B, TNF, CLEC4A(b), SIGLEC5(a), CCL2, ITGA4(b), CLEC1A(b), CLEC12A(a), CLEC12A(b) and CD101(b)*. Validation of differential expression was performed on 11 primers assigned with default efficiency. Expression levels from primers specific for *TLR3* could not be validated on the Rotor-Gene Q qPCR platform and was thus excluded from the analysis. For genes analyzed using two primer pairs, only one assay was analyzed further after checking the correlation coefficients between the two pairs. Thus, the following genes were excluded due to double primer assay (correlation coefficient between the two primer sets are shown in parentheses): *TLR4(a)* (0.81), *SLA-DRB1(b)* (0.95), *CD86(b)* (0.94), *CCR7(b)* (0.98), *TRAF6(a)* (0.97), *CCR5(b)* (0.97), *CXCR4(b)* (0.83), *IRF8(b)* (0.92), *FLT3(a)* (0.99), *CCR1(a)* (0.88), *IRF5(a)* (0.65), *BATF3(a)* (0.65), *ID2(a)* (0.97), *BCL11A(a)* (0.77), *BCL6(a)* (0.97), *TCF4(b)* (0.86), *CLEC2D(b)* (0.88), *CD163(b)* (0.99), *FCGR1A(a)* (0.82), *FCGR2B(a)* (0.96), *FCGR3B(a)* (0.83), *CD1a(b)* (0.99), *LAMP3(b)* (0.91) and *XCR1(a)* (0.91). Thus, a total of 46 genes were evaluated for differential gene expression, many of those with two highly correlated primer pairs targeting the same mRNA transcript, as a result of surface architecture (2D vs. 3D) and materials used for culturing. (see suppl. table S1 for complete list of primers).

3.3. The monocyte-derived cells show distinct gene expression when cultured on surfaces of alternative materials and dimension.

Principal component analysis (PCA) was performed on relative expression data of all 46 genes, to reveal patterns or clusters among samples based on co-expression patterns. Distinct clustering of cells isolated from 2D PS, 2D PDMS, 3D PS and 3D PDMS/pyrolysed 3D PDMS can be seen in Fig. 4. Most variation was explained by PC1 (eigenvalue = 30.4%) separating the cells grown on 2D compared to 3D. No separation, based on gene expression patterns, was seen between cells grown on the carbonized form of 3D PDMS and 3D PDMS. To see how the gene expression changed when cells were

cultured on alternative surfaces, the expression was compared relative to the expression on the conventional control surface (2D PS), set to 1. Both the gene expression from non-stimulated- and LPS-stimulated cells is shown in table 3. Out of the 46 genes analyzed, 29 genes had a fold change expression of ± 2 when cultured alternatively compared to control, and for the LPS-stimulated cells this number was 34. In agreement with results from the PCA, the two most variable groups of clusters (2D PS and 3D PDMS) also showed the highest number of differentially genes both in samples of no stimuli and LPS treatment. Fig. 5 summarizes the differently expressed genes across the alternative surfaces, with or without LPS.

In the non-stimulated cells, a common effect of changing the material from PS to PDMS (both 2D-, 3D- and pyrolysed 3D PDMS) was increased expression of *CD163* and decreased expression of *LAMP3* (*CD208*) and *ITGA4* (*CD49d*). The same applied for the LPS-stimulated cells, except here also the expression of *BATF3* was decreased in cells from the PDMS surfaces and the expression of *LAMP3* was, in addition to PDMS surfaces, also decreased in cells cultured on 3D PS. A common effect of changing the dimension from 2D to 3D in resting cells (both PS, PDMS and pyrolysed PDMS) was increased expression of *IL6, IL10, CCR5* and decreased expression of *BCL6, CD1a, CD209* (*DC-SIGN*) and *FCGR2B* (*CD32*). In the LPS-stimulated cells this was also the case only expression of *BCL6* was unchanged compared to control, and in addition the expression of *ID2* and *TCF4* was increased and decreased, respectively. The expression of *SLA-DRB1* (*MHCII*) was approximately the same in cells from 2D PDMS and 3D PS, but was decreased 2.3 fold (0.43) in cells from 3D PDMS and pyrolysed 3D PDMS. The same trend applied for cells stimulated with LPS. The expression of *CD86* was unchanged across the various surfaces, except for a 2 fold (0.46) downregulation in LPS-stimulated 3D PS cells. Common for all the four alternative surfaces tested was an increased expression of *IL23A* and a decreased expression of *TLR8* and *CD40* when compared to the conventional 2D PS culture surface. For the LPS-stimulated cells a decrease in the expression of *TLR8* and *LAMP3* was observed for all four alternative surfaces. The most important findings regarding the gene expression results for all tested surfaces are summarized in table 4.

Table 3:
Relative gene expression (fold change) in moDCs from alternative surfaces compared to conventional surface

	No stimuli (day 4)					LPS (day 5)				
	Control surface	Alternative surfaces				Control surface	Alternative surfaces			
	2D PS	2D PDMS	3D PS[a]	3D PDMS	Pyrolysed 3D PDMS	2D PS	2D PDMS	3D PS[b]	3D PDMS	Pyrolysed 3D PDMS
IL6	1±0.21	0.73±0.13	**4.16±1.03**	**10.31±0.99**	**11.87±0.87**	1±0.13	0.92±0.24	**6.03**	**12.12±2.03**	**22.37±4.50**
IL8	1±0.12	1.34±0.43	0.71±0.29	**4.25±1.41**	**4.42±1.19**	1±0.24	0.67±0.11	1.31	**2.61±0.42**	**4.02±0.69**
IL10	1±0.12	1.90±0.32	**8.43±2.06**	**13.56±2.87**	**18.58±3.56**	1±0.22	1.19±0.12	**7.76**	**9.68±0.88**	**12.63±0.49**
IL23A	1±0.16	**3.36±0.60**	**5.53±1.52**	**17.52±2.37**	**10.16±1.73**	1±0.15	0.61±0.07	1.81	1.16±0.38	1.60±0.48
TLR2	1±0.20	**2.20±0.22**	0.75±0.24	1.82±0.46	1.77±0.49	1±0.18	**2.35±0.25**	0.82	1.69±0.21	1.91±0.34
TLR4(b)	1±0.17	1.40±0.27	0.51±0.08	0.59±0.04	0.58±0.12	1±0.22	1.15±0.14	**0.39**	**0.45±0.07**	0.55±0.07
TLR7	1±0.30	1.00±0.31	0.77±0.04	0.91±0.32	0.84±0.26	1±0.32	0.72±0.24	**0.27**	0.71±0.25	0.62±0.17
TLR8	1±0.27	**0.09±0.05**	**0.08±0.02**	**0.01±0.00**	**0.03±0.01**	1±0.47	**0.03±0.00**	**0.04**	**0.02±0.01**	**0.01±0.00**
TLR9	1±0.53	0.83±0.47	1.34±0.69	1.17±0.60	1.00±0.40	1±0.48	**0.45±0.27**	**2.10**	0.76±0.39	0.87±0.44
IFNA	1±0.37	0.99±0.18	1.13±0.26	0.68±0.04	0.94±0.11	1±0.24	0.90±0.12	1.11	0.81±0.16	0.61±0.17
SLA-DRB1(a)	1±0.15	0.67±0.14	0.98±0.18	**0.43±0.10**	**0.43±0.11**	1±0.15	0.59±0.13	1.01	**0.32±0.05**	**0.35±0.02**
CD86(a)	1±0.16	0.97±0.04	0.67±0.02	0.90±0.06	0.95±0.15	1±0.11	0.76±0.09	**0.46**	0.67±0.04	0.71±0.09
CD40	1±0.14	**0.31±0.04**	**0.22±0.01**	**0.50±0.10**	**0.44±0.14**	1±0.17	**0.42±0.04**	0.53	**0.46±0.07**	0.57±0.06
CCR7(a)	1±0.40	**0.19±0.07**	1.16±0.60	0.74±0.23	0.57±0.17	1±0.30	**0.13±0.02**	0.61	0.66±0.16	**0.45±0.08**
TRAF6(b)	1±0.05	0.83±0.05	0.83±0.10	0.85±0.01	0.83±0.04	1±0.11	0.68±0.08	0.74	0.62±0.04	0.69±0.03
CLEC4A(a)	1±0.19	**2.21±0.62**	0.82±0.06	**2.19±0.35**	1.40±0.22	1±0.29	**3.29±0.90**	0.62	1.39±0.36	1.11±0.41
IRF1	1±0.08	1.28±0.07	0.78±0.05	1.29±0.23	1.38±0.17	1 ±0.11	0.98±0.04	0.77	0.76±0.04	0.99±0.03
CCR5(a)	1±0.23	1.91±0.59	**4.10±0.78**	**8.80±0.33**	**9.18±1.46**	1 ±0.13	1.63±0.35	**8.39**	**9.42±0.63**	**7.38±0.75**
CXCR4(a)	1±0.17	1.46±0.28	**0.27±0.01**	1.25±0.27	0.94±0.18	1±0.20	1.79±0.09	**0.41**	1.50±0.13	1.44±0.19
IRF8(a)	1±0.02	1.61±0.36	1.07±0.76	1.78±0.65	1.60±0.48	1±0.09	1.24±0.06	0.68	1.58±0.36	1.26±0.44
FLT3(b)	1±0.24	**0.40±0.11**	1.85±0.54	1.94±0.46	1.42±0.47	1±0.16	**0.20±0.08**	1.86	1.24±0.30	1.32±0.28
SIGLEC5(b)	1±0.07	1.24±0.20	1.54±0.50	**3.04±1.14**	**2.70±0.84**	1±0.28	1.24±0.31	1.49	**2.58±0.57**	**2.60±0.41**

CD209	1±0.10	**2.49±0.27**	**0.08±0.01**	**0.18±0.07**	**0.21±0.06**	1±0.18	**2.86±0.40**	**0.03**	**0.14±0.04**	**0.40±0.11**
ITGA4(a)	1±0.19	**0.32±0.03**	0.62±0.05	**0.39±0.04**	**0.49±0.05**	1±0.14	**0.23±0.05**	0.54	**0.36±0.05**	**0.49±0.08**
CCR1(b)	1±0.08	1.29±0.10	0.87±0.03	1.07±0.10	1.25±0.17	1±0.04	1.39±0.08	0.90	1.17±0.08	1.18±0.12
IRF5(b)	1±0.04	1.00±0.21	1.49±0.15	1.02±0.09	1.11±0.20	1±0.11	0.74±0.07	1.45	0.74±0.04	0.88±0.07
NFKB	1±0.06	0.59±0.04	**0.44±0.01**	0.59±0.04	0.58±0.03	1±0.06	0.56±0.10	0.59	**0.50±0.07**	0.61±0.08
BATF3(b)	1±0.14	0.85±0.05	0.56±0.07	0.83±0.15	0.76±0.14	1±0.20	**0.35±0.15**	0.80	**0.44±0.20**	**0.45±0.19**
ID2(b)	1±0.11	1.58±0.18	1.73±0.27	1.71±0.28	1.88±0.24	1±0.11	1.57±0.01	**3.19**	**2.18±0.21**	**2.76±0.07**
BCL11A(b)	1±0.15	**0.48±0.08**	0.69±0.14	1.23±0.18	0.82±0.19	1±0.17	**0.39±0.17**	0.86	0.65±0.14	**0.50±0.10**
BCL6(b)	1±0.11	0.59±0.06	**0.43±0.08**	**0.47±0.04**	**0.44±0.04**	1±0.18	0.63±0.07	0.57	0.57±0.12	0.64±0.09
TCF4(a)	1±0.21	0.73±0.21	**0.45±0.13**	0.51±0.16	0.54±0.13	1±0.24	0.60±0.14	**0.34**	**0.32±0.08**	**0.39±0.09**
MYD88	1±0.08	0.73±0.15	0.54±0.06	0.51±0.06	0.66±0.02	1±0.10	0.80±0.07	0.54	**0.43±0.04**	0.53±0.03
LY96	1±0.06	1.09±0.16	0.65±0.11	0.97±0.11	0.88±0.06	1±0.04	0.77±0.11	0.73	0.81±0.08	1.03±0.14
CLEC1A(a)	1±0.31	1.33±0.59	**0.44±0.04**	0.63±0.17	0.61±0.24	1±0.26	1.67±0.45	**0.41**	0.95±0.07	0.79±0.37
CLEC2D(a)	1±0.25	**0.33±0.00**	0.60±0.25	0.84±0.08	0.94±0.17	1±0.10	**0.32±0.02**	0.70	0.51±0.03	0.56±0.04
CXCL2	1±0.09	1.68±0.51	1.23±0.48	**5.01±1.42**	**4.82±1.41**	1±0.03	0.62±0.10	1.60	**2.31±0.56**	**3.35±0.95**
CD163(a)	1±0.30	**8.74±2.93**	**0.22±0.18**	**6.17±1.61**	**4.70±0.89**	1±0.30	**6.62±1.61**	1.20	**10.07±3.27**	**8.84±1.38**
IRF3	1±0.04	1.06±0.05	1.17±0.13	0.98±0.13	0.90±0.05	1±0.22	0.63±0.08	0.96	0.59±0.04	0.74±0.08
FCGR1A(b)	1±0.27	1.62±0.89	**0.38±0.10**	0.72±0.30	0.85±0.22	1±0.18	0.87±0.25	**0.30**	0.67±0.17	0.91±0.22
FCGR2B(b)	1±0.12	1.19±0.33	**0.17±0.01**	**0.40±0.09**	**0.38±0.11**	1±0.15	1.20±0.12	**0.25**	**0.39±0.09**	**0.42±0.07**
FCGR3B(b)	1±0.01	1.84±0.25	0.74±0.08	1.59±0.26	1.43±0.15	1±0.01	1.29±0.01	0.86	1.43±0.14	1.58±0.15
CD1a(a)	1±0.13	0.71±0.21	**0.28±0.14**	**0.03±0.00**	**0.05±0.01**	1±0.29	0.58±0.35	**0.06**	**0.02±0.01**	**0.02±0.00**
LAMP3(a)	1±0.12	**0.20±0.05**	0.62±0.20	**0.38±0.13**	**0.27±0.07**	1±0.16	**0.08±0.04**	**0.39**	**0.17±0.06**	**0.21±0.07**
XCR1(b)	1±0.20	1.12±0.28	0.56±0.11	0.79±0.13	0.81±0.10	1±0.03	1.01±0.12	1.28	0.95±0.06	1.12±0.01
CD101(a)	1±0.51	1.88±0.10	**2.05±0.35**	**2.86±0.96**	1.98±1.14	1±0.26	1.15±0.25	**2.65**	1.26±0.36	1.20±0.13
Genes with ≥2-fold regulation	**-**	**13**	**17**	**19**	**17**	**-**	**14**	**18**	**21**	**19**

Relative gene expression of moDCs from three pigs cultured on alternative material/scaffold relative to conventional culture surface (=1), analysed by qPCR±SEM. A two-fold or more regulation is marked by bold case. 2D, two-dimensional; 3D, three-dimensional; PS, polystyrene; PDMS, polydimethylsiloxane; qPCR, quantitative PCR; SEM, standard error of the mean. [a]Data generated from only two. [b]Data generated from only one pig. Please note that the data resulting from no stimuli and LPS treatment cannot be directly compared.

Table 4: Summary of findings

Culture setup	Regulation of selected genes compared to control surface[a]	Phenotype	Activation status of non-stimulated / LPS-stimulated cells
2D PS (control)	NA	MoDC	**- / +**
2D PDMS	*FLT3*[b]↓, *LAMP3*[b]↓, *BATF3*↓[b,e], *CD163*[c]↑, *IL23A*↑[d]	MDM	**+ / +**
3D PS	*CD1a*[b]↓, *FCGR2B*[b]↓, *CD163*[c]↓, *IL6*[d]↑, *IL10*[d]↑, *Il23A*[d]↑, CCR5[d]↑	MoDC/MDM	**+ + / + + +**
3D PDMS	*LAMP3*[b]↓, *CD1a*[b]↓, *FCGR2B*[b]↓, *BATF3*↓[b,e], *CD163*[c]↑, *IL6*[d]↑, *IL8*[d]↑, *IL10*[d]↑, *IL23A*[d]↑, CCR5[d]↑	MDM	**+ + / + + +**
Pyrolysed 3D PDMS	*LAMP3*[b]↓, *CD1a*[b]↓, *FCGR2B*[b]↓, *BATF3*↓[b,e], *CD163*[c]↑, *IL6*[d]↑, *IL8*[d]↑, *IL10*[d]↑, *IL23A*[d]↑, CCR5[d]↑	MDM	**+ + / + + +**

MoDC, monocyte-derived dendritic cell; MDM, monocyte-derived macrophage; NA, not applicable. [a]In non-stimulated cells; [b]DC marker; [c]macrophage marker; [d]activation marker; [e]In LPS-stimulated cells.

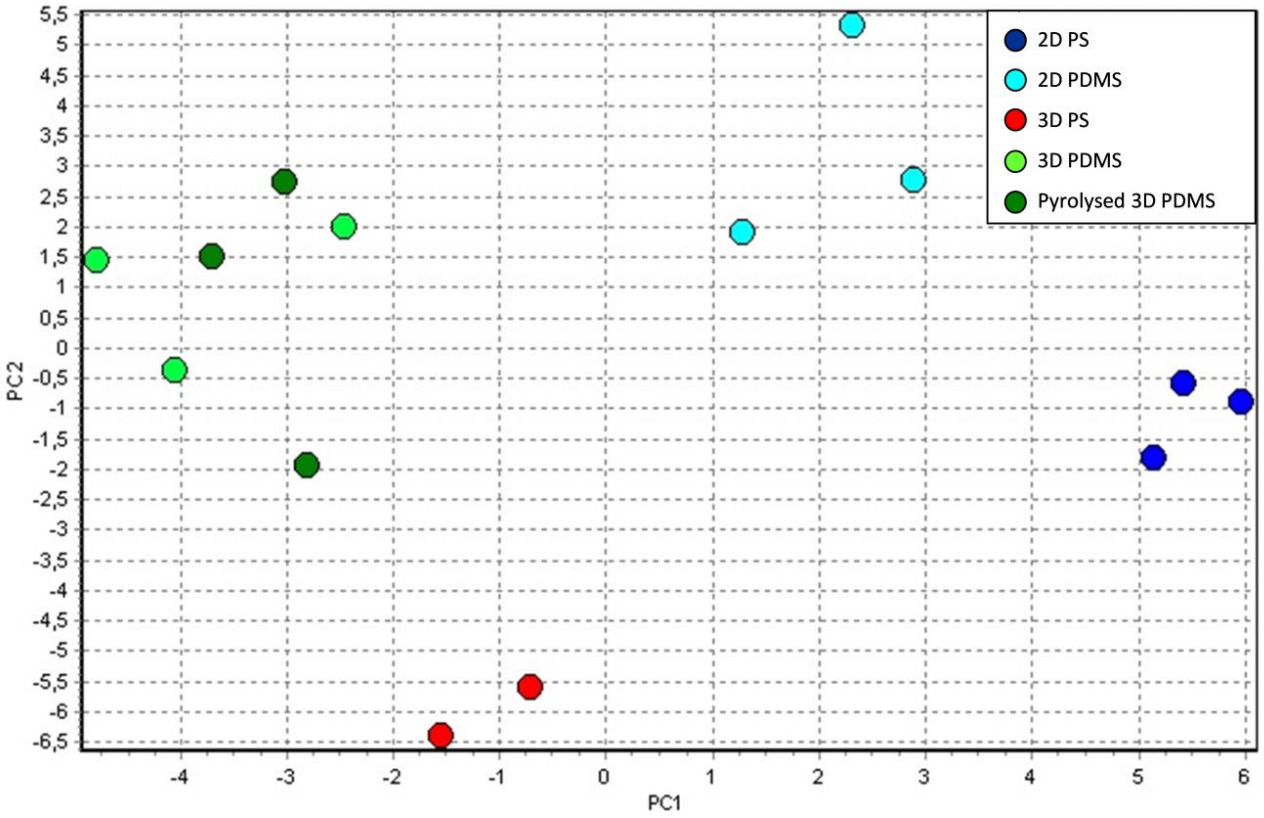

Fig. 4. Principal component analysis on LOG2, autoscaled expression data of all 47 genes. Distinct clustering of cells isolated from 2D PS (dark blue), 2D PDMS (light blue), 3D PS (red) and 3D PDMS/pyrolysed 3D PDMS (green) can be seen. The analysis is based on data from 3 pigs, except for the 3D PS culture where 2 pigs were analysed. Non-stimulated cells were used for the analysis.

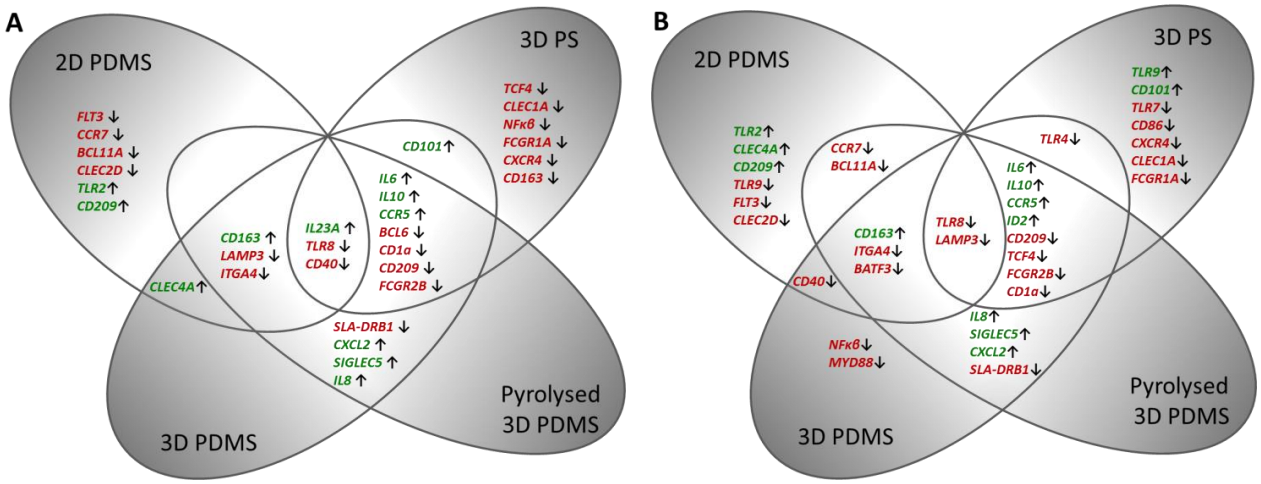

Fig. 5: Schematic illustration of the effect of culture surface on the gene expression of moDCs. Genes with at least a two-fold up- or down-regulation (see table 3) on the four alternative surfaces compared to conventional surface (2D PS) are shown for non-stimulated cells (A) and LPS-stimulated cells (B). Red = down-regulated genes, green = up-regulated genes.

4. Discussion

This study aimed at investigating the effect of changing the culture conditions when generating porcine moDCs *in vitro*. For this purpose conventional PS culture plates (2D PS) were compared with plates coated with a thin layer of PDMS (2D PDMS). The reason PDMS was chosen were because of its common usage within microfluidic cell culture devices, a field that have undergone significant growth in recent years (17,27,28). With PDMS it is easy to create highly complex fluidic features (29), a characteristic not shared by polystyrene mainly because of challenges with bonding of the material (30). The use of plastic ware for bioanalysis has evolved in two directions during the last 20 years; while engineers have become accustomed to use PDMS for fabrication of micro devices, biologists have almost entirely used PS as material of choice for culture ware, e.g. Petri dishes, culture flasks and microtiter plates (18). Therefore most of the *in vitro* biological data available today is from cells cultured on PS and thus comparison of data generated using other materials might be difficult. There is no doubt that fabricated micro devices for testing biological samples will become increasingly implemented within biomedical research, and thus generating knowledge of how cells respond to growth in/or contact with alternative materials and surface architecture is crucial.

The porcine monocytes-derived cells generated with a cocktail of GM-CSF and IL-4 had a surface phenotype typically for moDC when cultured on 2D PS (9,11,12). The phenotype when cultured on 2D PDMS was similar to 2D PS-cultured cells except for decreased expression of CD1 and MHCII. All the 3D-cultured cells had no or low expression of CD1, CD80/86 and MHCII. This was consistent with the gene expression analysis; when compared to control, the expression of *CD1a* was slightly decreased in 2D PDMS cells (a fold change of 1.4 (a relative-to-control expression of 0.71) which was, however, not categorized as being biologically significant; see material and methods), and decreased 3.5-33 fold (0.28-0.03) in cells from all three types of 3D surfaces, Table 1.

Equal weight of all 46 genes in the PCA analysis revealed a clear separation (and most variation) between cells grown at different surface architecture compared to material. Thirteen genes were expressed differently in cells from 2D PS and 2D PDMS surfaces. The most interesting observation was an increase in *CD163* and *IL23A*, and a decrease in *FLT3* and *LAMP3* expression in 2D PDMS cells compared to 2D PS. As *CD163* have been described as a monocyte/macrophage marker (6,31) and *FLT3* and *LAMP3* as markers expressed by DCs (32,33), it seems as if the cells cultured on PDMS in contrast to PS developed into macrophage-like cells with an increased activation state in the form of inflammatory cytokine expression even without the addition of LPS. Additionally, LPS-stimulated cells cultured on all three types of PDMS surfaces, had a decreased expression of *BATF3* compared to the control surface. *BATF3* is typically expressed by bona fide DC at higher levels (Gael Aurey and Artur Summerfield, unpublished data) and the downregulation on PDMS surfaces is in accordance with the cells having macrophage-like phenotypes. It was surprising to find expression of *FLT3* in the monocyte-derived cells as a previous study found this gene to be primarily expressed by bona fide DCs originating from bone marrow DC-precursors (32). An explanation could be that conventional DCs (cDCs) were present in our monocyte population to begin with as these cells also express CD172a (which was used to purify the monocytes), although at a much lower level than monocytes (34). Changing the surface to PDMS had a negative effect on the *FLT3* expression.

Adding a third dimension to the culture, i.e. 3D PDMS generated cells that in addition to the above mentioned differences in gene expression, also differed from cells on 2D PS by increased

expression of *IL6, IL8, IL10* and *CCR5*, inflammatory and regulatory cytokines and a chemokine receptor reflecting cells with higher activation status. In addition to *LAMP3*, also *CD1a* and *FCGR2b* which is usually expressed by DCs were downregulated. As shown in the PCA plot 3D PDMS and pyrolysed 3D PDMS surfaces constituted one cluster. In fact there was not much difference in their gene expression profile; only 2 genes were differently expressed compared to control on 3D PDMS but not on the pyrolysed version of the surface for non-stimulated cells. Also the level of expression was similar on the two surfaces. So the carbonization of PDMS had only minor effect on the gene expression.

Finally the effect of changing only the culture dimension was tested on the 3D PS surface. This surface clustered differently from the other surfaces and resulted primarily in downregulation of genes compared to control (12 genes were downregulated, 5 were upregulated). Cells from this surface were in an activated state based on upregulation of inflammatory and regulatory cytokines/chemokines as was the case for all 3D surfaces. Apart from the downregulation of the two DC markers, *CD1a* and *FCGR2b*, cells on this surface also downregulated the expression of the macrophage marker *CD163* which were upregulated on all the other alternative surfaces. This emphasizes that the skewing of cells toward a macrophage phenotype is dependent on surface material (PDMS) more than dimension (3D).

A concern when working with cells cultured on 3D scaffolds, is the harvesting process. It is obviously more complicated collecting cells cultured in a 3D setup compared to 2D. There is a risk of losing cells that are stuck in the scaffold and thus basing the further analysis on a fraction of the original cell pool. In this study, an equal number of cells were originally pipetted in each culture well. The cells were not counted after harvesting, but the quantity of total RNA after purification was measured, and this yield can be used as an indirect measure of initial cell quantity. All culture surfaces resulted in a relatively high total RNA yield, except for the 3D PS surface. This scaffold is a commercial available 200 µm thick porous PS membrane made using emulsion templating (35) and designed for 3D culture (36). The scaffold has a porosity of 90% and the pore size is approximately 40µm. This surface is more compact than the 3D PDMS and pyrolysed 3D PDMS scaffolds which have pore sizes of

300-600µm. We may only speculate if cells were left trapped within the pores of the 3D PS scaffold due to their relative compact architecture compared to 3D PDMS and pyrolysed 3D PDMS. The low RNA yield from 3D PS could also have to do with the material as a higher RNA yield from cells cultured on 2D PDMS compared to 2D PS was obtained. In a study on human breast cancer cells Zhang and colleagues reports a poor cell attachment on plasma oxygen-treated 2D PDMS compared to 2D PS surfaces (37). Thus the decreased RNA yield after retrieval of cells from 3D PS is probably due to a combination of cells sticking better to the polystyrene and being "trapped" in the relatively small pores of the scaffold. In any case, it seems as if the 3D PS scaffold is preferable for assays that do not require retrieval of cells after culture.

In conclusion, the effect of changing the culture setup when generating porcine moDC was tested and it was found that both material (PDMS) and architecture (3D) changed the gene expression of the cells. Even though one could wish for more biological replicates, multivariate analysis (PCA) suggest that architecture (2D vs. 3D) rather than material (PS vs. PDMS) results in differentially expression of genes involved in pattern recognition and inflammation. In contrast, genes involved in macrophage phenotype were dependent on surface material (PDMS) more than dimension (3D). These findings provide evidence of the necessity of detailed reporting of the culture conditions used when presenting gene expression results as it was found to influence the expression, which make comparisons difficult. The findings also highlight the challenges for future studies combining the analysis or generation of cells having specific phenotypes with for example microfluidic cell culture-devices fabricated using other materials than PS.

Funding information

This research received no specific grant from any funding agency in the public, commercial, or not-for-profit sectors.

Acknowledgement

We thank Ulla Riber for assistance with the flow cytometry, Karin Tarp and Panchale Olsen for assistance with the qRT-PCR, Sylvie Python for help with the cell culture protocol and William Winston Agace for discussions regarding gene selection.

References

1. Inaba K, Steinman RM, Pack MW, Aya H, Inaba M, Sudo T, et al. Identification of proliferating dendritic cell precursors in mouse blood. J Exp Med. 1992 May;175(5):1157–67.
2. Castiello L, Sabatino M, Jin P, Clayberger C, Marincola FM, Krensky AM, et al. Monocyte-derived DC maturation strategies and related pathways: a transcriptional view. Cancer Immunol Immunother. 2011 Apr;60(4):457–66.
3. Yang L, Carbone DP. Tumor-host immune interactions and dendritic cell dysfunction. Adv Cancer Res. 2004 Jan;92:13–27.
4. Kusmartsev S, Gabrilovich DI. Role of immature myeloid cells in mechanisms of immune evasion in cancer. Cancer Immunol Immunother. 2006 Mar;55(3):237–45.
5. Buonerba C, Ferro M, Di Lorenzo G. Sipuleucel-T for prostate cancer: the immunotherapy era has commenced. Expert Rev Anticancer Ther. 2011 Jan;11(1):25–8.
6. Fairbairn L, Kapetanovic R, Sester DP, Hume DA. The mononuclear phagocyte system of the pig as a model for understanding human innate immunity and disease. J Leukoc Biol. 2011 Jun;89(6):855–71.
7. Meurens F, Summerfield A, Nauwynck H, Saif L, Gerdts V. The pig: a model for human infectious diseases. Trends Microbiol. 2012 Jan;20(1):50–7.
8. Kyrova K, Stepanova H, Rychlik I, Polansky O, Leva L, Sekelova Z, et al. The response of porcine monocyte derived macrophages and dendritic cells to Salmonella Typhimurium and lipopolysaccharide. BMC Vet Res. 2014 Jan;10(1):244.
9. Johansson E, Domeika K, Berg M, Alm G., Fossum C. Characterisation of porcine monocyte-derived dendritic cells according to their cytokine profile. Vet Immunol Immunopathol. 2003 Feb;91(3-4):183–97.
10. Facci MR, Auray G, Buchanan R, van Kessel J, Thompson DR, Mackenzie-Dyck S, et al. A comparison between isolated blood dendritic cells and monocyte-derived dendritic cells in pigs. Immunology. 2010 Mar;129(3):396–405.

11. Carrasco CP, Rigden RC, Schaffner R, Gerber H, Neuhaus V, Inumaru S, et al. Porcine dendritic cells generated in vitro: morphological, phenotypic and functional properties. Immunology. 2001 Oct;104(2):175–84.

12. Chamorro S, Revilla C, Gómez N, Alvarez B, Alonso F, Ezquerra A, et al. In vitro differentiation of porcine blood CD163- and CD163+ monocytes into functional dendritic cells. Immunobiology. 2004 Jan;209(1-2):57–65.

13. Summerfield A, Auray G, Ricklin M. Comparative dendritic cell biology of veterinary mammals. Annu Rev Anim Biosci. 2015 Jan;3:533–57.

14. Summerfield A, McCullough KC. The porcine dendritic cell family. Dev Comp Immunol. 2009 Mar;33(3):299–309.

15. Pampaloni F, Reynaud EG, Stelzer EHK. The third dimension bridges the gap between cell culture and live tissue. Nat Rev Mol Cell Biol. Nature Publishing Group; 2007 Oct;8(10):839–45.

16. Ravi M, Paramesh V, Kaviya SR, Anuradha E, Solomon FDP. 3D cell culture systems: advantages and applications. J Cell Physiol. 2015 Jan;230(1):16–26.

17. El-Ali J, Sorger PK, Jensen KF. Cells on chips. Nature. 2006 Jul;442(7101):403–11.

18. Berthier E, Young EWK, Beebe D. Engineers are from PDMS-land, Biologists are from Polystyrenia. Lab Chip. The Royal Society of Chemistry; 2012 Mar;12(7):1224.

19. McDonald JC, Duffy DC, Anderson JR, Chiu DT, Wu H, Schueller OJ, et al. Fabrication of microfluidic systems in poly(dimethylsiloxane). Electrophoresis. 2000 Jan;21(1):27–40.

20. Łopacińska JM, Emnéus J, Dufva M. Poly(dimethylsiloxane) (PDMS) affects gene expression in PC12 cells differentiating into neuronal-like cells. PLoS One. 2013 Jan;8(1):e53107.

21. Mohanty S, Amato L, Heiskanen A, Keller SS, Boisen A, Wolff A, et al. Conducting pyrolysed carbon scaffold for tissue engineering. Proc 39th Int Conf Micro Nano Eng. 2012;

22. Cha KJ, Kim DS. A portable pressure pump for microfluidic lab-on-a-chip systems using a porous polydimethylsiloxane (PDMS) sponge. Biomed Microdevices. 2011 Oct;13(5):877–83.

23. Mohanty S, Sanger K, Heiskanen A, Trifol J, Szabo P, Dufva M, et al. Fabrication of scalable tissue engineering scaffolds with dual-pore microarchitecture by combining 3D printing and particle leaching. Mater Sci Eng C. 2016 Apr;61:180–9.

24. Skovgaard K, Mortensen S, Boye M, Poulsen KT, Campbell FM, Eckersall PD, et al. Rapid and widely disseminated acute phase protein response after experimental bacterial infection of pigs. Vet Res. Jan;40(3):23.

25. Vandesompele J, De Preter K, Pattyn F, Poppe B, Van Roy N, De Paepe A, et al. Accurate

normalization of real-time quantitative RT-PCR data by geometric averaging of multiple internal control genes. Genome Biol. BioMed Central Ltd; 2002 Jun;3(7):RESEARCH0034.

26. Andersen CL, Jensen JL, Ørntoft TF. Normalization of real-time quantitative reverse transcription-PCR data: a model-based variance estimation approach to identify genes suited for normalization, applied to bladder and colon cancer data sets. Cancer Res. 2004 Aug;64(15):5245–50.

27. Folch A, Toner M. Microengineering of cellular interactions. Annu Rev Biomed Eng. Annual Reviews 4139 El Camino Way, P.O. Box 10139, Palo Alto, CA 94303-0139, USA; 2000 Jan;2:227–56.

28. Tehranirokh M, Kouzani AZ, Francis PS, Kanwar JR. Microfluidic devices for cell cultivation and proliferation. Biomicrofluidics. 2013 Jan;7(5):51502.

29. Kartalov EP, Anderson WF, Scherer A. The Analytical Approach to Polydimethylsiloxane Microfluidic Technology and Its Biological Applications. J Nanosci Nanotechnol. 2006 Aug;6(8):2265–77.

30. Kim L, Toh Y-C, Voldman J, Yu H. A practical guide to microfluidic perfusion culture of adherent mammalian cells. Lab Chip. The Royal Society of Chemistry; 2007 Jun;7(6):681–94.

31. Sánchez C, Doménech N, Vázquez J, Alonso F, Ezquerra A, Domínguez J. The porcine 2A10 antigen is homologous to human CD163 and related to macrophage differentiation. J Immunol. American Association of Immunologists; 1999 May;162(9):5230–7.

32. Guzylack-Piriou L, Alves MP, McCullough KC, Summerfield A. Porcine Flt3 ligand and its receptor: generation of dendritic cells and identification of a new marker for porcine dendritic cells. Dev Comp Immunol. 2010 Apr;34(4):455–64.

33. Jamin A, Gorin S, Le Potier M-F, Kuntz-Simon G. Characterization of conventional and plasmacytoid dendritic cells in swine secondary lymphoid organs and blood. Vet Immunol Immunopathol. 2006 Dec;114(3-4):224–37.

34. Summerfield A, Guzylack-Piriou L, Schaub A, Carrasco CP, Tâche V, Charley B, et al. Porcine peripheral blood dendritic cells and natural interferon-producing cells. Immunology. 2003 Dec;110(4):440–9.

35. Barbetta A, Dentini M, Zannoni EM, De Stefano ME. Tailoring the porosity and morphology of gelatin-methacrylate polyHIPE scaffolds for tissue engineering applications. Langmuir. American Chemical Society; 2005 Dec;21(26):12333–41.

36. Maltman DJ, Przyborski SA. Developments in three-dimensional cell culture technology aimed at improving the accuracy of in vitro analyses. Biochem Soc Trans. Portland Press Limited; 2010

Aug;38(4):1072–5.

37. Zhang W, Choi DS, Nguyen YH, Chang J, Qin L. Studying cancer stem cell dynamics on PDMS surfaces for microfluidics device design. Sci Rep. Nature Publishing Group; 2013 Jan;3:2332.

Supporting information

Supplementary Table S1: List of primers used in this study.
87 primers are listed (9 primers were excluded as they did not work).

Gene symbol	Gene name	Sequence	Amplicon length
ACTB	β-actin	F: CTACGTCGCCCTGGACTTC R: GCAGCTCGTAGCTCTTCTCC	76
B2M	β-2-microglobulin	F: TGAAGCACGTGACTCTCGAT R: CTCTGTGATGCCGGTTAGTG	70
GAPDH	Glyceraldehyde-3-phosphate dehydrogenase	F: ACCCAGAAGACTGTGGATGG R: AAGCAGGGATGATGTTCTGG	79
HPRTI	Hypoxanthine phosphoribosyl-transferase I	F: ACACTGGCAAAACAATGCAA R: TGCAACCTTGACCATCTTTG	71
RPL13A	Ribosomal protein L13a	F: ATTGTGGCCAAGCAGGTACT R: AATTGCCAGAAATGTTGATGC	76
PPIA	peptidylprolyl isomerase A (cyclophilin A)	F: CAAGACTGAGTGGTTGGATGG R: TGTCCACAGTCAGCAATGGT	138
TBP	TATA box binding protein	F: ACGTTCGGTTTAGGTTGCAG R: CAGGAACGCTCTGGAGTTCT	96
YWHAE	Tyrosine 3-monooxygenase/ tryptophan 5-monooxygenase	F: GCTGCTGGTGATGATAAGAAGG R: AGTTAAGGGCCAGACCCAAT	124
IL1B	Interleukin 1b	F: CCAAAGAGGGACATGGAGAA R: GGGCTTTTGTTCTGCTTGAG	123
IL6	Interleukin 6	F: TGGGTTCAATCAGGAGACCT R: CAGCCTCGACATTTCCCTTA	116
IL8	Interleukin 8	F: GAAGAGAACTGAGAAGCAACAACA R: TTGTGTTGGCATCTTTACTGAGA	99
IL10	Interleukin 10	F: TACAACAGGGGCTTGCTCTT R: GCCAGGAAGATCAGGCAATA	110
IL12A	Interleukin 12 p35	F: GAACTAGCCACGAATGAGAGTTG R: ACTGCTAAGGCACAGGGTTG	114
IL12B	Interleukin 12 p40	F: GACCAGAAAGAGCCCAAAAAC R: AGGTGAAACGTCCGGAGTAA	70
IL23A	interleukin 23	F: GCTGTGATCCTCAGGGACTC R: TAGAGAAGGCTCCCCTGTGA	119
TLR2	Toll like receptor 2	F: CGGAGGTTGCATATTCCACAG R: TGTGAAAGGGAACAGGGAAC	128
TLR3	Toll like receptor 3 / toll-like receptor 3 variant 1 (TLR3)	F: ACATCTACTGAAAGATCCATTGTGC R: TCTTCGCAAACAGAGTGCAT	148
TLR4(a)	Toll like receptor 4	F: TTTCCACAAAAGTCGGAAGG	145

		R: CAACTTCTGCAGGACGATGA	
TLR4(b)	Toll like receptor 4	F: TGGTGTCCCAGCACTTCATA R: CAACTTCTGCAGGACGATGA	116
TLR7	Toll like receptor 7	F: AGAAGCCCCTTCAGAAGTCC R: GGTGAGCCTGTGGATTTGTT	93
TLR8	Toll like receptor 8	F: GCAAAGACCACCACCAACTT R: ATCCGTCAGTCTGGGAATTG	129
TLR9	Toll like receptor 9	F: CCTGTTCTATGATGCCTTCGTG R: GGTACCCAGTCTCGCTCCTC	144
IFNA	Interferon alpha 1	F: ATCGTCAGGGCAGAAGTCAT R: CCAGGTGTCTGTCACTCCTTC	86
IFNB	Interferon beta	F: AGCACTGGCTGGAATGAAAC R: TCCAGGATTGTCTCCAGGTC	83
IFNG	Interferon gamma	F: CCATTCAAAGGAGCATGGAT R: TTCAGTTTCCCAGAGCTACCA	76
TNF	Tumor Necrosis Factor alpha	F: CCCCCAGAAGGAAGAGTTTC R: CGGGCTTATCTGAGGTTTGA	92
SLA-DRB1(a)	Major Histocompatibility Complex, Class II, DR Beta 1	F: TGACGGTGTATCCTGCAAAG R: GTAGAACCCGGTCACAGAGC	74
SLA-DRB1(b)	Major Histocompatibility Complex, Class II, DR Beta 1	F: GAGGTCTACAGCTGCCGAGT R: ATCTTGCCCTGAGCAGATTC	92
CD86(a)	CD86	F: CATCGTCTGTGTCCTGCAAC R: CACAGGTGGCTTTGCATCTA	82
CD86(b)	CD86	F: GAACAGGAAGGCGAGTGAAC R: ATCACACTGGGCATCATCAG	73
CD40	CD40	F: TGAGAGCCCTGGTGGTTATC R: GCTCCTTGGTCACCTTTCTG	90
CCR7(a)	Chemokine (C-C Motif) Receptor 7	F: TCCACGTCTGCAAACTCATC R: GTCGATGCTGATGCAGAGAA	83
CCR7(b)	Chemokine (C-C Motif) Receptor 7	F: GCCATGAGCTTCTGCTACCT R: CCTTGTTGCGCTCGAAGT	70
TRAF6(a)	TNF Receptor-Associated Factor 6, E3 Ubiquitin Protein Ligase	F: CTGCCATGAAAAGATGCAGA R: GCGACTGGGTATTCTCTTGC	62
TRAF6(b)	TNF Receptor-Associated Factor 6, E3 Ubiquitin Protein Ligase	F: CCAGTTCCATGCACATTCAG R: GCGACTGGGTATTCTCTTGC	91
CLEC4A(a)	C-Type Lectin Domain Family 4, Member A	F: ATGGGGTTGGAATGATGTTC R: TCATGGAGAATGTTCCACTCAT	91
IRF1	interferon regulatory factor 1	F: TGAAGCTGCAACAGATGAGG R: CTTCCCATCCACGTTTGTCT	100
CCR5(a)	Chemokine (C-C Motif) Receptor 5	F: GCCGCAATGAGAAGAAGAAG R: AGGGAGCCCAGAAGAGAAAG	81
CCR5(b)	Chemokine (C-C Motif) Receptor 5	F: CAACTTGCTGGTTGTCCTCA R: GCCAGGTTGAGCAGGTAGAT	78
CXCR4(a)	Chemokine (C-X-C Motif) Receptor 4	F: ACGGGTTCCGTATATTCACTTC R: GGAAACAGGGTTCCTTTATGG	87
CXCR4(b)	Chemokine (C-X-C Motif) Receptor 4	F: CTGCTGGCTGCCATACTACA R: TCAAACTCACACCCTTGCTG	81
IRF8(a)	Interferon Regulatory Factor 8	F: TGGGAGAACGACCAGAAGAG R: CCAGGCCTTGAAGATGGAG	99
IRF8(b)	Interferon Regulatory Factor 8	F: CCGGATTTTGAGGAAGTGAC	84

		R: CTCTTCCTCGGGGACAATG	
FLT3(a)	Fms-Related Tyrosine Kinase 3	F: ATGGATCAGCCATTTTACGC R: CGTTTCCTGGAGTCAAAAGC	77
FLT3(b)	Fms-Related Tyrosine Kinase 3	F: GCTGGAGGAGGAAGAGGACT R: TCCCTTTGGCCACTTGATAG	77
SIGLEC5(b)	Sialic Acid Binding Ig-Like Lectin 5	F: ACGCCTCGATCAAGGTCAC R: AGCTGAGTCTGAGGCTGGAG	96
CCL2	Chemokine (C-C Motif) Ligand 2	F: GCAAGTGTCCTAAAGAAGCAGTG R: TCCAGGTGGCTTATGGAGTC	103
CD209	CD209	F: CGGAGCAGAAATTCCTGAAG R: CATTGCCAGGAACCTTCATT	94
ITGA4(a)	Integrin, Alpha 4 (Antigen CD49D, Alpha 4 Subunit Of VLA-4 Receptor)	F: TCCAGAGCCAAATCCAAAAG R: GCGTTTGGGTCTTTGATGAT	94
CCR1(a)	Chemokine (C-C Motif) Receptor 1	F: CTGGCCATTTCTGACCTGAT R: ACACATGTGATCGCCAAAAA	93
CCR1(b)	Chemokine (C-C Motif) Receptor 1	F: TCCAAGAATCCCTGTTCACC R: AGGCGATGACCTCTGTCACT	81
IRF5(a)	Interferon Regulatory Factor 5	F: TCTTCAGCCTGGAGCATTTT R: CTCCCCAAAGCAGAAGAAGA	98
IRF5(b)	Interferon Regulatory Factor 5	F: AACCCCGAGAGAAGAAGCTC R: CAAGAAAGCTCCCCTGAGAA	88
NFKB1	Nuclear Factor Of Kappa Light Polypeptide Gene Enhancer In B-Cells 1	F: CTCGCACAAGGAGACATGAA R: GGGTAGCCCAGTTTTTGTCA	97
BATF3(a)	Basic Leucine Zipper Transcription Factor, ATF-Like 3	F: GTTCTGCAGAGGAGCGTTTC R: TCTCTCCTTCGGACCTTCCT	86
BATF3(b)	Basic Leucine Zipper Transcription Factor, ATF-Like 3	F: AGGAAGGTCCGAAGGAGAGA R: TTTGTCAGCCTTCTGGGTTT	78
ID2(a)	Inhibitor Of DNA Binding 2, Dominant Negative Helix-Loop-Helix Protein	F: GGACATCAGCATCCTGTCCT R: AGAGCGCTTTGCTGTCACTT	74
ID2(b)	Inhibitor Of DNA Binding 2, Dominant Negative Helix-Loop-Helix Protein	F: CCAGTGAGGTCCGTTAGGAA R: GTTGTACAGCAGGCTCATCG	99
BCL11A(a)	B-Cell CLL/Lymphoma 11A (Zinc Finger Protein)	F: ATGCGAGCTGTGCAACTATG R: GTAAACGTCCTTCCCCACCT	88
BCL11A(b)	B-Cell CLL/Lymphoma 11A (Zinc Finger Protein)	F: GAATTCTCGCCCGAACCTC R: ACACGTGAGGAGGTCATGGT	99
BCL6(a)	B-Cell CLL/Lymphoma 6	F: ATCGTCAACAGGTCCCTGAC R: GGGTGCAGGTAGAGTGGAGA	71
BCL6(b)	B-Cell CLL/Lymphoma 6	F: CAAACCTGAAAACCCACACC R: ATGGGCCACCTGTACAAATC	89
TCF4(a)	Transcription Factor 4	F: GAGTGATAAGCCCCAGACCA R: TTCCTTTCTCGGACTTGCTG	87
TCF4(b)	Transcription Factor 4	F: TCCAGTCTTCCTCCGATGTC R: GGCAGGAGGTGTACAGGAAG	78
MYD88	myeloid differentiation primary response protein 88	F: CCAGACTAAGTTTGCACTCAGC R: AGGATGCTGGGGAACTCTTT	99
LY96	Lymphocyte Antigen 96 (MD2)	F: CAGTAAAGGTTGAGCCCTGTG R: TTTGCGCATTGGTAAAGTCA	140
CLEC1A(a)	C-Type Lectin Domain Family 1, Member A	F: CCAACACTCAGCAAGACAGC R. TTCCTGTTCTGGGTTTGGAG	91
CLEC2D(a)	C-Type Lectin Domain Family 2,	F: GTCACCACATCACGTTTGGA	82

	Member D	R: GGCACATTCTCCAACTCCTC	
CLEC2D(b)	C-Type Lectin Domain Family 2, Member D	F: CGCAAAGAACTGGACAGTCA R: TTCAGCTCCTCTTCGGTTTC	84
CXCL10	Chemokine (C-X-C Motif) Ligand 10	F: CCCACATGTTGAGATCATTGC R: GCTTCTCTCTGTGTTCGAGGA	141
CXCL2	Chemokine (C-X-C Motif) Ligand 2	F: GAAGATGCTAAACAAGAGCAGTG R: AGCCAAATGCATGAAACACA	147
CD163(a)	CD163	F: CACATGTGCCAACAAAATAAGAC R: CACCACCTGAGCATCTTCAA	130
CD163(b)	CD163	F: GGAAGTGAGCAGGTCTGGAG R: ACTCTGGTTCCCTGAGCAGA	141
IRF3	Interferon Regulatory Factor 3	F: GTCAAGAGGCTGGTGATGGTC R: CTGTTGGAAATGTGCAGGTC	119
FCGR1A(a)	Fc Fragment Of IgG, High Affinity Ia, Receptor (CD64)	F: GGCAGTGATCACCTTGCAG R: ATGGGGTCCCTCACATTGTA	79
FCGR1A(b)	Fc Fragment Of IgG, High Affinity Ia, Receptor (CD64)	F: GCCACAGAAGATGGAAAGGT R: CGACATGAAACCAGACAGGA	94
FCGR2B(a)	Fc Fragment Of IgG, Low Affinity IIb, Receptor (CD32)	F: AGGAGTGACTGGGCTGATTG R: AACAGGAGCCAGGAATAGCA	84
FCGR2B(b)	Fc Fragment Of IgG, Low Affinity IIb, Receptor (CD32)	F: ACCACCCAGTGGTTCCATAA R: TCTCCTGGCCTTAAAGCTGA	75
FCGR3B(a)	Fc Fragment Of IgG, Low Affinity IIIb, Receptor (CD16b)	F: CCGAAGTCTGTGGTGATCCT R: CCTGGCACTTCAGAGTCACA	76
FCGR3B(b)	Fc Fragment Of IgG, Low Affinity IIIb, Receptor (CD16b)	F: ACCACATTCCAAATGCAACA R: ACTTTCACAGCCTCCGAAGA	94
CD1A(a)	CD1a	F: TAGGAGGCCAGGACATCATC R: GGCACAATCACTGCCAATAA	76
CD1A(b)	CD1a	F: CACGTCTCTGGCTTCTACCC R: GATGTCACCTTGCTGAGTGC	87
LAMP3(a)	Lysosomal-Associated Membrane Protein 3	F: TTTGGAAATGTGGACGAGTG R: ACAATCAAACCCACAGCACA	95
LAMP3(b)	Lysosomal-Associated Membrane Protein 3	F: GCACTCCTTCAAGTGCGTAA R: CCTGAAGCTGGACGTTCATT	83
XCR1(a)	Chemokine (C Motif) Receptor 1	F: CTGCTGAAACTTGGGGTCAT R: CAGTGGGAGAAGGCAATGTT	92
XCR1(b)	Chemokine (C Motif) Receptor 1	F: CTGGATTACGCCTTGCTCAT R: AGACATAGAGCACCGGGTTG	73
CD101(a)	CD101	F: ATTGAAACTCAGGCCCACAG R: CCTGGCTGTGTTCTGTAGCA	80

Chapter 7 - General discussion

In this chapter, general considerations concerning *in vitro* culture is presented and discussed. Detailed discussions on topics related to study I and IIII is presented in paper I and II, respectively.

Conventional *in vitro* culture

Conventional *in vitro* culture of cells is usually performed in tissue culture treated 2D culture plates made in polystyrene, with varying well sizes. IGRA has been used for more than 25 years for measuring CMI responses within individuals for the purpose of testing vaccine efficacy or as a diagnostic tool. The test relies on the locomotion of one cell type, namely the T cell and its engagement with APCs presenting cognate antigen via pMHC complexes. In this sense it can be seen as a co-culture, where the two cell subtypes need to be in physical contact for the *de novo* production of IFN-γ to occur. The culture can be performed using whole blood or PBMCs. By using PBMCs, the "co-culture" is purest in the sense that only lymphocytes (T-, B- and NK-cells) and monocytes are present, whereas whole blood cultures also include erythrocytes and granulocytes. In cultures of PBMCs, cells sediment to the bottom of the well after some time, thus it may be expected that any migration that takes place is carried out directly on the plastic surface. As whole blood consist of app. 95% erythrocytes, in this type of culture erythrocytes "coat" the bottom well surface thus migration of T lymphocytes may take place within/on top of the erythrocyte layer. Whether this results in some migratory advantages/disadvantages needs to be confirmed.

An observation from study I was increased IFN-γ concentrations in polyclonal-activated cultures of whole blood compared to PBMCs, despite the cell concentration of PBMC cultures exceeding that of whole blood cultures (7.9 vs. $10x10^6$ cells/ml). This suggests that factors other than the overall cell concentration may influence the level of IFN-γ detected in the cultures used for IGRA. An interesting discovery from 2011 reported by Antunes and colleagues, revealed that erythrocytes are capable of releasing factors into the culture medium, increasing the survival and growth of $CD3^+$ T lymphocytes (Antunes et al. 2011). Previous studies had shown that the addition of erythrocytes to *in*

vitro cultured human T lymphocytes, resulted in increased proliferation regardless of the erythrocytes being added at the start of culture or 24 hours later, suggesting that the effect exerted by the erythrocytes were applicable for already activated lymphocytes (Arosa et al. 2004). Additionally, the mechanisms behind the inhibition of T lymphocyte apoptosis was found to be linked to upregulation of cytoprotective proteins and downregulation of oxidative stress within the T lymhocytes (Fonseca 2001; Fonseca et al. 2003).

Antunes and colleagues were able to show that the effect supporting proliferation and survival of activated T lymphocytes (not B lymphocytes or NK cells) originated from soluble protein/factors released by intact erythrocytes, which they termed EDGSF (*erythrocyte-derived growth and survival factors*). They concluded that erythrocytes are regulatory cells that support growth, proliferation and survival of dividing T cells by the release of novel factors. This correlates with the finding that addition of plasma could rescue PBMCs from apoptosis during culture (Hodge et al. 2000), as discussed in paper I. Thus, testing IFN-γ levels on cells in whole blood format may be desirable for cultures of intermediate length (overnight cultures) as this seems to protect the T lymphocytes from apoptosis, yet the nutrient supply should still be adequate within this timeframe.

However, the use of either PBMCs or whole blood cultures for measuring CMI responses is still under debate. When using IGRA for vaccine efficacy testing, the point is to measure the presence of antigen-responsive T lymphocytes. Therefore, creating a setting that, despite it being artificial, resemble the conditions surrounding the cells *in vivo*, would favor optimal T lymphocyte activation. In the 2D cultures (whole blood or PBMCs) this is not the case as T lymphocyte migration must be expected to occur in one plane with no directionality, thus possibly resulting in a sub-optimal setting for antigen presentation which could lead to decreased sensitivity of the assay. The consequence of this is rejection of drug/vaccine candidates that might have good *in vivo* effects, but suffer from poor *in vitro* performance due to insufficient antigen-presentation in the 2D culture well.

3D cultures

In the attempt to imitate *in vivo* conditions during *in vitro* culture, the obvious next step was to include a third dimension to the culture. The unnatural 2D environment when culturing cells *in vitro*

on glass or plastic surfaces, may provide inaccurate and unreliable data in regards to predictive outcomes of drug screening tests (Gurski et al. 2010). This "mismatch" between *in vitro* and *in vivo* outcome is causing huge economical losses due to money spent on clinical trials based on pre-studies using poor correlating *in vitro* cultures (Hartung 2013). A major limitation of the 2D model is that it cannot capture the complexity of the *in vivo* microenvironment, and cell-cell and cell-matrix interactions important for differentiation, proliferations and cellular functions, are lost (Mazzoleni et al. 2009). Furthermore studies performed using 2D cultures may also results in misrepresentation of findings since cells are forced to adapt to an artificial, flat and rigid surface (Mazzoleni et al. 2009).

The development of physiologically relevant 3D *in vitro* models has mostly focused on long term culture of cells used for drug screenings etc. In this thesis, focus was on short term culture of primary immune cells and the hypothesis was, that when culturing cells used for diagnostic measurements in 2D, as in the case of IGRA, this may not reproduce a CMI response similar to the response present *in vivo,* thus decreasing the diagnostic value of the tests. With this in mind, in the attempt to mimic the *in vivo* structure of a lymph node in order to increase the changes of T lymphocyte-APC encounter during *in vitro* culture, and at the same time keeping the culture format relatively simple, several 3D incubation setups were tested. The different 3D setups were based on the addition of 3D scaffolds acting as a network for cell attachment and migration. These were made from glass wool (with/without extended gravity flow), shavings made in PP, commercial available 3D scaffolds made in PS or PCL, filter paper disks and a PDMS scaffold. Additionally, coating of some of these scaffolds with ECM proteins (MaxGel or Matrigel) or CCL21 chemokine to improve cell attachment and migration, respectively, was also tested.

We did not succeed in developing a 3D platform for IGRA resulting in increased levels of secreted IFN-γ as compared to the standard assay platform in 2D. This could be due to several causes. First of all, it would have made sense to look at the kinetics of IFN-γ protein secretion, as was done for the mRNA expression. Even though the 20-22 hour culture time is a generally accepted and frequently used time interval when looking at IFN-γ protein, this might not be optimally for 3D cultures. It could

be speculated if the time interval was simply too short for the 3D architecture to add any advantages in regards to cell-cell contacts. Secondly, if the cells failed in attaching properly to the tested scaffolds, but rather "sank" to the bottom of the well, then obviously the scaffolds would lose their effect. Theoretically this could be the case for a fraction of the cultured cells, but most of the cells would be expected to reside within or on the scaffolds since caution was made when plating the cells. Also as some of the scaffolds tested had relatively small pore sizes (20 and 40µm in filter paper and 3D PS scaffolds, respectively), it would be unlikely if cells sank to the bottom. Also, in the case with ECM-coated scaffolds, which is believed to increase the surface attachment of the cells (Kleinman et al. 1987; Cooke et al. 2008), this did not seem to improve the assay. Retrospective it would have been relevant to confirm the inclusion of cells within the different scaffolds for example by scanning electron microscopy (SEM). Thirdly, 3D culture using artificially scaffolds may simply not be applicable for this type of short term assay, and it seems as if T lymphocytes are able to migrate (as shown in Figure 16) and engage with APCs in the 2D plane of a culture well surface even more efficiently than in an 3D environment, at least the for the type of 3D scaffolds tested in this thesis.

Non-specific activation

A common tendency was elevated background levels of IFN-γ in the 3D cultures compared with 2D cultures. This suggests that factors other than activation via antigen presentation must have led to the IFN-γ production in these 3D cultures. It has previously been reported that NK cells are capable of non-specific IFN-γ secretion in overnight antigen-stimulated cultures from young calves (Olsen et al. 2005). This does not explain the differential finding of non-specific activation in 3D compared to 2D cultures though. Flow cytometry combining surface labeling with intracellular staining of IFN-γ would clarify whether this non-specific IFN-γ originated from T lymphocytes or if other cells present in the cultures such as NK cells or γδ T lymphocytes contributed to the IFN-γ levels. Interestingly, the finding that 3D culture resulted in increased non-specific activation of cells (at least judged by the level of IFN-γ) in cultures used for IGRA, correlates with the finding that changing of culture surface architecture (2D to 3D) resulted in moDCs with increased activation status (paper II). This suggests that external factors mediated by the shift in culture architecture somehow activate the cells, and this

applies to both cells of porcine moDC origin and mixed cultures of bovine PBMCs. We only see what we look for, thus a broader analysis of the nature of activation in the PBMCs, or even in the different cell subtypes within the PBMC population, would be relevant.

Cells on chip

A lot of research is performed within the development of 3D culture models since they offer a somewhat complex microenvironment for the cells compared to 2D cultures. Also, the development of *in vivo*-correlating *in vitro* 3D culture models in general would contribute to a reduction in the use of animal models, which is in accordance to the ethical guidelines concerning the use of animals in research, defined by the three R´s: Replacement, Reduction and Refinement (Russell & Burch 1959). In fact, the US National Research Council has recommended that animal models are replaced with *in vitro* human cell based assays (Krewski et al. 2010). We aimed at developing a "lymph node-on-a-chip" system, combining a cell chamber that facilitated lymphocyte migration and activation with direct detection of IFN-γ using direct one-step qRT-PCR. This combination turned out to be a novel invention (cf. the novelty search report, appendix 3). It would not only be applicable as a diagnostic test, it would also be suitable for testing immune-stimulatory/inhibitory agents and thus contribute to reducing the use of *in vivo* animal models. Unfortunately we were far from reaching this goal since neither the 3D "lymph node like" scaffolds seemed to work (off chip), nor did the qRT-PCR reaction. A prototype chip with different incubation chambers was fabricated. The idea was that by applying a steady flow through the chamber, relevant cells would attach to the 3D scaffold and liquid be exchanged without flushing out the cells. The microstructures within the chambers were designed as a "plan b" if no scaffold-solution was found, and their function was to retain cells while shifting from blood-flow to qRT-PCR reagent flow. More research was needed for the chip to become a reality and unfortunately this exceeded the time-frame of the thesis.

Generation of moDCs

Paper II describes the generation of moDC cultured with GM-CSF and IL-4 on various culture surfaces. It has long been under debate whether *in vitro* generated moDC could be classified as DC or not (Artur

Summerfield, personal communication). Classification of DC subsets is complicated and it can be difficult to differentiate between DCs, macrophages and monocytes since many of the proposed unique markers and functions have been shown to be shared between cell types (Guilliams et al. 2014). Also the fact that specific markers are not conserved across species as well as the change in morphology and location of the cells further complicates the nomenclature. However, attempts are being made to standardize the nomenclature for DC subsets/precursors, and it has been proposed to simply group these cells under the term "monocyte-derived cells" (Guilliams et al. 2014). The monocyte-derived cells generated on alternative surfaces in the present study, appeared macrophage-like in their gene expression profile, whereas monocytes cultured on conventional surfaces showed "classical" moDC expression and morphology. The fact that external stimuli in the form of changes in culture surroundings could lead to the differentiation of what appeared to be a different cell type, argue for the huge plasticity of these cells and that the classification into either DC or macrophage may be misleading. In fact, this viewpoint is shared by others who suggest a "modular spectrum model" that argue that monocyte-derived cells being particular plastic are able to express combinations of multiple transcriptional modules depending on received signals from their microenvironment (Ginhoux et al. 2015; Xue et al. 2014; Guilliams & van de Laar 2015).

Immunotherapy using moDC generated *in vitro* have shown varying therapeutic effects and they often fail in activation of cytotoxic T lymphocytes (Barbuto 2013). In order to induce a strong response *in vivo*, the moDC must be able to migrate to the draining lymph node which requires them to be in an activated state. Lack of activation and migration is usually the reason for the poor therapeutic effect of these treatments (Wimmers et al. 2014). It would be interesting to investigate if the different culture methods, apart from changes in gene expression, also gave rise to differential antigen-presenting abilities and if the migratory capacities of these cells were affected as well. At least the cells cultured alternatively show an activated phenotype, and it could be speculated that the flat culture surface generally used for moDC culture is partly the reason for lack of migratory cells and instead results in "lazy" cells with a gene expression profile adapted to 2D and therefore are not able to migrate to the draining lymph node when re-introduced to the patient.

Chapter 8 - General conclusion

The work presented in this thesis included a revision of procedures commonly used when culturing cells for immunological studies. We questioned the reliability of IGRAs in terms of its sensitivity toward changes in culture setup, and challenged the traditional 2D culture by addition of an extra dimension in the form of 3D scaffolds. Additionally, we examined the effect of external factors on the differentiation of moDCs by means of changing the material of culture surfaces as well as dimension.

In study I, blood from pre-vaccinated calves with required CMI responses against a MAP peptide-antigen, was used to investigate factors of influence for the validity of IGRA performed with cultures of whole blood, diluted whole blood or purified PBMCs in concentrations ranging from 10-0.625x10^6 cells/ml. We found large differences in the optimal diagnostic culture conditions with each individual animal; some calves showed highest specific IFN-γ responses in cultures of whole blood whereas PBMC cultures of 10x10^6 or 5x10^6 cells/ml were found optimal in other calves. Furthermore, we did the worrying discovery that PBMC cultures were amenable to differences in cellular composition compared to whole blood; by analyzing the percentages of cellular subsets using flow cytometry, we found a significantly reduced population of γδ T lymphocytes. Lastly, we were able to show effect of culture plates from different suppliers, although not significant, and following specific activation, six out of eight calves tested had optimal response in the same plate from Corning®. These findings highlights the need for caution when analyzing and comparing IGRA data, as different conditions infer different results in the same animal.

Culturing cells in 2D is unnatural and cell activation requiring cell-cell contact and thus migration, is forced down on one plane as opposed to the migration *in vivo*. In study II, we sought to alleviate the process of cell activation by facilitating the *in vitro* migration of cultured cells using 3D scaffolds and protein coatings. However, these 3D IGRAs did not show superior qualities in terms of increased cell activation and thus concentrations of IFN-γ compared to 2D IGRAs. A surprising discovery was that the addition of an extra dimension to the cultures seemed to activate the cells in a

non-specific manner. We did not go into detail regarding the circumstances behind this non-specific activation.

The finding that 3D cultures had an activating effect on cells as well as previous reports showing a dramatic effect on the gene expression levels of PC12 cells when changing culture material (Łopacińska et al. 2013), led us to investigate possible effects of changing the culture condition during the *in vitro* differentiation of porcine moDC in study IIII. We compared traditional culture surface material (PS) with an untraditional culture surface made from PDMS, a material frequently used for lab-on-a-chip device fabrication. The results showed that both the culture surface material (PS vs. PDMS) as well as the dimension (2D vs. 3D) caused changes in gene expression. PDMS generated cells with a macrophage-like phenotype and 3D cultures had a positive effect on the activation profile of the cells. Thus, this study show how sensitive moDCs are to their surrounding environment and it opens up for the possibility of influencing the expression profile of cultured cells simply by designing culture setups that favor a desired differentiation path.

Taken together, a microfluidic diagnostic chip for direct detection of CMI responses in a blood sample was not developed as planned originally. A prototype chip was produced (study III), consisting of eight chambers having space for a 3D scaffold or with varying microstructures for the capture of cells. However, neither the detection platform, consisting of direct qRT-PCR nor a 3D scaffold for increased activation was established. Instead focus within this thesis changed into optimization of *in vitro* cell culture conditions. In conclusion, IGRAs, as well as *in vitro* assays in general, suffer from severe limitations in terms of imitating *in vivo* conditions. This might have detrimental consequences when translating *in vitro* results into *in vivo* predictions. Therefore, improved *in vivo*-like culture formats applicable for both long and short term routine cultures would be useful and is worth pursuing.

9 References

Antunes, R.F. et al., 2011. Red blood cells release factors with growth and survival bioactivities for normal and leukemic T cells. *Immunology and cell biology*, 89(1), pp.111–21.

Arosa, F.A., Pereira, C.F. & Fonseca, A.M., 2004. Red blood cells as modulators of T cell growth and survival. *Current pharmaceutical design*, 10(2), pp.191–201.

Assenmacher, M. et al., 1998. Sequential production of IL-2, IFN-gamma and IL-10 by individual staphylococcal enterotoxin B-activated T helper lymphocytes. *European journal of immunology*, 28(5), pp.1534–43.

Bajénoff, M. et al., 2007. Highways, byways and breadcrumbs: directing lymphocyte traffic in the lymph node. *Trends in immunology*, 28(8), pp.346–52.

Barbuto, J.A.M., 2013. Are dysfunctional monocyte-derived dendritic cells in cancer an explanation for cancer vaccine failures? *Immunotherapy*, 5(2), pp.105–7.

Barker, S.L. & LaRocca, P.J., 1994. Method of production and control of a commercial tissue culture surface. *Journal of Tissue Culture Methods*, 16(3-4), pp.151–153.

Berthier, E., Young, E.W.K. & Beebe, D., 2012. Engineers are from PDMS-land, Biologists are from Polystyrenia. *Lab on a Chip*, 12(7), p.1224.

Billman-Jacobe, H. et al., 1992. A comparison of the interferon gamma assay with the absorbed ELISA for the diagnosis of Johne's disease in cattle. *Australian veterinary journal*, 69(2), pp.25–8.

Blum, J.S., Wearsch, P.A. & Cresswell, P., 2013. Pathways of antigen processing. *Annual review of immunology*, 31, pp.443–73.

Boehm, U. et al., 1997. Cellular responses to interferon-gamma. *Annual review of immunology*, 15, pp.749–95.

Bousso, P. & Robey, E., 2003. Dynamics of CD8+ T cell priming by dendritic cells in intact lymph nodes. *Nature immunology*, 4(6), pp.579–85.

Chen, J. & Liu, X., 2009. The role of interferon gamma in regulation of CD4+ T-cells and its clinical implications. *Cellular immunology*, 254(2), pp.85–90.

Choi, Y.W. et al., 1989. Interaction of Staphylococcus aureus toxin "superantigens" with human T cells. *Proceedings of the National Academy of Sciences of the United States of America*, 86(22), pp.8941–5.

Cooke, M.J. et al., 2008. Enhanced cell attachment using a novel cell culture surface presenting functional domains from extracellular matrix proteins. *Cytotechnology*, 56(2), pp.71–79.

Curtis, A.S. et al., 1983. Adhesion of cells to polystyrene surfaces. *The Journal of Cell Biology*, 97(5), pp.1500–1506.

Danilova, N., 2012. The evolution of adaptive immunity. *Advances in experimental medicine and biology*, 738, pp.218–35.

Davis, M.M. & Bjorkman, P.J., 1988. T-cell antigen receptor genes and T-cell recognition. *Nature*, 334(6181), pp.395–402.

Dhillon, N.K. et al., 2007. PDGF Synergistically Enhances IFN- -Induced Expression of CXCL10 in Blood-Derived Macrophages: Implications for HIV Dementia. *The Journal of Immunology*, 179(5), pp.2722–2730.

Diao, J. et al., 2006. In situ replication of immediate dendritic cell (DC) precursors contributes to conventional DC homeostasis in lymphoid tissue. *Journal of immunology (Baltimore, Md. : 1950)*, 176(12), pp.7196–206.

Eagle, H., 1955. Nutrition needs of mammalian cells in tissue culture. *Science (New York, N.Y.)*, 122(3168), pp.501–14.

Farrar, M.A. & Schreiber, R.D., 1993. The molecular cell biology of interferon-gamma and its receptor. *Annual review of immunology*, 11, pp.571–611.

Fonseca, A.M., 2001. Red blood cells inhibit activation-induced cell death and oxidative stress in human peripheral blood T lymphocytes. *Blood*, 97(10), pp.3152–3160.

Fonseca, A.M. et al., 2003. Red blood cells upregulate cytoprotective proteins and the labile iron pool in dividing human T cells despite a reduction in oxidative stress. *Free radical biology & medicine*, 35(11), pp.1404–16.

Van Furth, R. et al., 1972. [Mononuclear phagocytic system: new classification of macrophages, monocytes and of their cell line]. *Bulletin of the World Health Organization*, 47(5), pp.651–8.

Van Furth, R., 1980. Identification of Mononuclear Phagocytes: Overview and Definitions. In *Methods for Studying Mononuclear Phagocytes*. Academid Press, pp. 243–52.

Förster, R., Braun, A. & Worbs, T., 2012. Lymph node homing of T cells and dendritic cells via afferent lymphatics. *Trends in immunology*, 33(6), pp.271–80.

Gay, D. et al., 1993. Receptor editing: an approach by autoreactive B cells to escape tolerance. *The Journal of experimental medicine*, 177(4), pp.999–1008.

Ginhoux, F. et al., 2015. New insights into the multidimensional concept of macrophage ontogeny, activation and function. *Nature immunology*, 17(1), pp.34–40.

Girard, J.-P., Moussion, C. & Förster, R., 2012. HEVs, lymphatics and homeostatic immune cell trafficking in lymph nodes. *Nature reviews. Immunology*, 12(11), pp.762–73.

Goldszmid, R.S. & Trinchieri, G., 2012. The price of immunity. *Nature immunology*, 13(10), pp.932–8.

Gollmer, K. et al., 2009. CCL21 mediates CD4+ T-cell costimulation via a DOCK2/Rac-dependent pathway. *Blood*, 114(3), pp.580–8.

Gretz, J.E. et al., 1996. Sophisticated strategies for information encounter in the lymph node: the reticular network as a conduit of soluble information and a highway for cell traffic. *Journal of immunology (Baltimore, Md. : 1950)*, 157(2), pp.495–9.

Guilliams, M. et al., 2014. Dendritic cells, monocytes and macrophages: a unified nomenclature based on ontogeny. *Nature reviews. Immunology*, 14(8), pp.571–8.

Guilliams, M. & van de Laar, L., 2015. A Hitchhiker's Guide to Myeloid Cell Subsets: Practical Implementation of a Novel Mononuclear Phagocyte Classification System. *Frontiers in immunology*, 6, p.406.

Gurski, L. et al., 2010. 3D matrices for anti-cancer drug testing and development. *Oncology Issues*.

Haig, D.M. & Miller, H.R.P., 1990. Differentiationof bone marrow cells into effector cells. In J. M. Behnke, ed. *Parasites: Immunity And Pathology: The Consequences Of Parasitic Infections In Mammals*. CRC Press, p. 437.

Harrison, R.G., 1911. ON THE STEREOTROPISM OF EMBRYONIC CELLS. *Science (New York, N.Y.)*, 34(870), pp.279–81.

Hartley, S.B. et al., 1993. Elimination of self-reactive B lymphocytes proceeds in two stages: arrested development and cell death. *Cell*, 72(3), pp.325–35.

Hartung, T., 2013. Look back in anger - what clinical studies tell us about preclinical work. *ALTEX*, 30(3), pp.275–91.

Hiromatsu, K. et al., 1992. A protective role of gamma/delta T cells in primary infection with Listeria monocytogenes in mice. *The Journal of experimental medicine*, 175(1), pp.49–56.

Hodge, G., Hodge, S. & Han, P., 2000. Increased levels of apoptosis of leukocyte subsets in cultured PBMCs compared to whole blood as shown by Annexin V binding: relevance to cytokine production. *Cytokine*, 12(12), pp.1763–8.

Italiani, P. & Boraschi, D., 2014. From Monocytes to M1/M2 Macrophages: Phenotypical vs. Functional Differentiation. *Frontiers in Immunology*, 5, p.514.

Janikashvili, N., Larmonier, N. & Katsanis, E., 2010. Personalized dendritic cell-based tumor immunotherapy. *Immunotherapy*, 2(1), pp.57–68.

Jenkins, M.K. & Moon, J.J., 2012. The role of naive T cell precursor frequency and recruitment in dictating immune response magnitude. *Journal of immunology (Baltimore, Md. : 1950)*, 188(9), pp.4135–40.

Jungersen, G. et al., 2002. Interpretation of the gamma interferon test for diagnosis of subclinical paratuberculosis in cattle. *Clinical and diagnostic laboratory immunology*, 9(2), pp.453–60.

Jungersen, G., Mikkelsen, H. & Grell, S.N., 2012. Use of the johnin PPD interferon-gamma assay in control of bovine paratuberculosis. *Veterinary immunology and immunopathology*, 148(1-2), pp.48–54.

Kennedy, H.E., 2002. Modulation of Immune Responses to Mycobacterium bovis in Cattle Depleted of WC1+gammadelta T Cells. *Infection and Immunity*, 70(3), pp.1488–1500.

King, D.P. et al., 1999. Cutting edge: protective response to pulmonary injury requires gamma delta T lymphocytes. *Journal of immunology (Baltimore, Md. : 1950)*, 162(9), pp.5033–6.

Kleinman, H.K. et al., 1987. Use of extracellular matrix components for cell culture. *Analytical biochemistry*, 166(1), pp.1–13.

Korohoda, W., 1972. Some aspects of the interrelation among cell locomotion, contact phenomena, and cellular multiplication. *Acta Protozoologica*, 11.

Krewski, D. et al., 2010. Toxicity testing in the 21st century: a vision and a strategy. *Journal of toxicology and environmental health. Part B, Critical reviews*, 13(2-4), pp.51–138.

Kwok, W.W. et al., 2012. Frequency of epitope-specific naive CD4(+) T cells correlates with immunodominance in the human memory repertoire. *Journal of immunology (Baltimore, Md. : 1950)*, 188(6), pp.2537–44.

Liu, M. & Schatz, D.G., 2009. Balancing AID and DNA repair during somatic hypermutation. *Trends in immunology*, 30(4), pp.173–81.

Łopacińska, J.M., Emnéus, J. & Dufva, M., 2013. Poly(dimethylsiloxane) (PDMS) affects gene expression in PC12 cells differentiating into neuronal-like cells. *PloS one*, 8(1), p.e53107.

Maltman, D.J. & Przyborski, S.A., 2010. Developments in three-dimensional cell culture technology aimed at improving the accuracy of in vitro analyses. *Biochemical Society transactions*, 38(4), pp.1072–5.

Manz, A., Graber, N. & Widmer, H.M., 1990. Miniaturized total chemical analysis systems: A novel concept for chemical sensing. *Sensors and Actuators B: Chemical*, 1(1-6), pp.244–248.

Mazurek, G.H. & Villarino, M.E., 2003. Guidelines for using the QuantiFERON-TB test for diagnosing latent Mycobacterium tuberculosis infection. Centers for Disease Control and Prevention. *MMWR. Recommendations and reports : Morbidity and mortality weekly report. Recommendations and reports / Centers for Disease Control*, 52(RR-2), pp.15–8.

Mazzoleni, G., Di Lorenzo, D. & Steimberg, N., 2009. Modelling tissues in 3D: the next future of pharmaco-toxicology and food research? *Genes & nutrition*, 4(1), pp.13–22.

Medzhitov, R., 2008. The Innate Immune System. In W. E. Paul, ed. *Fundamental Immunology*. Lippincott Williams & Wilkins.

Menegatti, E. et al., 2013. Lab-on-a-chip: emerging analytical platforms for immune-mediated diseases. *Autoimmunity reviews*, 12(8), pp.814–20.

Mikkelsen, H., Jungersen, G. & Nielsen, S.S., 2009. Association between milk antibody and interferon-gamma responses in cattle from Mycobacterium avium subsp. paratuberculosis infected herds. *Veterinary Immunology and Immunopathology*, 127(3-4), pp.235–241.

Miller, M.J. et al., 2004. T cell repertoire scanning is promoted by dynamic dendritic cell behavior and random T cell motility in the lymph node. *Proceedings of the National Academy of Sciences of the United States of America*, 101(4), pp.998–1003.

Moser, B. & Loetscher, P., 2001. Lymphocyte traffic control by chemokines. *Nature immunology*, 2(2), pp.123–8.

Munoz, M.A., Biro, M. & Weninger, W., 2014. T cell migration in intact lymph nodes in vivo. *Current opinion in cell biology*, 30, pp.17–24.

Muramatsu, M. et al., 2000. Class switch recombination and hypermutation require activation-induced cytidine deaminase (AID), a potential RNA editing enzyme. *Cell*, 102(5), pp.553–63.

Murphy, K., 2012. *Janeway's Immunobiology* 8th ed., New York, USA & Abingdon, UK: Garland Science.

Naik, S.H. et al., 2007. Development of plasmacytoid and conventional dendritic cell subtypes from single precursor cells derived in vitro and in vivo. *Nature immunology*, 8(11), pp.1217–26.

Naik, S.H. et al., 2006. Intrasplenic steady-state dendritic cell precursors that are distinct from monocytes. *Nature immunology*, 7(6), pp.663–71.

Olsen, I. et al., 2005. Bovine NK cells can produce gamma interferon in response to the secreted mycobacterial proteins ESAT-6 and MPP14 but not in response to MPB70. *Infection and immunity*, 73(9), pp.5628–35.

Palucka, K. & Banchereau, J., 2012. Cancer immunotherapy via dendritic cells. *Nature reviews. Cancer*, 12(4), pp.265–77.

Pinchuk, I. V, Beswick, E.J. & Reyes, V.E., 2010. Staphylococcal enterotoxins. *Toxins*, 2(8), pp.2177–97.

Ramos, R.N. et al., 2012. Monocyte-derived dendritic cells from breast cancer patients are biased to induce CD4+CD25+Foxp3+ regulatory T cells. *Journal of leukocyte biology*, 92(3), pp.673–82.

Randolph, G.J., Jakubzick, C. & Qu, C., 2008. Antigen presentation by monocytes and monocyte-derived cells. *Current opinion in immunology*, 20(1), pp.52–60.

Ravi, M. et al., 2015. 3D cell culture systems: advantages and applications. *Journal of cellular physiology*, 230(1), pp.16–26.

Romagnani, S., 1994. Lymphokine production by human T cells in disease states. *Annual review of immunology*, 12, pp.227–57.

Romani, N. et al., 1994. Proliferating dendritic cell progenitors in human blood. *The Journal of experimental medicine*, 180(1), pp.83–93.

Rothel, J.S. et al., 1990. A sandwich enzyme immunoassay for bovine interferon-gamma and its use for the detection of tuberculosis in cattle. *Australian veterinary journal*, 67(4), pp.134–7.

Rothel, J.S. et al., 1992. The gamma-interferon assay for diagnosis of bovine tuberculosis in cattle: conditions affecting the production of gamma-interferon in whole blood culture. *Australian veterinary journal*, 69(1), pp.1–4.

Ruhwald, M., Aabye, M.G. & Ravn, P., 2012. IP-10 release assays in the diagnosis of tuberculosis infection: current status and future directions. *Expert review of molecular diagnostics*, 12(2), pp.175–87.

Russell, W. & Burch, R., 1959. The principles of humane experimental technique.

Sallusto, F. & Lanzavecchia, A., 1994. Efficient presentation of soluble antigen by cultured human dendritic cells is maintained by granulocyte/macrophage colony-stimulating factor plus interleukin 4 and downregulated by tumor necrosis factor alpha. *The Journal of experimental medicine*, 179(4), pp.1109–18.

Savina, A. & Amigorena, S., 2007. Phagocytosis and antigen presentation in dendritic cells. *Immunological reviews*, 219, pp.143–56.

Schatz, D.G., 2004. V(D)J recombination. *Immunological reviews*, 200, pp.5–11.

Schoenborn, J.R. & Wilson, C.B., 2007. Regulation of interferon-gamma during innate and adaptive immune responses. *Advances in immunology*, 96, pp.41–101.

Schroder, K. et al., 2004. Interferon-gamma: an overview of signals, mechanisms and functions. *Journal of leukocyte biology*, 75(2), pp.163–89.

Snapka, R.M., 1979. Glass wool as a surface for cell growth in vitro. *Tissue Culture Association Manual*, 5(3), pp.1117–1120.

Sobocinski, G.P. et al., 2010. Ultrastructural localization of extracellular matrix proteins of the lymph node cortex: evidence supporting the reticular network as a pathway for lymphocyte migration. *BMC immunology*, 11(1), p.42.

Tanaka, H. & Taniuchi, I., 2014. The CD4/CD8 lineages: central decisions and peripheral modifications for T lymphocytes. *Current topics in microbiology and immunology*, 373, pp.113–29.

Teach, W.C. & Kiessling, G.C., 1960. *Polystyrene*, New York, NY: Reinhold Publishing Corp.

Terry, S., 1975. A gas chromatographic air analyser fabricated on silicon wafer using integrated circuit technology. Ph.D. Thesis, Stanford University.

Thakur, A., Pedersen, L.E. & Jungersen, G., 2012. Immune markers and correlates of protection for vaccine induced immune responses. *Vaccine*, 30(33), pp.4907–20.

Tonegawa, S., 1983. Somatic generation of antibody diversity. *Nature*, 302(5909), pp.575–81.

Weninger, W., Biro, M. & Jain, R., 2014. Leukocyte migration in the interstitial space of non-lymphoid organs. *Nature reviews. Immunology*, 14(4), pp.232–46.

Wilson, R.A. et al., 1996. T-cell subsets in blood and lymphoid tissues obtained from fetal calves, maturing calves, and adult bovine. *Veterinary immunology and immunopathology*, 53(1-2), pp.49–60.

Wimmers, F. et al., 2014. Paradigm Shift in Dendritic Cell-Based Immunotherapy: From in vitro Generated Monocyte-Derived DCs to Naturally Circulating DC Subsets. *Frontiers in immunology*, 5, p.165.

Wood, P.R., Corner, L.A. & Plackett, P., 1990. Development of a simple, rapid in vitro cellular assay for bovine tuberculosis based on the production of gamma interferon. *Research in veterinary science*, 49(1), pp.46–9.

Wood, P.R., Kopsidas, K., Milner, A.R., Hill, J., Gill, I., Webb, R., Mack, W.N., Coates, K., 1989. The development of an in vitro cellular assay for Johne's disease in cattle. In A. R. Milner & P. R. Wood, eds. *Johne's Disease: Current Trends in Research, Diagnosis and Management*. East Melbourne, Australia: CSIRO Publications, pp. 164–167.

Woolf, E. et al., 2007. Lymph node chemokines promote sustained T lymphocyte motility without triggering stable integrin adhesiveness in the absence of shear forces. *Nature immunology*, 8(10), pp.1076–85.

Worbs, T., Bernhardt, G. & Förster, R., 2008. Factors governing the intranodal migration behavior of T lymphocytes. *Immunological reviews*, 221, pp.44–63.

Xue, J. et al., 2014. Transcriptome-based network analysis reveals a spectrum model of human macrophage activation. *Immunity*, 40(2), pp.274–88.

Yamada, K.M. & Cukierman, E., 2007. Modeling tissue morphogenesis and cancer in 3D. *Cell*, 130(4), pp.601–10.

Yang, H. & Parkhouse, R.M., 2000. Characterization of the porcine gammadelta T-cell receptor structure and cellular distribution by monoclonal antibody PPT27. *Immunology*, 99(4), pp.504–9.

Yang, H. & Parkhouse, R.M., 1996. Phenotypic classification of porcine lymphocyte subpopulations in blood and lymphoid tissues. *Immunology*, 89(1), pp.76–83.

Zhang, C., Zhang, J. & Tian, Z., 2006. The regulatory effect of natural killer cells: do “NK-reg cells” exist? *Cellular & molecular immunology*, 3(4), pp.241–54.

Aabye, M.G. et al., 2012. A simple method to quantitate IP-10 in dried blood and plasma spots. *PloS one*, 7(6), p.e39228.

10 Appendices

Appendix 1 – images of 3D scaffolds used in the thesis

Scaffolds used in study II:

(PP, Polypropylene; PCL, polycaprolactone; PS, polystyrene; PDMS, polydimethylsiloxane)

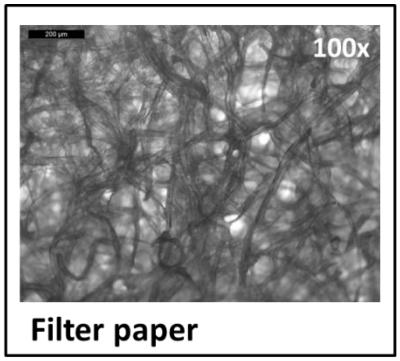

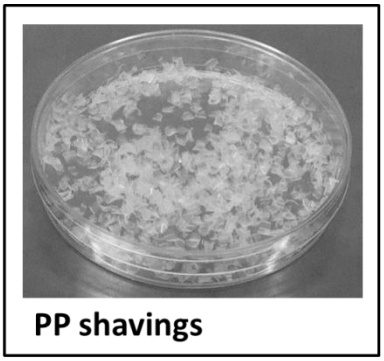

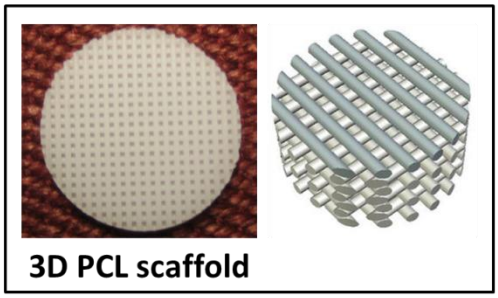

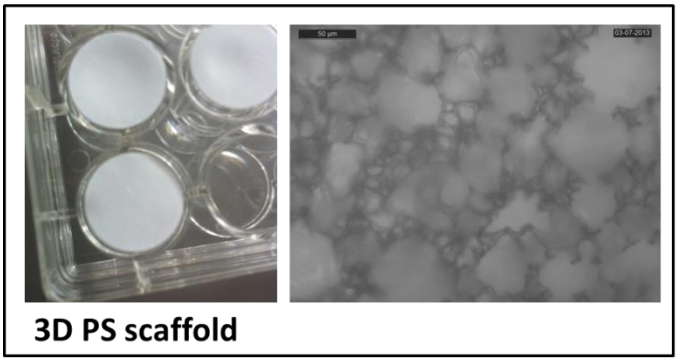

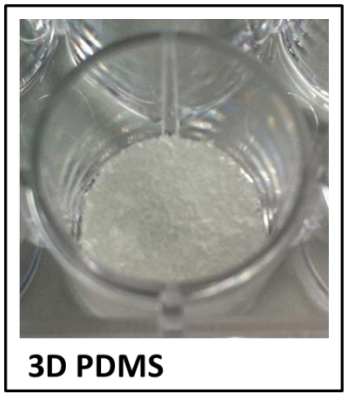

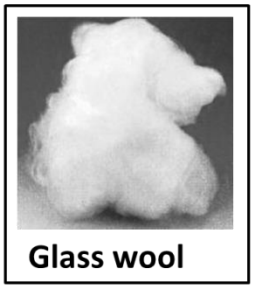

Additional scaffolds/surfaces used in study IIII:

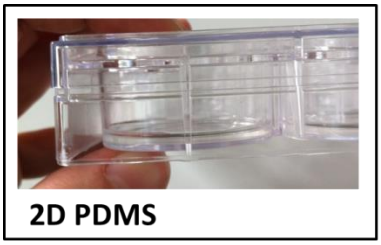

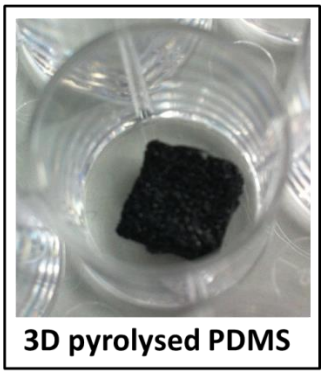

Appendix 2 - List of primers used in study II and III

List of primers used with the Rotor-Gene Q platform

Symbol	Gene	Sequence
IFNG[a,b]	*IFN-γ*	F: AAATTCCGGTGGATGATCTG R: TTCTCTTCCGCTTTCTGAGG
CXCL10[a,b]	*IP10*	F: TCATTCCTGCAAGTCAATCCT R: CAGACATCTTTTCTCCCCATTC
CXCL10[b]	*IP10*	F: TGGGGAGAAAAGATGTCTGAA R: CTCTTTCCGTGTTCGAGGAG
PPIA[a]	*Peptidylprolyl isomerase A*	F: CGCGTCTCTTTTGAGCTGTT R: TCCTTTCTCTCCAGTGCTCAG
GAPDH[a,b]	*Glyceraldehyde 3-phosphate dehydrogenase*	F: GAGCTCAATGGGAAGCTCAC R: GGCAGGTCAGATCCACAACT
HPRT1[a]	*Hypoxanthine phosphoribosyltransferase 1*	F: TGGCTCGAGATGTGATGAAG R: CAACAGGTCGGCAAAGAACT
HPRT1[b]	*Hypoxanthine phosphoribosyltransferase 1*	F: CACTGGGAAGACAATGCAGA R: ACACTTCGAGGGGTCCTTTT
ACTB[b]	*β-actin*	F: TCCCTGGAGAAGAGCTACGA R: ATTCCATGCCCAGGAAGG

[a]Used for testing 3D IGRA, [b]Used for optimization of direct one-step blood qRT-PCR SYBR Green Kit

Appendix 3 - Novelty Search Report (study II)

Diagnostic reticular chip combining micro fluidics with qRT-PCR for the detection of antigen-specific cell-mediated immune responses

Aim and background of the invention

The present invention aims at developing a chip that can be used as a simple and quick diagnostic tool for the indirect detection of an intracellular infection (e.g. tuberculosis) in a blood sample by detecting the presence of a specific cell-mediated immune response directed against antigens from the infectious agent.

In the diagnostic methods presently used for testing a cell-mediated immune response against tuberculosis, blood is incubated together with antigen in a plate or tube for 16-24 hours. The supernatant is harvested and tested for the presence of cytokines using ELISA (QuantiFERON-TB Gold or QuantiFERON-TB Gold In-Tube), or the specific cytokine-producing T cells are counted using ELISPOT (T-SPOT.TB). In the plate or tube, the T cells will have to interact with antigen-presenting monocytes to become activated and start to produce the cytokines that are used as a measure for the presence of a specific cell-mediated immune response. The cell-cell contact is a concern, however, since there is the risk that some specific T cells will not become activated because they do not interact with the monocytes. This would give rise to false negative results (i.e. where a positive blood sample does not give a positive read-out because of lack of specific T cell-monocyte interaction in the test tube/plate).

In vivo, once activated, the antigen-presenting cells (APCs), mainly dendritic cells, will migrate via the lymphatic system to the draining lymph node. Lymph nodes are specialized structures located in the interface of the blood and the lymphatic system, and therefore facilitate the interaction between APCs entering through the lymph and naïve T cells entering via blood vessels. In this way the lymph

nodes contribute efficiently to the initiation of adaptive immune responses. Lymph nodes are divided into different areas termed B-cell zones and T-cell zones, according to the primary type of lymphocyte found in these areas. Naïve T cells, as well as antigen-experienced T cells, constantly circulate the body via blood and lymph in search for antigen presented to them by APCs. When T cells arrive at a lymph node they enter the T cell zone. Here, special cells called fibroblastic reticular cells (FRCs) produce and ensheath a 3 dimensional (3D) reticular network consisting of extracellular matrix proteins, including collagens, laminin, fibronectin and tenascin[1]. T cells travel along this network via chemotaxis toward "trapped", activated APCs. This extracellular lymph node-architecture is a clever solution to the challenge of enabling physical contact between specific cells that are only present in negligible numbers.

Description of the invention

In the context of diagnostics, imitating the extracellular reticular network of a lymph node using a protein matrix, increases the chance of specific cell-cell contact. In the present invention, a stabilized blood sample is applied to a chip, together with antigens from the pathogen of interest, and lead through the extracellular protein matrix. Due to the "stickiness" of the monocytes (APC precursor cells) present in the blood sample, these cells will stick to the matrix, take up the antigen, process it, and present it on their cell surface. Additionally, they will start to secrete chemokines as a result of their activation. T cells, which are less sticky, are able to "travel" along the matrix following the chemokine gradients created by the stationary, activated APCs. This will increase the chance of specific T cell-APC encounter and thus increase the reliability of the results, since the risk of false negatives is decreased. Only if the specific T cells already have been exposed to the antigen prior to the test (hence in an infected individual), the induced immune-response in the form of cytokine release, will exceed a threshold and yield a positive readout. The result is read directly on the chip using a built-in quantitative reverse transcriptase polymerase chain reaction (qRT-PCR). Since the

[1] *Sobocinski GP, Toy K, Bobrowski WF, Shaw S, Anderson AO, Kaldjian EP (2010): Ultrastructural localization of extracellular matrix proteins of the lymph node cortex: evidence supporting the reticular network as a pathway for lymphocyte migration. BMC Immunol. Aug; 11(42).*

readout is based on the presence of mRNA and not proteins the result is expected to be ready after only a few hours.

The main advantages of this chip compared to presently used *in vitro* cell culture tests, is that since the result is expected to be read after only a few hours, the patient tested can get the result within the same day. This is important when diagnosing for example patients in developing countries that might have travelled a long way to get to the clinic, and does not have the possibility to wait a few days for the result. In developed countries the chip will ease the diagnosis of, for example, homeless people that do not have a contact address. Instead they can get the results directly at the clinic after a few hours, and a treatment can be initiated. Another advantage is that the blood is directly added to the chip, and therefore does not need to first be transported to a laboratory, thus it is not a concern whether the cells are still viable. Since the blood does not need to be incubated and then analyzed by trained personnel and since the volume of blood, and therefore also reagents, is minimal, this diagnostic chip will be cheaper than the present solutions. It is, however, a necessity that the clinics that are performing the tests have a reader that can translate the qRT-PCR results, but this is a one-time expense.

This invention is generic – the chip is not restricted to one specific disease, but can in principle be used to diagnose other infections that elicit a cell-mediated immune response in humans as well as animals, such as HIV, malaria, brucellosis and paratuberculosis. Also it might be useful in the prognosis of cancer since the activity of the cancer-specific cell-mediated immune response is important in controlling cancer development.

Intellectual property right (IPR) landscape - Novelty search

Searched patent/literature databases:

- Patents
  - Derwent Innovations Index
- Papers
  - Web of Science
  - PubMed – NCBI
- Others
  - Google search

Search profile (words used):

- Same words used when searching for patents and papers:

1. Topic=(chip* or micro chip* or microchip* or nano chip* or nanochip* or lab on a chip* or lab-on-a-chip* or LOC)
2. Topic=(polymerase chain reaction or PCR or qRT PCR or qRT-PCR or quantitative real time polymerase chain reaction)
3. Topic=(diagnostic* or diagnose*)
4. Topic=(cell-mediated immune respons* or CMI or cell mediated immune respons* or cell mediated immunerespons*)
5. Topic=(micro fluidic* or microfluidic*)
6. Topic=(detect* or discover* or measure*)
7. Topic=(interferon gamma* or IFN-g or interferon-gamma or interferon-g or interferon* or IFN)

- ***Derwent***
  - (Chemical Section, Electrical and Electronic Section, Engineering Section, Timespan = All Years)
- ***Web of Science***
  - (Databases = Science Citation Index Expanded, Social Sciences Citation Index, Arts & Humanities Citation Index, Timespan = All Years)
- ***PubMed –NCBI***
  - (All Fields)
- **Google**

- "tuberculosis + low cost + diagnostic + blood"
- "artificial lymph node"

Patents or papers from cooperative scientists:

Patents

- Hansen, Mikkel Fougt; Damsgaard, Christian Danvad; Larsen, Niels Bent; **Wolff, Anders** (2011) Sample processing device and method. Patent No 20110818

- Christer Spegel, Simon Pedersen, Ras K. Vestergaard, Tautgirdas Ruzgas, Rafel, Taboryski, **Anders Wolff** (2007)**.** Determining and monitoring system for properties in single particle e.g. biological cell, has one interface used for interfacing the substrate with an analyzing system. WO2007104565

Papers

- **Gregers Jungersen**

References related to diagnosis of cell-mediated immunity

- Cordes H., Riber, U., Jensen, T.K., and Jungersen, G. Cell-mediated and humoral immune responses in pigs following primary and challenge-exposure to *Lawsonia intracellularis*. *Veterinary Research* In press

- Thomsen, V.T., Nielsen, S.S., Thakur, A., Jungersen, G. Characterization of the long-term immune response to vaccination against *Mycobacterium avium* subsp*. paratuberculosis* in Danish dairy cows. *Veterinary Immunology and Immunopathology* In press

- Jungersen G., Mikkelsen, H. and Grell, S.N. Use of the johnin PPD interferon-gamma assay in control of bovine paratuberculosis. 2011. *Veterinary Immunology and Immunopathology* In press

- Mikkelsen H, Aagaard C, Nielsen SS, Jungersen G. 2011. Novel antigens for detection of cell mediated immune responses to Mycobacterium avium subsp. paratuberculosis infection in cattle. *Veterinary Immunology and Immunopathology* 143: 46-54.

- H Mikkelsen, C Aagaard, S S Nielsen, and G Jungersen. 2011. Review of *Mycobacterium avium* subsp. *paratuberculosis* antigen candidates with diagnostic potential. *Veterinary Microbiology* 152: 1-20.

- Riber, U., Boesen, H.T., Jakobsen, J.T., Nguyen, L.T.M. and Jungersen, G. 2011. Co-incubation with IL-18 potentiates antigen-specific IFN-γ response in a whole-blood stimulation assay for measurement of cell-mediated immune responses in pigs experimentally infected with *Lawsonia intracellularis*. *Veterinary Immunology and Immunopathology* 139: 257-263.

- D J Begg, K de Silva, K Bosward, L Di Fiore, D L Taylor, G Jungersen and R J Whittington. 2009. Enzyme Linked Immuno Spot: An alternative method for the detection of Interferon gamma in Johne's disease. *Journal of Veterinary Diagnostic Investigation* 21: 187-196.

- H Mikkelsen, G Jungersen and S S Nielsen. 2009. Association between milk antibody and interferon-gamma responses in cattle from *Mycobacterium avium* subsp. *paratuberculosis* infected herds. *Veterinary Immunology and Immunopathology* 127: 235-241.

- Riber, U. and Jungersen, G. 2007. Cell-mediated immune responses differentiate infections with *Brucella suis* from *Yersinia enterocolitica* serotype O:9 in pigs. *Veterinary Immunology and Immunopathology* 116: 13-25.

- Olsen, I., Boysen, P., Kulberg, S., Hope, J.C., Jungersen, G. and Storset, A. 2005. Bovine NK cells can produce gamma interferon in response to the secreted mycobacterial proteins ESAT-6 and MPP14, but not in response to MPB70. *Infection and Immunity* 73: 5628-5635.

- Huda, A., Jungersen, G. and Lind, P. 2004. Longitudinal study of interferon-gamma, serum antibody and milk antibody responses in cattle infected with *Mycobacterium avium* subsp. *paratuberculosis*. *Veterinary Microbiology* 104: 43-53.

- Huda, A., Lind, P., Christoffersen, A.B. and Jungersen, G. 2003. Analysis of repeated tests for interferon-gamma (IFN-γ) response and faecal excretion for diagnosis of subclinical paratuberculosis in Danish cattle. *Veterinary Immunology and Immunopathology* 94: 95-103.

- Jungersen, G., Huda, A., Hansen, J.J. and Lind, P. 2002. Interpretation of gamma-interferon test for diagnosis of subclinical paratuberculosis in cattle. *Clinical and Diagnostic Laboratory Immunology* 9, 453-460.

Papers submitted to peer-reviewed journals:

- Mikkelsen H, Aagaard C, Nielsen SS, Jungersen G. Correlation of antigen-specific IFN-γ responses of fresh blood samples from *Mycobacterium avium* subsp. *paratuberculosis* infected cattle with responses of day-old samples co-cultured with IL-12 or anti-IL-10 antibodies. *Veterinary Immunology and Immunopathology.*

- **Anders Wolff**

References related to lab-on-a-chip and PCR

- Bui, Thanh Xuan; Wolff, Anders; Madsen, Mogens; Bang, Dang Duong (2011) Reverse transcriptase real-time PCR for detection and quantification of viable Campylobacter jejuni directly from poultry faecal samples. *Research in Microbiology*, p. 1-9 (2011)

- Yi Sun, Raghuram Dhumpa, Dang Duong Bang, Jonas Høgberg, Kurt Handberg and Anders Wolff (2011) A lab-on-a-chip device for rapid identification of avian influenza viral RNA by solid-phase PCR. *Lab Chip*, 2011, 11 (8) Pages: 1457-1463 DOI: 10.1039/c0lc00528b

- Yi Sun, Raghuram Dhumpa, Dang Duong Bang, Kurt Handberg, Anders Wolff (2011). DNA microarray-based solid-phase RT-PCR for rapid detection and identification of influenza virus type A and subtypes H5 and H7. *Diagnostic Microbiology and Infectious Disease* 2011, 69(4) 432-439

- Haukur Gudnason, Martin Dufva, D.D. Bang and Anders Wolff, Comparison of multiple DNA dyes for real-time PCR: effects of dye concentration and sequence composition on DNA amplification and melting temperature. *Nucleic Acids Research*, 35, (19) Art No e127 (8 pages) Oct (2007)

- Christensen, T.B., Pedersen, C.M., Gröndahl, K.G., Jensen, T.G., Bang, D.D. & Wolff, A. PCR biocompatibility of Lab-on-a-chip and MEMS materials. *J. Micromech. Microeng.* 17, 1527-1532 (2007).

- Ahlford, A; Brivio, M; Gudnason, H; Wolff, A; Sylvanen, A. Development of a lab-on-a-chip for point-of-care genetic diagnostics. *European Journal of Clinical Investigation.* 37, 82 (2007)

- Zhenyu Wang, Andrea Sekulovic, Jörg P. Kutter, Dang. D. Bang and Anders Wolff. Towards a portable microchip system with integrated thermal control and polymer waveguides for real-time PCR. *Electrophorecis,* 2006, 27, (24), 5051-5058.

Publications in Refereed Proceedings

- Minqiang Bu, Ivan R. Perch-Nielsen, Yi Sun, and Anders Wolff (2011) A Microfluidic Control System With Re-Usable Micropump/Valve Actuator and Injection Moulded Disposable Polymer Lab-on-a-Slide. *Transducers '11, 16th International Conference on Solid-State Sensors, Actuators and Microsystems, Beijing, China (2011),* pages 1244-1247

- Dang Duong Bang, Dhumpa Raghuram, Cao Cuong, Flora laouenan, Berganzo Javier, Rafal Walczak, Yuliang Liu, Minqiang Bu, Jan Dziuban, Jesus Miguel Ruano, and Anders Wolff A Trip from a Tube to a Chip Applied Micro and Nanotechnology in Biotechonology, Veterinary and Life Sciences. Proceedings of the 3rd International Conference on the Development of BioMedical Engineeering in Vietnam, 11-14th Jan 2010 Publisher: Springer (ISSN: 1680-0737) , pages: 290-293, 2010

- Dang Duong Bang, Raghuram Dhumpa, M. Agirregabiria, Rafal Walczak, Yuliang Liu, Mingiang Bu, Sun Yi, Jan Dzuiban, Jesus Miguel Rruano, and Anders Wolff (2009) From a Tube to a Chip - Application of Micro and Nanotechnology in Biotechnology, Veterinary and Life Sciences. Smart Systems Integration Brussels Belgium On line publication March 2009 (Keynote lecture) http://www.mesago.de/en/SSI/Proceedings/index.htm

- Xuan Thanh Bui, Anders Wolff, Dang Duong Bang. Detection and quantification of *Campylobacter jejuni* and *Campylobacter coli* mRNA in poultry fecal samples. Proceedings of CHRO 2009. pp 68-

- M. Brivio, D. Snakenborg, E. Søgaard, A. Ahlford, A.-C. Syvänen, J.P. Kutter, and A.Wolff On-Chip Integration of Sample Pretreatment and Multiplex Polymerase Chainreaction (PCR) for DNA Analysis. *Proc. Micro Total Analysis Systems 2008*, Kluwer Academic Publisher, Dordrecht, The Netherlands, pp. 1737-1739, (2008).

- Patrycja Szczepańska, Rafał Walczak, Anders Wolff, Jan A. Dziuban (2008). SU-8 planar waveguides for real-time PCR chips. Proceedings of EUROSENSORS XXII 2008 Pp 383-386

Number of found and discarded patents/papers

- Patents (searched February 7, 2012 and February 20, 2012 in Derwent)

Combination of Search words	# found patents /applications	# relevant patents /applications	Patent /application ID
Search 1			
(chip* or micro chip* or microchip* or nano chip* or nanochip* or lab on a chip* or lab-on-a-chip* or LOC)	>100.000	-	-
(chip* or micro chip* or microchip* or nano chip* or nanochip* or lab on a chip* or lab-on-a-chip* or LOC) **AND** (polymerase chain reaction or PCR or qRT PCR or qRT-PCR or quantitative real time polymerase chain reaction)	911	-	-
(chip* or micro chip* or microchip* or nano chip* or nanochip* or lab on a chip* or lab-on-a-chip* or LOC) **AND** (polymerase chain reaction or PCR or qRT PCR or qRT-PCR or quantitative real time polymerase chain reaction) **AND** (diagnostic* or diagnose*)	217	0	-
Search 2			
(chip* or micro chip* or microchip* or nano chip* or nanochip* or lab on a chip* or lab-on-a-chip* or LOC)	>100.000	-	-
(chip* or micro chip* or microchip* or nano chip* or nanochip* or lab on a chip* or lab-on-a-chip* or LOC) **AND** (micro fluidic* or microfluidic*)	1.461	-	-
(chip* or micro chip* or microchip* or nano chip* or nanochip* or lab on a chip* or lab-on-a-chip* or LOC) **AND** (micro fluidic* or microfluidic*) **AND** (polymerase chain reaction or PCR or qRT PCR or qRT-PCR or quantitative real time polymerase chain reaction)	83	-	-
(chip* or micro chip* or microchip* or nano chip* or nanochip* or lab on a chip* or lab-on-a-chip* or LOC) **AND** (micro fluidic* or microfluidic*) **AND** (polymerase chain reaction or PCR or qRT PCR or qRT-PCR or quantitative real time polymerase chain reaction) **AND** (diagnostic* or diagnose*)	18	2	US2009317874-A1 WO2008117209-A1
Search 3			
(detect* or discover* or measure*)	>100.000	-	-

(detect* or discover* or measure*) **AND** (cell-mediated immune respons* or CMI or cell mediated immune respons* or cell mediated immunerespons*)	752	-	-
(detect* or discover* or measure*) **AND** (cell-mediated immune respons* or CMI or cell mediated immune respons* or cell mediated immunerespons*) **AND** (interferon gamma* or IFN-g or interferon-gamma or interferon-g or interferon* or IFN)	20	3	WO2009144478-A2 WO200259605-A1 US5334504-A1

- Papers (searched February 7, 2012 in PubMed)

Combination of Search words	# found papers	# relevant papers	Paper(s)
Search 1			
(chip* or micro chip* or microchip* or nano chip* or nanochip* or lab on a chip* or lab-on-a-chip* or LOC)	32346	-	-
(chip* or micro chip* or microchip* or nano chip* or nanochip* or lab on a chip* or lab-on-a-chip* or LOC) **AND** (polymerase chain reaction or PCR or qRT PCR or qRT-PCR or quantitative real time polymerase chain reaction)	3257	-	-
(chip* or micro chip* or microchip* or nano chip* or nanochip* or lab on a chip* or lab-on-a-chip* or LOC) **AND** (polymerase chain reaction or PCR or qRT PCR or qRT-PCR or quantitative real time polymerase chain reaction) **AND** (diagnostic* or diagnose*)	348	-	-
(chip* or micro chip* or microchip* or nano chip* or nanochip* or lab on a chip* or lab-on-a-chip* or LOC) **AND** (polymerase chain reaction or PCR or qRT PCR or qRT-PCR or quantitative real time polymerase chain reaction) **AND** (diagnostic* or diagnose*) **AND** (cell-mediated immune respons* or CMI or cell mediated immune respons* or cell mediated immunerespons*)	1	1	Chang *et al.,* 2010
Search 2			
(chip* or micro chip* or microchip* or nano chip* or nanochip* or lab on a chip* or lab-on-a-chip* or LOC)	32346	-	-
(chip* or micro chip* or microchip* or nano chip* or nanochip* or lab on a chip* or lab-on-a-chip* or LOC) **AND** (micro fluidic* or microfluidic*)	4749	-	-
(chip* or micro chip* or microchip* or nano chip* or nanochip* or lab on a chip* or lab-on-a-chip* or LOC) **AND** (micro fluidic* or microfluidic*) **AND** (polymerase chain reaction or PCR or qRT PCR or qRT-PCR or quantitative real time polymerase chain reaction)	343	-	-

(chip* or micro chip* or microchip* or nano chip* or nanochip* or lab on a chip* or lab-on-a-chip* or LOC) **AND** (micro fluidic* or microfluidic*) **AND** (polymerase chain reaction or PCR or qRT PCR or qRT-PCR or quantitative real time polymerase chain reaction) **AND** (diagnostic* or diagnose*)	61	0	-
Search 3			
(detect* or discover* or measure*)	3377434	-	-
(detect* or discover* or measure*) **AND** (cell-mediated immune respons* or CMI or cell mediated immune respons* or cell mediated immunerespons*)	3379	-	-
(detect* or discover* or measure*) **AND** (cell-mediated immune respons* or CMI or cell mediated immune respons* or cell mediated immunerespons*) **AND** (interferon gamma* or IFN-g or interferon-gamma or interferon-g or interferon* or IFN)	535	-	-
(detect* or discover* or measure*) **AND** (cell-mediated immune respons* or CMI or cell mediated immune respons* or cell mediated immunerespons*) **AND** (interferon gamma* or IFN-g or interferon-gamma or interferon-g or interferon* or IFN) **AND** (diagnostic* or diagnose*)	44	3	Harrington *et al.,* 2007 Cesur *et al.,* 2005 Pai 2005

Additional papers found using the same search profile in Web of Science (February 21, 2012)

Combination of Search words	**# found papers**	**# relevant papers**	**Paper(s)**
Search 1			
(chip* or micro chip* or microchip* or nano chip* or nanochip* or lab on a chip* or lab-on-a-chip* or LOC)	89648	-	-
(chip* or micro chip* or microchip* or nano chip* or nanochip* or lab on a chip* or lab-on-a-chip* or LOC) **AND** (polymerase chain reaction or PCR or qRT PCR or qRT-PCR or quantitative real time polymerase chain reaction)	3340	-	-
(chip* or micro chip* or microchip* or nano chip* or nanochip* or lab on a chip* or lab-on-a-chip* or LOC) **AND** (polymerase chain reaction or PCR or qRT PCR or qRT-PCR or quantitative real time polymerase chain reaction) **AND** (diagnostic* or diagnose*)	404	-	-
(chip* or micro chip* or microchip* or nano chip* or nanochip* or lab on a chip* or lab-on-a-chip* or LOC) **AND** (polymerase chain reaction or PCR or qRT PCR or qRT-PCR or quantitative real time polymerase chain reaction) **AND** (diagnostic* or diagnose*) **AND** (cell-mediated immune respons* or CMI or cell mediated immune respons* or cell mediated immunerespons*)	0	-	-
Search 2			
(chip* or micro chip* or microchip* or nano chip* or nanochip* or lab on a	89648	-	-

chip* or lab-on-a-chip* or LOC)			
(chip* or micro chip* or microchip* or nano chip* or nanochip* or lab on a chip* or lab-on-a-chip* or LOC) **AND** (micro fluidic* or microfluidic*)	7538	-	-
(chip* or micro chip* or microchip* or nano chip* or nanochip* or lab on a chip* or lab-on-a-chip* or LOC) **AND** (micro fluidic* or microfluidic*) **AND** (polymerase chain reaction or PCR or qRT PCR or qRT-PCR or quantitative real time polymerase chain reaction)	750	-	-
(chip* or micro chip* or microchip* or nano chip* or nanochip* or lab on a chip* or lab-on-a-chip* or LOC) **AND** (micro fluidic* or microfluidic*) **AND** (polymerase chain reaction or PCR or qRT PCR or qRT-PCR or quantitative real time polymerase chain reaction) **AND** (diagnostic* or diagnose*)	132	1	Park *et al.,* 2011
Search 3			
(detect* or discover* or measure*)	4762821	-	-
(detect* or discover* or measure*) **AND** (cell-mediated immune respons* or CMI or cell mediated immune respons* or cell mediated immunerespons*)	8675	-	-
(detect* or discover* or measure*) **AND** (cell-mediated immune respons* or CMI or cell mediated immune respons* or cell mediated immunerespons*) **AND** (interferon gamma* or IFN-g or interferon-gamma or interferon-g or interferon* or IFN)	2492	-	-
(detect* or discover* or measure*) **AND** (cell-mediated immune respons* or CMI or cell mediated immune respons* or cell mediated immunerespons*) **AND** (interferon gamma* or IFN-g or interferon-gamma or interferon-g or interferon* or IFN) **AND** (diagnostic* or diagnose*)	77	2	Kalis *et al.,* 2003 Schiller *et al.,* 2010

Summary of relevant patents, papers and others

Patents

- **Apparatus for performing thermocyclic process such as amplifying DNA comprises microfluidic chip with fluid channel formed in it, and at least two temperature zones; and thermal distribution elements disposed over portions of the chip**

  Patent Number(s): US2009317874-A1

  Inventor(s): DALE G A, HASSON K C, STONE M, ZENG S

  Patent Assignee Name(s) and Code(s):CANON US LIFE SCI INC(CANO-C)

  Derwent Primary Accession Number: 2009-S64755 [02]

  Abstract: NOVELTY - Apparatus (100) to perform thermocyclic process comprises microfluidic chip (200) having fluid channel (202), and is formed with at least two temperature zones; and thermal distribution element(s) disposed on portions of the chip. Each thermal distribution element is constructed to distribute thermal energy from external thermal energy source uniformly over the portion of chip thus defining the portions as one of the temperature zones within chip. The channel is arranged so that fluid flowing through the channel would enter and exit several times from each temperature zone.

  USE - for performing thermocyclic process such as amplifying DNA (claimed).

  ADVANTAGE - The microfluidic chips are prepackaged for optimized assay designs, e.g. specific diagnostic/analytical tests that optimize the PCR reaction. During chip fabrication, a label is affixed to the chip so that the instrument readily identifies the chip via an optical detector reading the label. The microfluidic chips are preferably disposable.

  DETAILED DESCRIPTION - An apparatus (100) for performing a thermocyclic process comprises a microfluidic chip (200) having a fluid channel (202), and is configured with at least two temperature zones; and at least one thermal distribution element in thermal communication with an associated portion of the chip. The thermal distribution element is constructed and arranged to distribute thermal energy from an external thermal energy source uniformly over the associated portion of the chip thus defining the associated portion as one of the

temperature zones within the chip. The channel is arranged such that a fluid flowing through the channel would enter and exit several of times from each temperature zones of the chip. The thermal distribution element comprises a thermally conductive material adhered to the associated portion of the microfluidic chip. The thermal distribution element comprises a metal plate, and a rectangular metal block. The apparatus further comprises a label including information which is used to identify characteristics of the thermocyclic process that can be performed with the apparatus based on characteristics of the temperature zones of the chip. The label comprises a machine-readable label; a bar code; and radiofrequency identification tag. The apparatus also comprises a thermal energy source associated with each thermal distribution element and configured to apply thermal energy to the thermal distribution element; and a detector (115) configured to detect emissions originating from at least one location within the channel. An INDEPENDENT CLAIM is included for a DNA amplification method involving providing the apparatus for amplifying DNA; applying thermal energy to the thermal distribution elements to generate temperatures in the portion of the chip; and pumping a solution containing a nucleic acid sample through the channel so that the solution alternately flows through the first, second, and third portions of the chip and is alternately exposed to the temperatures, while the solution is pumped, detecting emission originating from solution flowing through a portion of the channel disposed within one of the first, second, and third portions of the chip.

- **Integrated micro-fluidic device for molecular diagnostics of fluids e.g. blood, has chamber circuit integrated on substrate switches signals related to chambers accommodating fluids and chip has controller coupled to chamber circuit**

  Patent Number(s): WO2008117209-A1

  Inventor(s): FIH D A, HOEVENAARS A A M

  Patent Assignee Name(s) and Code(s):KONINK PHILIPS ELECTRONICS NV(PHIG-C)

  Derwent Primary Accession Number: 2008-M80548 [59]

  Citing Patents: 1

Abstract: NOVELTY - The integrated micro-fluidic device comprises several polymerase chain reaction (PCR) chambers (11-MN) provided on a glass substrate for accommodating fluids. A chamber circuit such as thin film transistor (TFT) is integrated on the substrate for switching signals related to the chambers. An integrated circuit (IC) chip bonded to the substrate comprises a controller which is coupled to the chamber circuit. The TFT comprises a polycrystalline, microcrystalline or amorphous semiconductor material and the IC chip comprises a monocrystalline semiconductor material.

USE - Integrated micro-fluidic device with local temperature control for molecular diagnostics of fluidic samples such as blood, urine, saliva, anal and vaginal secretions, agricultural samples, soil samples, bacteria, viruses, fungi or parasites.

ADVANTAGE - The improved integrated micro-fluidic device enables more uniform heating of the chamber with local temperature control.

- **Detecting a cell-mediated immune response to purified antigens of Mycobacterium avium subsp. paratuberculosis (Map) comprises detection of a cell-mediated immune response by measuring extent of lymphocyte activation and/or proliferation**

  Patent Number(s): WO2009144478-A2; WO2009144478-A9; WO2009144478-A3; AU2009252922-A1; EP2286230-A2; US2011135578-A1; CN102159952-A

  Inventor(s): HUGHES V M, STEVENSON K, HUGHES V

  Patent Assignee Name(s) and Code(s): MOREDUN RES INST (MORE-Non-standard), STEVENSON K(STEV-Individual), HUGHES V M(HUGH-Individual)

  Derwent Primary Accession Number: 2009-R90374 [60]

  Abstract: NOVELTY - Detecting a cell-mediated immune response to purified antigens of Mycobacterium avium subsp. paratuberculosis (Map) in an animal comprises detection of a cell-mediated immune response by measuring the extent of lymphocyte activation and/or proliferation in response to the purified antigens of Map.

  USE - The method is useful for detecting a cell-mediated immune response to purified antigens of Map in an animal; diagnosing Map infection in an animal; and for protecting an

animal against Map infection or for reducing Map colonization or the severity of a disease caused or contributed to by Map, where the disease caused or contributed to by Map is Johne's disease (all claimed).

DETAILED DESCRIPTION - INDEPENDENT CLAIMS are:

(1) a kit for carrying out a method of diagnosing a Map infection comprising purified Map-specific proteins or immunogenic fragments capable of eliciting a cell-mediated immune response, further comprising other reagents for use in the method of diagnosis, such as an anti-interferon gamma (IFN- gamma) antibody;

(2) proteins, e.g. mitogen activated protein (MAP) 0268c; MAP1297; MAP1365; and MAP3651c; and fragments, for raising an immune response in an animal;

(3) an immunogenic formulation vaccine comprising proteins, e.g. MAP0268c; MAP1297; MAP1365; and MAP3651c; and their fragments;

(4) a method of vaccinating or immunizing an animal against a MAP infection comprising administering MAP antigens, e.g. MAP0268c; MAP1297; MAP1365; and MAP3651c; and their fragments; and

(5) use of proteins, e.g. MAP0268c; MAP1297; MAP1365; and MAP3651c; and their fragments, for protecting an animal against Map infection or for reducing Map colonization or the severity of a disease caused or contributed to by Map.

Technology Focus/Extension Abstract: TECHNOLOGY FOCUS - BIOTECHNOLOGY - Preferred Method: In detecting a cell-mediated immune response to one or more purified antigens of Map in an animal, the cell-mediated immune response is measured by detecting a level of cytokine such as IFN- gamma , tumor necrosis factor alpha (TNF- alpha), transforming growth factor beta (TGF- beta), interleukins (IL-2, IL-6, IL-10, IL-12, IL-17) and granulocyte-macrophage colony-stimulating factor (GM-CSF) using antibodies or indirectly from mRNA by reverse transcription (RT)-PCR or microarray. The method is carried out on a blood sample or fraction, isolated from a subject, or a skin test such as a delayed hypersensitivity skin test. The sample of blood or fraction is incubated with the one or more purified Map antigens, to allow any cell-mediated response to develop. The antigens are proteins or fragments that are

expressed by Map and elicit a detectable immune response in animals infected by Map greater than that elicited by the antigens of other closely related subspecies of M. avium (M. avium subsp. avium and M. avium subsp. silvaticum). The antigens are display little or no cross-reactivity with other related species such as other subspecies of M. avium, M. bovis, and/or Mycobacterium tuberculosis. The method uses two or more Map-specific antigens, e.g. MAP0268c; MAP1297; MAP1365 and MAP3651c.

- **In vitro detection of a human or animal cell-mediated immune response to one or more specific antigens from the Mycobacterium tuberculosis complex, comprises using erythrocyte lysing buffer and detecting presence of gamma interferon**

  Patent Number(s): WO200259605-A; WO200259605-A1; AU2002219017-A1

  Inventor(s): MUNK M, ANDERSEN P

  Patent Assignee Name(s) and Code(s):STATENS SERUM INST (STAT-Non-standard)

  Derwent Primary Accession Number: 2002-608468 [51]

  Patents Cited by Examiner: 12, Articles Cited by Examiner: 6

  Abstract: NOVELTY - Detecting in vitro a cell-mediated immune response to specific antigens from the Mycobacterium tuberculosis complex, comprises treating a blood sample containing lymphocytes within a leukocyte population and erythrocytes to lyse the erythrocytes present, incubating the lymphocytes with the antigen from the complex, and detecting the cell-mediated immune response of the lymphocytes to the antigen.

  USE - The method above is useful in in vitro detection of a human or animal cell-mediated immune response within a small fresh whole blood sample to one or more specific antigens such as those from the Mycobacterium tuberculosis complex (claimed).

  ADVANTAGE - The method is capable of decreasing the time and expenses for a cell-mediated tuberculosis diagnostic test, and it provides a significantly higher IFNgamma release, with less amount of cells, compared to other method that uses fresh blood samples. Thus, this method is reliable and suitable for specific T-cell response purposes.

  DETAILED DESCRIPTION - Detecting in vitro a cell-mediated immune response to one or more

specific antigens from the Mycobacterium tuberculosis complex (M. tuberculosis, M. africanum and M. bovis) in a human or animal, comprises treating a whole blood sample containing lymphocytes within a leukocyte population and erythrocytes to lyse the erythrocytes present, incubating the lymphocytes with the antigen from the complex, and detecting the cell-mediated immune response of the lymphocytes to the antigen.
AN INDEPENDENT CLAIM is also included for a diagnostic kit suitable for use in the above method, comprising a source of one or more specific antigens, latex beads coated with one or more specific antigens, and erythrocyte lysing buffer.

Technology Focus/Extension Abstract: TECHNOLOGY FOCUS - BIOTECHNOLOGY - Preferred Method: The lymphocyte concentration in the above method is concentrated between the steps of treating the whole blood sample and incubating the lymphocytes. The lymphocytes are enriched by centrifugation and are resuspended in the cell culture medium to produce a resuspension volume that is less than the volume of the whole blood sample by a factor of at least 1.5. The step of detecting the cell-mediated immune response is carried out by detecting the presence of gamma-interferon (IFNgamma) released by sensitized lymphocytes from the whole blood sample to indicate a cell-mediated immune response to the antigen. The IFNgamma released from the sensitized lymphocytes can be detected in an immunoassay, such as an enzyme-linked immunosorbant assay (ELISA). The lymphocytes cited above are also contacted with latex beads that are coated with the antigen.

EXAMPLE - Peripheral blood cells from each of several donors (healthy individuals or patients with tuberculosis) was either left untreated (fresh whole blood) or enriched (improved whole blood). In this procedure, 200 mul from the enriched leukocyte cell suspension were added into each well of a 96-well flat-bottom plate in the presence or absence of PHA (1 mug/ml), PPD (5 mug/ml), ESAT6 (5 mug/ml), or CFP7 (5 mug/ml) and incubated at 37 degreesC in 5% CO2 air saturation. After 4-6 days in the culture, 100 mul/well of supernatant samples were removed and added into another 96-well plate for storage or for further use. Quantitative determination of IFNgamma secreted into the cell-culture supernatants were analyzed by ELISA technique using monoclonal antibodies specific for human IFNgamma. Briefly, 96-well

plates were incubated with a catching anti-human IFNgamma monoclonal antibody diluted in PBS at 4 degreesC for 18 hours. After washing and blocking of the wells, cell culture supernatants were added and the wells wee incubated for 2 hours. The wells were washed and biotin-labelled polyclonal goat-anti-human IFNgamma antibodies were added. The reaction is visualized by adding alkaline phosphatase-conjugated streptavidin followed by p-nitrophenyl phosphate diluted in the appropriate buffer. Concentrations of IFNgamma in the samples were calculated using the standard curve generated from the recombinant human IFNgamma and results were expressed in pg/ml. The minimum assay sensitivity was 10 pg/ml. The absence of interfering erythrocytes increased cell contact and performance of IFNgamma production by enriched cells.

- **In vitro assay for detecting cell-mediated immune responses - by incubating whole blood with specific antigen and detecting gamma interferon**

  Patent Number(s): US5334504-A1; US5494799-A1; WO8705400-A1; WO8705400-A; AU8771659-A ; JP63502695-W; EP296158-A; CA1299099-C ; EP296158-B1; DE3779909-G ; US5334504-A; EP296158-A4; US5494799-A; JP2642112-B2

  Inventor(s): CORNER L A, WOOD P R, WOOD R P, CORNER A L

  Patent Assignee Name(s) and Code(s): COMMONWEALTH SCI & IND RES ORG(CSIR-C), WOOD P R(WOOD-Individual)

  Derwent Primary Accession Number: 1987-264177 [74]

  Citing Patents: 21, Patents Cited by Examiner: 34, Articles Cited by Inventor: 1, Articles Cited by Examiner: 56

  Abstract: An in vitro method of detecting a cell-mediated immune response to a specific antigen in a human or animal comprises (a) incubating a whole blood sample from the human or animal with the specific antigen and (b) detecting the presence of gamma interferon (gamma IFN) released by sensitised lymphocytes in the whole blood sample to indicate a cell-mediated immune response to the specific antigen. Pref. the gamma IFN is detected using an emxyme-linked immunosorbent assay or a radioimmunoassay.

USE/ADVANTAGE-The assay is far simpler and faster than those previously described. A single blood sample provides sufficient material for testing a patient's responsiveness to a wide variety of antigens. The method is used esp. for detecting immune response to the M.bovis antigen, tuberculin purified protein deriv. (PPD) in whole blood samples from cattle. The assay does not compromise the immune status of animals as does the current in vivo tuberculin skin test. The assay can also be used in detecting cellular responses to e.g. M. leprae, M. tuberculosis, mumps, Candida, Brucella, histoplasmin, trichophyton, coccidioidin and malaria.

Papers

- **Chang HJ, Huang MY, Yeh CS, Chen CC, Yang MJ, Sun CS, Lee CK, Lin SR (2010): Rapid diagnosis of tuberculosis directly from clinical specimens using a gene chip. Clin Microbiol Infect. Aug;16(8):1090-6.**

  Abstract: The aim of this study was to explore a gene chip capable of detecting the presence of Mycobacterium tuberculosis isolates directly in clinical sputum specimens and to compare it with current molecular detection techniques. At first, we selected 13 M. tuberculosis-specific target genes to construct a gene chip for rapid diagnosis. Using the membrane array method, we diagnosed M. tuberculosis by gene chip directly from 246 sputum specimens from patients suspected of having tuberculosis. Among 80 M. tuberculosis complex (MTBC) culture-positive sputum specimens, the MTBC detection rate was 62.5% (50/80) by PCR-restriction fragment length polymorphism (RFLP), 70% (56/80) by acid-fast staining, and 85% (68/80) by the membrane array method. Furthermore, subspecies showed different gene expression patterns in the membrane array. In conclusion, MTBC could be detected directly in sputum by the membrane array method. The rapidity of detection and the capability of differentiating subspecies could make this method useful in the control and prevention of tuberculosis.

- **Harrington NP, Surujballi OP, Waters WR, Prescott JF (2007): Development and evaluation of a real-time reverse transcription-PCR assay for quantification of gamma interferon mRNA to**

diagnose tuberculosis in multiple animal species. Clin Vaccine Immunol. Dec;14(12):1563-71.
Abstract: Tuberculosis of free-ranging and captive wildlife, including species implicated in the maintenance and transmission of Mycobacterium bovis, is a difficult disease to diagnose and control. Historically, diagnosis of tuberculosis has relied largely upon assays of cell-mediated immunity (CMI), such as tuberculin skin testing. This approach, however, is problematic or impractical for use with many wildlife species. Increasingly, in vitro diagnostic tests, including gamma interferon (IFN-gamma)-based assays, are replacing or complementing skin testing of cattle and humans. Analogous assays are unavailable for most wildlife because of a lack of species-specific immunological reagents. This report describes the development and validation of a whole-blood assay to quantify antigen-specific IFN-gamma mRNA expression by quantitative real-time reverse transcription-PCR. Oligonucleotide primers and probes were designed and tested for reactivity towards several susceptible species of interest with respect to tuberculosis infection. The assay was subsequently optimized to quantify the IFN-gamma mRNA expression in elk and red deer (Cervus elaphus) and was evaluated for its ability to detect mycobacterial antigen-specific responses of experimentally tuberculosis-infected animals. The assay was a simple, rapid, and sensitive measure of antigen-specific CMI. The IFN-gamma mRNA responses correlated well with IFN-gamma protein production and showed performance in determining an animal's infection status superior to that of either lymphocyte proliferation or IFN-gamma protein enzyme-linked immunosorbent assay methods. An additional advantage is the ease with which the assay can be modified to reliably quantify IFN-gamma expression by using consensus sequences of closely related species or of other species for which IFN-gamma sequence information is available.

- **Cesur S, Saka D, Tarhan G, Ceyhan I, Calişir H, Ogretensoy M (2005): [Evaluation of a commercial enzyme immunoassay for the detection of interferon gamma levels in active tuberculosis patients and vaccinated healthy subjects]. Mikrobiyol Bul. Jan;39(1):73-7. [Article in Turkish].**

Abstract: The detection of plasma interferon gamma (IFN-g) levels has an important value for the evaluation of cell mediated immune response to Mycobacterium tuberculosis. The aim of this study was to investigate the plasma IFN-g levels by a commercial enzyme immunoassay (ELISA) and to compare the levels between recently diagnosed culture positive lung tuberculosis patients and BCG vaccinated healthy controls. Twenty-three patients with active lung tuberculosis (13 males, 10 females) and 34 BCG vaccinated healthy adults (16 male, 18 female) have been included in the study. The control subjects were questioned about passed tuberculosis infection and/or a contact with tuberculosis patients. No risk factors for exposure to M. tuberculosis were found in the control group. IFN-g levels were measured by QuantiFERON-TB (Cellestis, Australia) kit, and 22 of patients and 17 of control subjects were found to be positive. As a result, the sensitivity of QuantiFERON-TB test was high (95.6%), however its specificity was quite low (50%). In conclusion, QuantiFERON-TB may be used as a supplementary diagnostic test in patients considered to have active tuberculosis, before treatment. As BCG is in routine vaccination programme and the number of active tuberculosis cases is high in our country, this test seems to be invalid for the diagnosis of latent tuberculosis. Therefore, more specific tests that are not affected by the vaccine response, are required for the diagnosis of latent tuberculosis.

- **Pai M (2005): Alternatives to the tuberculin skin test: interferon-gamma assays in the diagnosis of mycobacterium tuberculosis infection. Indian J Med Microbiol. Jul;23(3):151-8.**
  Abstract: For nearly a century, there were no alternatives to the tuberculin skin test (TST) for diagnosing latent tuberculosis infection. Because of advances in immunology and genomics, for the first time, an alternative has emerged in the form of T cell based interferon-g (IFN-gamma) assays, a new generation of in vitro tests of cellular immunity. These assays measure cell mediated immune response by quantifying IFN-gamma released by T cells in response to stimulation by Mycobacterium tuberculosis antigens. Although early versions of IFN-gamma assays used purified protein derivative (PPD) as the stimulating antigen, newer versions use antigens that are significantly more specific to M. tuberculosis. These specific antigens include

ESAT-6 and CFP-10. These proteins, encoded by genes located within the region of difference 1 (RD1) segment of the M. tuberculosis genome, are more specific to M. tuberculosis than PPD because they are not shared with any BCG substrains or several nontuberculous mycobacterial species. A review of current evidence on the performance of IFN-gamma assays and TST suggests that both the TST and IFN-gamma assays have advantages and limitations, and both tests appear to be useful at this time. The emergence of IFN-gamma assays is a much anticipated, welcome development that has, for the first time, increased the choice of tests available for diagnosing latent tuberculosis infection. Because both tests have their strengths and limitations, the decision to select one over the other will depend on the population, the goal of testing, and the resources available. To fully evaluate the utility of IFN-gamma assays in high burden countries such as India, long-term cohort studies are needed to determine the association between positive IFN-gamma results and the subsequent risk of active disease.

- **Kalis CHJ, Collins MT, Hesselink JW, Barkema HW (2003): Specificity of two tests for the early diagnosis of bovine paratuberculosis based on cell-mediated immunity: the Johnin skin test and the gamma interferon assay. Veterinary Microbiology. Dec;97(1-2):73-86.**
  Abstract: Paratuberculosis in cattle is a chronic debilitating infectious disease caused by Mycobacterium paratuberculosis. Control of paratuberculosis is based on tests that principally detect advanced stages of infections: faecal culture and serology. Tests measuring cell-mediated immunity (CMI) could improve control of paratuberculosis if able to diagnose mycobacterial infections earlier, before animals become infectious. A drawback of CMI tests for paratuberculosis has been a reported low specificity. This study re-examined CMI specificity and factors that may affect it. The specificities of the Johnin skin test and its in vitro equivalent, the gamma interferon (IFNgamma) assay, were estimated in 35 uninfected dairy herds. In each herd a random sample of 20 young (6-24 months old) and 20 adult (greater than or equal to24 months old) female dairy cattle were tested by both tests simultaneously. Skin test specificity was 93.5% using a skin thickness increase of greater than or equal to4 mm as the cut-off value. IFNgamma assay specificity when interpreted using a newly developed

algorithm was 93.6%. When interpreted according to two alternative algorithms provided by the IFNgamma kit suppliers, the assay had specificities of 66.1 and 67.0%. If the skin test and IFNgamma assay were used in parallel, and only animals positive on both tests were considered as M. paratuberculosis-infected, the specificity was 97.6%. Agreement between skin test and IFNgamma assay on 1631 total animals was fair (kappa = 0.41). Antigen batch influenced the specificity of both the skin test, ranging from 92 to 95%, and the IFNgamma assay, ranging from 71 to 99% among batches. Test specificity also varied among herds ranging from 58 to 100% for the skin test and 57 to 100% for the IFNgamma assay. While factors affecting CMI test specificity and agreement need further evaluation, the high specificity and general agreement among these CMI tests, coupled with the excellent results obtained in the control of bovine tuberculosis using CMI tests, support their potential value in the early diagnosis and control of paratuberculosis.

- **Schiller I, Oesch B, Vordermeier HM, Palmer MV, Harris BN, Orloski KA, Buddle BM, Thacker TC, Lyashchenko KP, Waters WR (2010): Bovine Tuberculosis: A Review of Current and Emerging Diagnostic Techniques in View of their Relevance for Disease Control and Eradication. Transboundary And Emerging Diseases. Aug; 57(4): 205-220.**
  Abstract: Existing strategies for long-term bovine tuberculosis (bTB) control/eradication campaigns are being reconsidered in many countries because of the development of new testing technologies, increased global trade, continued struggle with wildlife reservoirs of bTB, redistribution of international trading partners/agreements, and emerging financial and animal welfare constraints on herd depopulation. Changes under consideration or newly implemented include additional control measures to limit risks with imported animals, enhanced programs to mitigate wildlife reservoir risks, re-evaluation of options to manage bTB-affected herds/regions, modernization of regulatory framework(s) to re-focus control efforts, and consideration of emerging testing technologies (i.e. improved or new tests) for use in bTB control/eradication programs. Traditional slaughter surveillance and test/removal strategies will likely be augmented by incorporation of new technologies and more targeted control efforts. The present review provides an overview of current and emerging bTB testing

strategies/tools and a vision for incorporation of emerging technologies into the current control/eradication programs.

- **Park S, Zhang Y, Lin S, Wang TH, Yang S (2011): Advances in microfluidic PCR for point-of-care infectious disease diagnostics. Biotechnology Advances. Nov-Dec; 29(6): 830-839.**
  Abstract: Global burdens from existing or emerging infectious diseases emphasize the need for point-of-care (POC) diagnostics to enhance timely recognition and intervention. Molecular approaches based on PCR methods have made significant inroads by improving detection time and accuracy but are still largely hampered by resource-intensive processing in centralized laboratories, thereby precluding their routine bedside- or field-use. Microfluidic technologies have enabled miniaturization of PCR processes onto a chip device with potential benefits including speed, cost, portability, throughput, and automation. In this review, we provide an overview of recent advances in microfluidic PCR technologies and discuss practical issues and perspectives related to implementing them into infectious disease diagnostics.

Other (found on Google)

Search words: "tuberculosis + low cost + diagnostic + blood"

- **Pai NP and Pai M (2012): Point-of-Care Diagnostics for HIV and Tuberculosis: Landscape, Pipeline, and Unmet Needs. Discov Med. Jan;13(68):35-45.**
  Abstract: Early diagnosis and rapid initiation of treatment remains a key strategy to control both HIV and tuberculosis (TB). However, HIV and TB control programs have had completely contrasting successes, especially with the development and deployment of point-of-care (POC) diagnostics. Clinicians, researchers, and public health staff who work at the frontlines of HIV care and control have had access to an outstanding array of POC diagnostics at their disposal, including those used for screening, initial diagnosis, staging, treatment monitoring, and early infant diagnosis. The field has also advanced to consider over-the-counter, self-testing options for HIV and the use of multiplexed platforms that allow for simultaneous detection of

infections associated with HIV. In sharp contrast to HIV, suboptimal and delayed diagnosis of TB has perpetuated the epidemic in many high-burden countries. Although the TB diagnostics pipeline is substantially better today than it was even five years ago, absence of a simple POC test continues to be a gaping hole in the pipeline. In this review, we compare the POC diagnostics landscape and pipelines for these two important infectious diseases, and highlight gaps and unmet needs.
(http://www.discoverymedicine.com/Nitika-Pant-Pai/2012/01/18/point-of-care-diagnostics-for-hiv-and-tuberculosis-landscape-pipeline-and-unmet-needs/)

- **Post.doc, Ph.D. Thomas Steen Hansen's Project: Low cost polymer device for tuberculosis diagnostics using electrical readout.**

  Abstract: Tuberculosis is a serious threat to the people in numerous developing countries. One of the reasons this dangerous disease is difficult to control is the lack of a cheap and reliable diagnostic tool. In our project we aim at developing a polymer device that with a high sensibility can diagnose TB without the use of advanced laboratory equipment. The device is based on a new type of advanced polymer that can both conduct electricity and bind molecules with biological relevance. We can e.g. bind antibodies that are distinct in the manner that they can very specifically recognize a given molecule. Using this setup we can measure the presence of a TB related molecule in a blood sample from a patient. This is to be used in association with collaborators from Hvidovre Hospital who have identified a new signal protein in the blood from TB patients. In this project we will combine the advanced polymer with antibodies against the new signal protein to produce a simple and cheap polymer device that can diagnose TB in a health clinic in developing countries. The method is generic and can be transferred to other areas where antibodies are used for diagnostics, herein HIV.
  (http://www.nanotech.dtu.dk/English/Research/Externally_Funded_Projects/Low_Cost_Polymer_Device.aspx)

Search words: "artificial lymph node"

- **Okamoto N, Chihara R, Shimizu C, Nishimoto S, Watanabe T (2007): Artificial lymph nodes induce potent secondary immune responses in naive and immunodeficient mice. *J Clin Invest.*April;117(4):997–1007.**

  Abstract: We previously demonstrated that artificial lymph nodes (aLNs) could be generated in mice by the implantation of stromal cell–embedded biocompatible scaffolds into their renal subcapsular spaces. T and B cell domains that form in aLNs have immune response functions similar to those of follicles of normal lymphoid tissue. In the present study, we show that the aLNs were transplantable to normal as well as SCID mice, where they efficiently induced secondary immune responses. Antigen-specific secondary responses were strongly induced in aLNs even 4 weeks after their transplantation. The antigen-specific antibody responses in lymphocyte-deficient SCID mice receiving transplanted aLNs were substantial. The cells from the aLNs migrated to the SCID mouse spleen and BM, where they expanded to generate large numbers of antigen-specific antibody-forming cells. Secondary responses were maintained over time after immunization (i.e., antigen challenge), indicating that aLNs can support the development of memory B cells and long-lived plasma cells. Memory $CD4^+$ T cells were enriched in the aLNs and spleens of aLN-transplanted SCID mice. Our results indicate that aLNs support strong antigen-specific secondary antibody responses in immunodeficient mice and suggest the possibility of future clinical applications.
  (http://www.jci.org/articles/view/30379)

- **Patent application title: ARTIFICIAL LYMPH NODE FOR TREATING CANCER**
  Inventors: Takeshi Watanabe (Yokohama-Shi, JP) Kouji Tanaka (Yokohama-Shi, JP)
  Assignees: RIKEN
  IPC8 Class: AA61K3900FI
  USPC Class: 4242771
  Class name: Cancer cell or component thereof

Publication date: 10/22/2009

Patent application number: 20090263428

Abstract: Provided is an artificial lymph node that is persistently effective in cancer treatment in vivo. A method of producing an artificial lymph node capable of inducing cancer antigen-specific immune responses, comprising the following steps: (a) a step for immunizing a non-human animal using a cancer antigen and an adjuvant capable of inducing cellular immunity; and (b) a step for transplanting an artificial lymph node material consisting of a polymeric biomaterial comprising cytokine-producing stromal cells and dendritic cells to the immunized non-human animal, an artificial lymph node capable of inducing cancer antigen-specific immune responses obtained by the method of production, a cancer therapeutic agent comprising the artificial lymph node, and a kit for producing an artificial lymph node for cancer treatment comprising the following: (a) a cancer antigen; (b) an adjuvant capable of inducing cellular immunity; (c) a cytokine expression vector and stromal cells, or stromal cells incorporating a cytokine expression vector; (d) dendritic cells; and (e) a polymeric biomaterial. (http://www.faqs.org/patents/app/20090263428)

Information about closest relevant techniques

In the “lab-on-a-chip”- field, most devises combining micro fluidics with on-chip PCR are designed to identify the presence of an infection in a sample by detecting the pathogen and not the immune response directed against it. One method for on-chip detection of proteins is the use of antibodies coated on the chip surface. The binding of proteins to these antibodies can either result in a detectable change in the conductivity of the coated surface or the binding can be visualized via fluorescence.

Presently used methods of diagnosing tuberculosis consist of either *in vitro* cell culture test such as QuantiFERON-TB Gold, QuantiFERON-TB Gold In-Tube, and T-SPOT.TB, or tuberculin skin test such as the Mantoux test. In the latter test, purified protein derivatives (PPD) tuberculin is intradermally injected in the skin of a test person and the result is read 48 to 72 hours later. If the person is infected, this will result in a local swelling due to a rapidly activated immune response.